Activity Report
2004

Association
EURATOM / IPP.CR

INSTITUTE OF PLASMA PHYSICS
ACADEMY OF SCIENCES OF THE CZECH REPUBLIC

TABLE OF CONTENTS

3

PREFACE

This report summarizes main activities and achieved results of the Association EURATOM/IPP.CR in the year 2004. The Association participates in the joint European effort in mastering controlled fusion by carrying out relevant plasma physics and technology R&D, including participation in JET and other European devices and design activities related to the proposed experimental reactor ITER.

The Association was founded on December 22, 1999 through a contract between the European Atomic Energy Community (EURATOM) represented by the European Commission and the Institute of Plasma Physics, Academy of Sciences of the Czech Republic (IPP). Several other institutions have been included in the Research Unit to contribute to the work programme in physics and technology research:

- Faculty of Mathematics and Physics, Charles University in Prague (FMP)
- Institute of Physical Chemistry, Academy of Sciences of the Czech Republic (IPCH)
- Faculty of Nuclear Science and Physical Engineering, Czech Technical University (FNSPE)
- Nuclear Physics Institute, Academy of Sciences of the Czech Republic (NPI)
- Nuclear Research Institute, Rez, Plc (NRI)
- Institute of Applied Mechanics, Brno (IAM)

The overall manpower involved in the Association's fusion research at the end of 2004 was 78, of which 67 were professionals (those with a University degree). The total effort expended is about 47 person years of which roughly 70% is devoted to physics tasks and the remaining 30% to underlying technology and technology tasks. The overall annual budget is about 1.8 M€.

Our activities in physics were based on the approved Work programs 2004 both in experiment and theory. The fusion-relevant plasma physics is experimentally studied on the small tokamak CASTOR. The research is focused on the study of phenomena at the plasma edge, such as biasing, impurity radiation, and the measurement of the structure of edge turbulence by arrays of electric probes. In addition, new advanced probes are being developed. A part of our activities was devoted to studies of wave-plasma interaction, in particular in the range of lower hybrid and electron cyclotron frequencies. Some selected atomic processes relevant to fusion plasmas, such as the interaction of molecular ions with first wall elements, were studied in test-bed experiments.

The existing collaborations with other Associations were further strengthened. The Czech scientists took an active part in experiments on TORE-SUPRA, TCV and MAST. On the other hands, several experimental campaigns on the CASTOR tokamak were performed with a significant contribution of our colleagues from Associations CEA, the Belgium state, ENEA (RFX) and ŐAW. The further progress was achieved in the Association's participation in the collective exploitation of the JET facilities under EFDA.

In the technology area, the R&D was substantially enhanced and focused on the fields Vessel/In Vessel, Tritium Breeding and Materials and Physics Integration. In total 15 Technology Tasks, mostly exploiting the cyclotron at the NPI, the fission reactor at the NRI and computational capabilities at the IAM.

In what follows, more details of our activities are presented.

Jan Stöckel
Head of Research Unit
Association EURATOM/IPP.CR

I RESEARCH UNIT

1 Association EURATOM/IPP.CR

Composition of the Research Unit

IPP **Institute of Plasma Physics,**
Academy of Sciences of the CR
Address: Za Slovankou 3,
182 21 Praha 8, Czech Republic
Tel: +420 286 890 450
Fax: +420 286 586 389
Contact Person: Jan Stöckel
e-mail: stockel@ipp.cas.cz

IPCH **Institute of Physical Chemistry,**
Academy of Sciences of CR
Address: Dolejškova 3,
182 23 Praha 8, Czech Republic
Tel: +420 266 053 514 (3485-
laboratoř)
Fax: +420 286 582 307
Contact person: Zdeněk Herman
zdenek.herman@jh-inst.cas.cz

NPI **Institute of Nuclear Physics,**
Academy of Sciences of the CR
Address: 250 68 Řež, Czech Republic
Tel: +420 266 172 105 (3506)
Fax: +420 220 941 130
Contact person: Pavel Bém
e-mail: bem@ujf.cas.cz

IAM **Institute of Applied Mechanics Brno,**
Ltd.
Address: Veveří 85,
611 00 Brno, CR
Phone: +420 541 321 291
Fax: +420 541 211 189
Contact person: Lubomír Junek
e-mail: junekl.uam@telecom.cz

FMP **Faculty of Mathematics and Physics,**
Charles University
Address: V Holešovičkách 2,
182 00 Praha 8, Czech Republic
Tel: +420 221 912 305
Fax: +420 221 912 332
Contact person: Milan Tichý
tichy@mbox.troja.mff.cuni.cz

FNSPE **Faculty of Nuclear Science and**
Physical Engineering,
Czech Technical University
Address: Břehová 7,
115 19 Praha 1, Czech Republic
Tel: +420 224 358 296
Fax: +420 222 320 862
Contact person: Vojta Svoboda
svoboda@br.fjfi.cvut.cz

NRI **Nuclear Research Institute pls., Řež**
Address: 250 68 Řež, Czech Republic
Tel: +420 266 172 453
Fax: +420 266 172 045
Contact person: Milan Zmítko
e-mail: zmi@ujv.cz

Steering Committee

EURATOM	**IPP.CR**
Johannes P.M. Spoor, Head Unit J7, DG RTD	Ivan Wilhelm (Charles University)
David Campbell, Unit J6, DG RTD	Petr Křenek (Ministry of Education, Youth and Sports)
Barry Green, Unit J6, DG RTD	Pavel Chráska (Institute of Plasma Physics)

Head of Research Unit	**Secretary of the SC**
Jan Stöckel	Pavol Pavlo

International Board of Advisors of the Association EURATOM-IPP.CR

Dr. Michael Endler	Max-Planck-Institut für Plasmaphysik, Greisfwald, Germany
Dr. Carlos Hidalgo	CIEMAT, Madrid, Spain
Dr. Jochen Linke	Forschungszentrum Jülich GmbH, Jülich, Germany
Dr. Yves Peysson	CEA, Cadarache, France
Prof. Michael Tendler	Royal Inst. of Technology, Alfven Laboratory, Stockholm, Sveden
Dr. Martin Valovič	UKAEA, Culham laboratory, United Kingdom
Prof. Guido Van Oost	Ghent University, Gent, Belgium
Dr. Henri Weisen	EPFL, Lausanne, Switzerland
Prof. Hannspeter Winter	Technische Universitaet, Wien, Austria

The Board was established to help with the formulation of scientific program, and assess the scientific achievements of the Association.

Representatives of the Association in European Committees

Consultative Committee for the EURATOM Specific Programme on Nuclear Energy Research - Fusion

Pavel Chráska	Institute of Plasma Physics, Academy of Sciences of the Czech Republic
Milan Tichý	Faculty of Mathematics and Physics, Charles University, Prague

Scientific and Technical Advisory Committee

Jan Stöckel	Institute of Plasma Physics, Academy of Sciences of the Czech Republic
Pavol Pavlo	Institute of Plasma Physics, Academy of Sciences of the Czech Republic

EFDA Steering Committee

Jan Dobeš	Institute of Nuclear Physics, Academy of Sciences of the Czech Republic

2 Manpower and Budget

Manpower Analysis of the Association EURATOM/IPP.CR 2004

	Institution	Professional Person	Professional PY	Non-Prof Person	Non-Prof PY	Total Person	Total PY	%
Physics	IPP	28	23,2	6	5	34	28,2	
	IPCH	5	2,6	0	0	5	2,6	
	FNSPE	1	0,5	0	0	1	0,5	
	FMP	5	1,8	0	0	5	1,8	
	Total	**39**	**28,1**	**6**	**5**	**45**	**33,1**	**70.4**
Technology	FNSPE	1	0,5	0	0	1	0,5	
	NPI	10	4,8	2	1,5	12	6,3	
	NRI	15	5,3	3	0,85	18	6,15	
	IAM	2	1	0	0	2	1	
	Total	**28**	**11,6**	**5**	**2,35**	**33**	**13,95**	**29.6**
TOTAL		**67**	**39,7**	**11**	**7,35**	**78**	**47,05**	

Expenditures 2004

	Euro
Physics	709 411
Underlying Technologies	192 950
Inertial Fusion Energy	13 189
Sub-total	**915 550**
Technology tasks Art 5.1a	647 282
Technology tasks Art 5.1b	170 876
EFDA Article 6.3 Contracts	10 963
EFDA Article 9 - secondment to Culham	12 195
EFDA Article 9 - secondment to Garching	7 475
Sub-total	**848 791**
Mobility Actions	**49 570**
TOTAL	**1 813 911**

3   International Collaboration

Collaborative Projects 2004

PROJECT NO.1: **Fluctuation measurements and edge plasma biasing**
Measurement of the edge fluctuations by Langmuir probe arrays in ohmic regime and in discharges with the edge plasma biasing.
Collaborating Associations:
- *CEA Cadarache*
- *IST*
- *Etat Belge- Ghent University*
- *CIEMAT*
- *ENEA - Conzorcio RFX, Padova*
- *VR*

PROJECT NO. 2: **Development of advanced probes**
Development of advanced probe for the edge plasma diagnostics, such as the tunnel probe for electron and ion temperature measurements, emissive probe, etc.
Collaborating Associations:
- *CEA Cadarache*
- *ÖAW (Innsbruck Uni)*
- *Etat Belge- Ghent University*
- *CIEMAT*
- *ENEA - Conzorcio RFX, Padova*

PROJECT NO. 3: **Edge plasma measurements on Tore Supra**
Measurements of the edge plasma parameters (electron temperature, density, ion temperature and ion flows) in large - scale devices (Tore Supra, JET) and interpretation of experimental data.
Collaborating Associations:
- *CEA Cadarache*
- *JET*

PROJECT NO. 4: **Edge plasma modelling**
Modeling of the particle transport (bulk ions + impurities) at the plasma edge and comparison with experiment.
Collaborating Associations:
- *ÖAW (Innsbruck Uni)*
- *VR*

PROJECT NO. 5: **USX and VUV diagnostics on TCV and CASTOR**
Optimization of the USX and VUV diagnostics for spectroscopy measurements and study the transport of impurities on TCV and CASTOR tokamak.
Collaborating Associations:
- Confederation Suisse

PROJECT NO. 6: **EBW on MAST and CASTOR**
Modelling of conversion of the Electron Bernstein Waves and comparison of the results with measurements of microwave radiation by means of radiometers.
Collaborating Associations:
- *UKAEA*

PROJECT NO. 7: **Generation of fast particles in front of LH grills**
Modeling of the generation of fast particles in front of Lower Hybrid grills and comparison with experiment.
Collaborating Associations:
- *CEA Cadarache*
- *JET*
- *TEKES*
- *ÖAW (Innsbruck Uni)*

PROJECT NO. 8: **Atomic data**
Study of interaction of hydrocarbon ions with fusion-relevant surface.
Collaborating Associations:
- *ÖAW (Innsbruck Uni)*

4 Main Facilities

The CASTOR Tokamak

The CASTOR tokamak is a small device built in the year 1958 in the Kurchatov Institute in Moscow, which is in operation in the IPP Prague since 1977. The vacuum vessel and plasma control systems were substantially reconstructed in the year 1985. The basic characteristics of the device are:

Major radius	40 cm
Minor radius	8,5 cm
Toroidal magnetic field	0,5-1,5 T
Plasma current	5-20 kA
Pulse length	<50 ms
Working gas	Hydrogen

The vacuum vessel (minor radius 100 mm) is made of stainless steel. The plasma cross section is defined by the poloidal limiter made of Molybdenum. Auxiliary microwave power (f=1.25GHz, P=40kW) can be injected into the ohmic plasma via a multijunction grill for the non-inductive current drive. A graphite electrode is routinely used to polarize the edge plasma.

A great advantage of CASTOR is its flexibility. Good quality plasma discharges can be achieved within 1-2 days after opening the vessel to the atmospheric pressure which makes it ideal for testing new diagnostics. Up to 70 reproducible discharges can be achieved during one experimental day. Typical plasma parameters are:

Central electron temperature	100-300eV
Central ion temperature	50-100 eV
Line average density	$0.5\text{-}3.10^{19}$ m^{-3}
Energy confinement time	<1 ms

Diagnostics:
- Magnetic diagnostics
- Microwave interferometer at 70GHz
- Photomultipliers with interference filters for measurement of hydrogen and light impurities lines
- VUV spectrometer Seya-Namioka with a high spatial resolution
- XUV spectrometer with multi-layer mirror as disperse element
- Bolometer array for measurements of radiation losses
- Langmuir probe arrays for edge plasma monitoring both in radial and poloidal directions
- Advanced probes for measurements of ion and electron temperatures, plasma potential, and flows in the edge plasma
- Array of coils for measurement of magnetic fluctuations
- Radiometer of electromagnetic radiation at 17-27 GHz and 27-40 GHz
- Microwave reflectometer at 29, 33, and 35 GHz
- Charge exchange analyzer for measurement of ion temperature

Measured signals are digitalized by several A/D converters. Basic data (24 channels) are digitalized with the sampling frequency 40 kHz. For fluctuation data, the digitizers with a higher sampling frequency (80 channels, 1 MHz) are used. Data are stored in a database and processed *a posteriori* either by IDL or Matlab based software.

NRI Fission reactor LVR-15

LVR-15 is a light water moderated and cooled tank nuclear reactor with forced cooling, operated by the Nuclear Research Institute in Rez . The maximum power of the reactor is 10 MW. The reactor core is situated in the reactor vessel (outer diameter 2300 mm, total height of the vessel 6235 mm), which is made of stainless steel, the internal part of the rector are made of an aluminium alloy. The reactor has a forced circulation of the coolant. The generated heat is transported via three cooling circuits to the river.

The irradiation capacity

Main irradiation channels	Thermal neutron flux density ($cm^{-2}.s^{-1}$)
Irradiation channels 60 mm in fuel	1.10^{14}
Irradiation channels 60 mm, core periphery	7.10^{13}
Irradiation channels 60/40 mm in reflector	$3-5.10^{13}$
Horizontal channels 100/60 mm	1.10^{8}
Graphite thermal column	1.10^{11}
High pressure water loop	5.10^{13}
Doped silicon facility	1.10^{13}

The irradiation facilities are complemented with well-equipped hot chambers, which allow the irradiated specimens handling.

Experimental facilities: Light water loops

RVS-3: The loop is designed for material and radioactivity transport investigation under PWR/VVER conditions. It enables to perform irradiation experiments in wide range of operational parameters limited by the following maximum parameters:

Pressure	16,5 MPa
Temperature	345°C
Water flow rate	10 000 kg/hour
Neutron flux	10^{18} n/m^2s^{-1}
Electrical capacity heat	100 kW

BWR-1: The loop is designed for investigation of structural materials behaviour and radioactivity transport under BWR conditions

Pressure	10MPa
Temperature	300°C
Water flow rate	2 000 kg/hour
Neutron flux	10^{18} n/m^2s^{-1}

BWR-2: The loop is designed for material research simulating conditions of BWR reactors

Pressure	12MPa
Temperature	300°C
Water flow rate	1 000 kg/hour
Force applied to the specimen	152 kN
Duration of the specimen loading cycle	30 hours
Working fluid	ultra-pure water

The NPI cyclotron-based Fast Neutron Facility (NPI FNF)

The project of International Fusion Material Irradiation Facility (IFMIF) aims to provide neutron irradiation tests of fusion materials at fusion-reactor relevant fluency. For testing the neutronic calculations of the IFMIF test cell, the NPI cyclotron-based Fast Neutron Facility (FNF) provides neutron beams with the IFMIF-like spectrum – the only such source operated within EU countries.

Accelerator

The variable-energy cyclotron U-120M (K=40) of the Nuclear Physics Institute Rez is a versatile machine operating in both positive and negative regimes and accelerating light particles with the mass-to-charge ratio A/Z = 1-2.8. Accelerated beams and energy ranges are shown in the Table 1.

Table 1. *Beam parameters of the cyclotron U-120M*

Accelerated ions	H(+)	D(+)	^{3}He(++)	^{4}He(++)	H(-)	D(-)
Energy range (MeV)	10 - 24	10 - 17	17 - 53	20 - 40	10 - 37	10 - 18
Internal beam current (μA)	100	80	40	40	40 -15	25 -10
External beam current (μA)	3	3	3	3	40 -15	25 -10

Beam-line system with ion-optic equipments and target stations consists of three lines in the experimental hall (positive-ion mode, extraction by the deflection system) and one line in the cyclotron hall (negative-ion mode, extraction by the stripping-foil method). Two of them are dedicated to fast-neutronic experiments within the IFMIF project.

Neutron-spectrometry facility NG1

The cross-section data of neutron emitting reactions induced by charged-particle beams on investigated nuclides are experimentally investigated at the NG1 target station. The angular distributions of emitted fast neutrons (in the energy range from 0.7 to 35 MeV) are measured by the scintillator pulse-height unfolding technique based on the n-gamma discrimination hardware and many-parameter data-acquisition on PC. Different target technique (including solid, liquid and gas samples) can be utilized on the NG1 target station. To conduct the benchmark tests of neutron-transport calculations provided for fusion relevant materials the neutron source reactions $D_2O(^3He,xn)$ and $D_2O(p,xn)$ were investigated and for the first time employed as the best simulation of the IFMIF spectrum.

High-power neutron beam facility NG2

To reach a high-fluence neutron field for the activation-cross-section benchmark tests relevant to IFMIF neutronic calculations, the novel fast-neutron source was developed taking advantage in high beam current of a negative-ion mode of cyclotron operation. With this aim, the proton-induced reaction on heavy-water flow target was investigated for the first time and utilized for the NG2 target station. Besides, the standard Be-targets for protons and deuterons of the NG2 beam line are routinely operated as well. The white-spectrum neutron fields with energy range up to 35 MeV and the flux density up to 3 x 10^{11} n/cm^2/s are available for the irradiation purposes.

II   PHYSICS

EXECUTIVE SUMMARY - PHYSICS

Main topics and the results of the research undertaken in the Association EURATOM/IPP.CR in 2004 were as follows:

1. Edge Plasma, Plasma-Wall Interaction and Magnetic Confinement Physics

Investigation of the edge plasma on the CASTOR tokamak was focused on fluctuation studies in ohmic and biasing phase of a discharge. In particular, properties of the edge plasma were studied with biasing electrode immersed into the scrape-off layer (SOL). In contrary to a standard case with the biasing electrode located deep in the confinement region, it was found that only a flux tube associated with the electrode is biased. A non-uniform poloidal electric field is formed and changes sign periodically around the minor circumference of the torus. The resulting $E_p \times B_t$ flows cause a strong modification of the edge density profiles in the scrape-off layer. This method can be applied for a local broadening of power deposition profile in larger tokamak facilities. The results on the SOL biasing were presented at [45] and submitted for publication to PPCF.

Properties of edge plasma fluctuations were studied by several probe arrays. The radial profile of the Reynolds stress was measured with a probe array designed specifically for this purpose in collaboration with Belgian Association. Simultaneously, poloidal and parallel flow velocities were measured. It was found that under certain conditions in the ohmic discharges, large gradients of the Reynolds stress are present, which may play an important role in accelerating the flow [46].

The radial profiles of the ion saturation current, electron temperature and floating potential were simultaneously measured by means of the tunnel probe. These measurements reveal a strong reduction of electron temperature fluctuations in the $E \times B$ shear layer during electrode biasing [47].

Experiments on interaction of hot plasma with solid targets were carried out in tokamak CASTOR. The edge plasma is similar to that proposed in the divertor of the next generation fusion devices with exception of fast high-power wall loads. The Imaging Seya-Namioka Spectrometer has been installed for monitoring the radial profiles of the low-Z impurity line intensities in the spectral range from 60 to 200 nm. The solid target surface becomes a source of the hydrogen and low-Z atoms, due to the recombination of the plasma ions. The radial profiles of chord-integrated intensity of Lyα and chosen lines of CIII, NV and OVI were determined. [4], [30], [51].

Several different plasma-sprayed tungsten-based specimens have been manufactured at IPP Prague, and tested in the CASTOR tokamak. A special movable holder has been constructed, that the influence of different insertion depth on main plasma parameters changes was studied. No significant changes of tokamak discharge and its radiation could be seen for $r > r_{crit}$ (critical radius), excluding only a local shielding effect of specimens. Pure plasma-sprayed W specimens could be moved deeper up to radius $\sim a/3$. After specimen removal from the vacuum vessel, a strong surface oxidation resulting in a surface colour

change was observed. Small bright "branches" were observed on all irradiated plasma sprayed specimens. No traces of deep erosion or local melting were observed. However, few isolated microscopic surface holes and cracks on the irradiated W+Cu specimen were detected. [32], [50].

2. Diagnostics Development

Fast bolometric system, consisting of AXUV-20EL silicon photodiode linear array from IRD, was installed on the CASTOR tokamak in cooperation with KI Moscow. Its main features are fast response time (1 μs with fast data acquisition system) and improved signal-to-noise ratio achieved owing to utilization of semiconductor detectors with wide-band spectral sensitivity. The system ensures 16-channel measurements, which allow obtaining of radial profiles of the radiation losses. Scans over all main plasma parameters (I_p, n_e, B_T) and plasma column positions in OH discharges were done and analyzed [42].

Radial profiles of the lithium-like oxygen lines O^{5+} 103.2 nm and 103.7 nm were measured by tilting of the Imaging VUV Spectrometer. The shapes of the radial profiles were investigated in ohmic heating regime and plasma biasing. In OH discharge, the radial profile is axially symmetric. The maximum profile value achieves around 25 mm apart from the centre, where the local minimum of intensity is usually located. In the case of biasing at 50 mm and applied potential is +150V, the emission radial profile does displace from the polarization electrode, consequently the intensity falls almost to zero near to the polarization electrode. The radial profile shape of the O^{5+}(103.2 nm) and O^{4+}(63.0 nm) lines were also modelled by the emission/transport code STRAHL. The calculated radial profile shape leads to the diffusion coefficient of oxygen near $D_\perp$ ~2 m^2/s, if constant value at radius is assumed [14], [39].

The 4-channel ultrasoft X-ray (USX) monochromator on TCV was modified for radial emission profile measurements in specially designed radially swept discharges. The results show that the line integrated radial emission profiles provide a significant constraint for determining the diffusion coefficient in the outer part ρ_{pol}>0.6 of the discharge. A series of discharges in different conditions show that there is no simple proportionality between the Carbon ion diffusion coefficient and the effective heat diffusivity. The currently used instrument was only intended as a feasibility demonstration and is not adapted for routine measurements of ionization balance [20], [31].

A novel probe and approach to the direct measurements of the plasma potential in a strong magnetic field have been tested. The principle of this method is to reduce the electron saturation current to the same magnitude as that of the ion saturation current. In this case, the floating potential of the probe becomes identical to the plasma potential. This goal is attained by a shield, which screens off an adjustable part of the electron current from the probe collector due to the much smaller gyro–radius of the electrons. First systematic measurements have been performed in the CASTOR tokamak [5], [27].

3. Wave Interactions in Plasmas

Using a random field representation in agreement with the CASTOR tokamak measurements, we numerically demonstrated that the enhancement of electron acceleration in front of LH grills by the random fluctuating fields can lead to a significantly high fast particle production, even if the content of high $N_{//}$ components in the LH grill spectrum is low [35]. Therefore, even advanced LH wave launchers, like the PAM launcher for ITER, can at high level of turbulence produce high thermal loads at magnetically connected components of the tokamak vessel.

To check the theoretically predicted [35] enhancement of electron acceleration by fluctuating random fields, radio frequency (RF) probe and retarding field analyzer (RFA) measurements were performed [34] during lower hybrid current drive (LHCD) Tore Supra experiments. It was found that the normalized number of the accelerated electrons (given by the normalized RFA signal) is higher, when the fluctuation level is lower, but only when the probe is magnetically connected to the wave-guide row. This could indicate dissipation of the random fields by accelerated particles.

A quasi-neutral particle-in-cell (QPIC) code was developed for the description of the collisionless presheath and applied to the problem of edge plasma interaction with the lower hybrid antenna electric field [26]. A new technique of integrating particle equations of motion in QPIC was developed and tested [11]. The simulation CPU time using QPIC is reduced by a factor of about 100 over standard PIC [26]. The plasma response in the grill region as well as the floating potential and Langmuir probe volt-ampere characteristics were calculated. The self-consistent QPIC code is a valuable tool for the interpretation of probe measurements in the presence of arbitrary, generally non-Maxwellian, distributions. A new method of analyzing three-wave nonlinear parametric interactions was developed [1].

It has been shown on tokamak CASTOR by using an emissive Langmuir probe that the positive plasma "biasing" takes place in a radially very narrow layer just at the grill mouth [42]. The effect scales linearly with the power applied. Apparently, this positive biasing results from the charge separation due to the escaping electrons, accelerated by the near field lower hybrid wave effects in this region, along the magnetic field lines.

The code for simulation of electron cyclotron emission and Bernstein modes, already used for interpretation of NSTX EBW emission, has been rebuilt for application to MAST ECE emission. In order to interpret the experimental results, we have developed a realistic 3D model of the MAST plasma, and performed first attempts to derive the radiative temperature from the measured ECE emission. The aim of the work is to with the help of ECE simulation and the detected signal [7], [16], [33].

4. Atomic Physics and Data for Edge Plasma and Plasma Wall Interactions

Interaction of $C_3H_n^+$ (n= 2-8) hydrocarbon ions with room-temperature carbon (HOPG) surfaces was investigated over the range of incident energies 11 – 46 eV and an incident angle of 30^0 with respect to the surface. Mass spectra, translational energy distributions and angular distributions of product ions were measured. The mass spectra showed both surface-induced dissociation of the projectiles and – in case of radical cation projectiles – chemical reactions with the hydrocarbons on the surface, namely - to a limited extent - H-atom transfer to the projectile, formation of protonated projectiles, and their subsequent fragmentation. Formation of C_4 -hydrocarbons in a carbon chain build-up reaction could not be detected. The products were formed in strongly inelastic collisions. Angular distributions of reaction products showed peaking at sub-specular angles close to 20^0 [64], [65].

5. JET Collaboration

In 2004, our Association continued to support the EFDA JET Public Information activities in form of a full time secondment to CSU. This work significantly contributed, among others, to the following outputs: 3 issues of the EFDA JET Bulletin, 6 articles on JET in the EFDA Newsletters, the 2005 European Fusion calendar, 4 exhibition posters for the SOFT conference, 4 "Focus On" articles for the JET public webpage, finalisation of the multilingual presentations for the JET webpage and an invited talk at the 2004 SPPT Conference in Prague [3].

The continuous work in data analysis using inverse reconstruction methods resulted in new and successful application of Minimum Fisher Regularisation in the spectra deconvolution. This way, JET neutron spectra from NE213 scintillators were validated [52].

Selected results are presented in more detail in sections II.1 – II.5 of this report.

LIST OF PUBLICATIONS 2004 – PHYSICS

[1] **Fuchs V.:** Asymptotic treatment of the three-wave nonlinear parametric interaction. *J. Plasma Physics* **71**, part 2 (2004) 1-6.

[2] **Gunn J.P., Schrittwieser R., Balan P., Ionita C., Stöckel J., Adámek J., Ďuran I., Hron M., Pánek R., Barina O., Hrach R., Vicher M., Van Oost G., Van Rompuy T, Martines E:** Tunnel probes for measurements of the electron and ion temperature in fusion plasmas. *Review of Scientific Instruments* **75**, No. 10, Part 2 (2004) 4328-4330.

[3] **Mlynář J., Ongena J., Ďuran I., Hron M., Pánek R., Petržílka V., Žáček F. and contributors to the EFDA-JET Workprogramme:** JET: preparing the future in fusion, invited talk at 22th Symposium on Plasma Physics and Technology, Prague, Czech Republic, 14-17.6. 2004, *Czech. J. Phys.* **54**, Suppl. C (2004) C28.

[4] **Piffl V., Weinzettl V., Burdakov A., Polosatkin S.:** Intensity radial profiles of VUV line radiation near the solid target in hot plasma. *Czech. J. Phys.* **54**, Suppl. C (2004) C89-C94.

[5] **Adámek J., Hron M., Stöckel J., Ryszawy J., Balan P., Schrittwieser R, Ionita C., Martines E., Tichý M., Van Oost G.:** A novel approach to direct measurement of the plasma potential. *Czech. J. Phys.* **54**, Suppl. C (2004) C95.

[6] **Hron M., Ďuran I., Stöckel J., Hidalgo C.:** Decay of enhanced density and damping of plasma flows after the electrode biasing termination on the CASTOR tokamak. *Czech. J. Phys.* **54**, Suppl. C (2004) C22.

[7] **Preinhaelter J., Shevchenko V., Valovic M., Pavlo P., Vahala L., Vahala G., Urban J. and the MAST team:** ECE from MAST- Gaussian beams and antenna problem. *Czech. J. Phys.* **54**, Suppl. C (2004) C116-C122.

[8] **Urban J., Preinhaelter J.:** Adaptive finite elements method for the solution of the Maxwell equations in inhomogeneous magnetized plasma. *Czech. J. Phys.* **54**, Suppl. C (2004) C109-C115.

[9] **Zajac J., Preinhaelter J., Žáček F., Nanobashvili S.:** Microwave experiments on the tokamak CASTOR: fundamental ECE radiometry. *Czech. J. Phys.* **54**, Suppl. C (2004) C68-C73.

[10] **Sedláček Z.:** Nonlinear free streaming in Vlasov plasma. *Czech. J. Phys.* **54**, Suppl. C (2004) C82-C88.

[11] **Fuchs V., Gunn J.P.:** Numerical stability of 2nd order Runge-Kutta integration algorithm for use in particle-in-cell codes. *Czech. J. Phys.* **54**, Suppl. C (2004) C100.

[12] **Pánek R., Pitts R.A., Gunn J.P., Erents S.K.:** Particle-in-cell simulations of the impact of retarding field analyzer probe head geometry on ion saturation current measurements. *Czech. J. Phys.* **54**, Suppl. C (2004) C150.

[13] **Krlín L., Pánek R., Pavlo P., Petržílka V., Stöckel J., Svoboda V., Kuhn S., Tskhakaya D., Tendler M.:** Anomalous impurity diffusion in models of tokamak edge plasma turbulence. *Czech. J. Phys.* **54**, Suppl. C (2004) C157-C163.

[14] **Burdakov A.V., Weinzettl V., Piffl V., Polosatkin S.V., Postupaev V.V.:** A Complex of Imaging Diagnostic Devices of Vacuum UV Radiation for the GOL-3 Multimirror Trap. *Instruments and Experimental Techniques* **47**, No. 2 (2004) 234–239.

[15] **Krlín L., Zápotocký M., Svoboda V.:** Role of finite Larmor radius in chaotic regime of waves-particle interaction. *Czech. J. Phys.* **54**, No. 7 (2004) 759-774.

[16] **Preinhaelter J., Urban J., Pavlo P., Shevchenko V., Valovic M., Vahala L., Vahala G.:** Influence of antenna aiming on ECE in MAST. 15th Topical Conference on High Temperature Plasma Diagnostic, San Diego 19-22 April 2004. *Review of Scientific Instruments* **75** (2004) 3804.

[17] **Pánek R., Krlín L., Tskhakaya D., Kuhn S., Stöckel J., Pavlo P., Tendler M., Svoboda V., Petržílka V.:** Anomalous diffusion and radial electric field generation due to edge plasma turbulence. *Contrib. Plasma Phys.* **44** (2004) 203-204.

[18] **Žáček F., Petržílka V., Goniche M., Devynck P., Nanobashvili S.:** Radially scanned probe measurements in front of the CASTOR lower hybrid antenna. *Contrib. Plasma Phys.* **44**, No.7-8 (2004) 635-642.

[19] **Balan P., Schrittwieser R., Adámek J., Bařina O., DeBeule P., Ďuran I., Gunn J.P., Hrach R., Hron M., Ionita C., Martines E., Pánek R., Stöckel J., Van Den Berge G., Van Oost G., Van Rompuy T., Vicher M.:** Measurement of the Parallel and Perpendicular Ion Temperatures by means of an Ion sensitive Segmented Tunnel Probe. *Contrib. Plasma Phys.* **44**, No 7-8 (2004) 683-688.

[20] **Piffl V., Weisen H., Zabolotski A.:** Ultra-soft X-ray spectroscopy using multilayer mirrors on TCV. *Plasma Phys. Contr. Fus.* **46**, No.11 (2004), 1659-1674.

[21] **Sedláček Z.:** A study of the non-linear Landau damping in the Fourier transformed velocity space, *Transport Theory and Statistical Phys.*, in press.

[22] **Preinhaelter J., Shevchenko V., Valovic M., Wilson H., Urban J., Pavlo P., Vahala L., Vahala G.:** The role of magnetic equilibria in determining ECE in MAST, *46th APS Meeting of Division of Plasma Physics*, Savannah Nov 16-20, 2004, GA, USA, *Bull. Am. Phys. Soc.* **49**, No.11 (2004)

[23] **Preinhaelter J., Shevchenko V., Valovic M., Pavlo P., Vahala L., Vahala G., Urban J. and the MAST Team:** Comparison of Theory and Experiment on Electron Cyclotron Emission from Spherical Tori, *ibid.*, Paper # 6P14.

[24] **Pitts R.A., Andrew P., Bonnin X., Chankin A.V., Corre Y., Corrigan G., Coster D., Duran I., Eich T., Erents S.K., Fundamenski W., Huber A., Jachmich S., Kirnev G., Lehnen M., Lomas P.J., Loarte A., Matthews G.F., Rapp J., Silva C., Stamp M.F., Strachan J.D., Tsitrone E. and contributors to the EFDA-JET Workprogramme:** Edge and divertor physics with reversed toroidal field in JET, invited paper on *16th International Conference on Plasma Surface Interactions in Controlled Fusion Devices, 24 - 28 May 2004, Portland, Maine*, to be published in J. of Nucl. Mat.

[25] **Bolshakova I., Holyaka R., Ďuran I., Kulikov S., Kumada M., Leroy K.:** Radiation resistant magnetic sensors for accelerators. *Proc. of the 9th European Particle Accelerator Conference, 5-9 July 2004, Luzern, Switzerland.*

[26] **Fuchs V., Gunn J.P., Petržílka V., Goniche M.:** Quasineutral simulations of plasma response to the lower hybrid antenna electric field". *31th EPS Conference on Contr. Fusion and Plasma Physics, London, UK, 28 June – 2 July, 2004,* ECA Vol. **28G**, P-5.142.

[27] **Adámek J., Hron M., Stöckel J., Ryszawy J., Balan P., Schrittwieser R., Ionita C., Martines E., Tichý M., Van Oost G.:** Direct plasma potential measurement by a novel probe, *ibid.*, P5-120.

[28] **Martines E., Cavazzana R., Spolaore M., Zuin M., Adamek J., Antoni V.:** Synchronization of drift waves in a DC magnetron sputtering device, *ibid.*, P4-227.

[29] **Hidalgo C., Gonçalves B., Silva C., Erents K., Falchetto G., Garbet X., Hron M., Matthews G., Pedrosa M.A.:** On the momentum re-distribution via turbulence in fusion plasmas, *ibid.*, P-4.168

[30] **Piffl V., Weinzettl V., Burdakov A., Polosatkin S.:** Intensity radial profiles of VUV lines near the carbon target in the CASTOR tokamak, *ibid.*, P-5.138.

[31] **Piffl V., Zabolotsky A., Weisen H. and TCV Team:** Carbon impurity transport studies in the TCV tokamak using spatially resolved ultrasoft X-ray spectroscopy, *ibid.*, P-2.142

[32] **Weinzettl V., Matějíček J., Piffl V., Polosatkin S.:** First tests of plasma-sprayed tungsten specimens in CASTOR tokamak discharges, *ibid.*, P-5.139.

[33] **Preinhaelter J., Shevchenko V., Valovic M., Wilson H., Urban J., Pavlo P., Vahala L., Vahala G., and the MAST team:** The sensitivity of ECE simulations in MAST to different magnetic equilibria models, *ibid.*, P-4.184.

[34] **Goniche M., Petržílka V., Devynck P., Gunn J., Žácek F., Achard J., Gauthier E., Ekedahl A., Fuchs V., Pascal J.Y.:** Exploration of fast particle generation and density fluctuations in front of the lower hybrid grills on Tore Supra, *ibid.*, P-4.110.

[35] **Petržílka V., Fuchs V., Goniche M., Krlín L., Žáček F.:** Modelling of the Effects of Random Fields in Front of LH Grills on the Local Fast Particle Production, *ibid.*, P-1.41.

[36] **Petržílka V., Krlín L., Ullschmied J., Tataronis J.A.:** External Magneto-static Field Effects on Plasma Flows Arising from Primary Electron Acceleration in Two Crossed Laser Beam, *ibid.*, P-2.011.

[37] **Ďuran I., Hron M., Stöckel J., Viererbl L., Všolák R., Červa V., Bolshakova I., Holyaka R., Vayakis G.:** Stability of Hall sensors performance under neutron irradiation. *16th Topical Conference on High-Temperature Plasma Diagnostics, San Diego, California, USA, 19-22 April, 2004.*

[38] **Pedrosa M.A., Hidalgo C., Gonçalves B., Silva C., Erents K., Falchetto G., Garbet X., Hron M., Matthews G., Orozco R.O., Pitts R., Sánchez E.:** On the momentum re-distribution via turbulence in

fusion plasmas: experiments in tokamaks and stellarators. *IAEA 2004 Conf., Vilamoura, Portugal.*

[39] **Plyusnin V.V., Riccardo V., Jaspers R., Alper B., Kiptily V.G., Mlynar J., Popovichev S., de La Luna E., Helander P., Andersson F. and JET EFDA contributors:** Study of runaway electron generation process during major disruptions in JET, *ibid*

[40] **Polosatkin S.V., Burdakov A.V., Piffl V., Postupaev V.V., Weinzettl V.:** Investigation of Impurity Dynamics at GOL-3 Facility. *5th International Conference on Open Magnetic Systems for Plasma Confinement, Novosibirsk, 2004.*

[41] **Martines E., Cavazzana R., Spolaore M., Zuin M., Adámek J., Serianni G., Antoni V.:** Synchronization of drift waves in DC magnetron sputtering device. *12th International Congress on Plasma Physics, 25-29 October 2004, Nice, France,* P1-61.

[42] **Žáček F., Petržílka V., Adámek J., Goniche M.:** Positive plasma biasing in front of the LH grill of CASTOR tokamak, *ibid.*, P1-70.

[43] **Hron M., Weinzettl V., Dufková E., Hidalgo C., Ďuran I., Stöckel J.:** Relaxation of potential, flows, and density in the edge plasma of CASTOR tokamak, *ibid.*, P1-83.

[44] **Ďuran I., Hron M., Stöckel J., Viererbl L., Všolák R., Červa V., Bolshakova I., Holyaka R., Vayakis G.:** Stability of the Hall sensors performance under neutron irradiation, *ibid.*, P2-66.

[45] **Stöckel J., Devynck P., Gunn J., Martines E., Bonhomme G., Van Oost G., Hron M., Adámek J., Brotánková J., Dejarnac R., Ďuran I., Görler T., Hansen T., Pánek R., Stejskal P., Svoboda V., Žáček F.:** Formation of convective cells in the SOL of the CASTOR tokamak, oral contribution, *ibid.*

[46] **Vergote M., Van Schoor M., Xu Y., Jachmich S., Stöckel J., Hron M.:** The possible role of the Reynolds Stress in the creation of a transport barrier in Tokamak edge plasmas. *Workshop on Electric Fields, Structures and Relaxation in Edge Plasmas, Nice, October 26-27, 2004*, Paper #12.

[47] **Gunn J.P., Pánek R., Stöckel J., Van Oost G., Van Rompuy T.:** Simultaneous measurements of ion current, electron temperature and floating potential fluctuations with a tunnel probe. *Ibid.*, Paper #15

[48] **Adámek J., Balan P., Hron M., Ionita C., Martines E., Pánek R., Ryszawy J., Schrittwieser R., Stöckel J., Tichý M., Van Oost G.:** The ball-pen probe for direct space potential measurements in magnetized plasmas. *Ibid.*, Paper #16

[49] **Pánek R., Gunn J.P., Bucalossi J., Ďuran I., Geraud A., Hron M., Loarer T., Pégourié B., Stöckel J., Tsitrone E.:** The response of the Tore Supra edge plasma to different gas fuelling techniques. *16th PSI conference 24-28 May 2004, Portland, Maine, USA*, will be published in the Journal of Nucl. Mat.

[50] **Sánchez E., Hidalgo B., Gonçalves B., Silva C., Pedrosa M.A., Hron M., Erents K.:** On the energy transfer between flows and turbulence in the plasma boundary of fusion devices, *ibid.*

[51] **Matějíček J., Koza Y., Weinzettl V.:** Plasma Sprayed Tungsten-based Coatings and their Performance under Fusion Relevant Conditions. *23rd Symposium on Fusion Technology, Venice, Sep 20-24, 2004,* Fusion Engineering and Design, in press

[52] **Mlynář J., Adams J., Bertalot L., Conroy S.:** First Results of Minimum Fisher Regularisation as Unfolding Method in JET Neutron Spectrometry. *ibid*

[53] **Aržannikov V., Burdakov A.V., Weinzettl V., Ivanov I.A., Kojdan V.S., Piffl V., Polosatkin S.V., Postupaev V.V., Rovenskich A.F., Sinickij S.L.:** High-Temperature Plasma-Surface Interaction Using VUV and Visible Spectroscopy. *31st Zvenigorod Conference on Plasma Physics, 2004, Zvenigorod, Russia*, paper # PS-1-9, p. 203

[54] **Ďuran I., Hron M., Stöckel J., Viererbl L., Všolák R., Červa V., Bolshakova I., Holyaka R., Vayakis G.:** Irradiation effects on candidate Hall probes. *EFDA Task TW3-TPDC-IRRCER final report for 2003.*

[55] **Mlynář J.:** *ITER: cesta ke zvládnutí řízené termojaderné syntézy* PMFA 49 2 (2004) 129 [BOOK: ITER: the way to master controlled thermonuclear fusion; in Czech].

[56] **Ďuran I.:** *Turbulence magnetického pole na tokamaku CASTOR,* disertační práce, kat. elektroniky a vakuové fyziky, 2004, MFF UK, Praha. [Magnetic field turbulence in the CASTOR tokamak, PhD Thesis, in Czech].

[57] **Urban J.:** *Metoda adaptivních konečných prvků pro řešení Maxwellových rovnic v nehomogenním magnetoaktivním plazmatu,* diplomová práce, FJFI ČVUT, obor Inženýrská informatika, 2004, Praha. [Adaptive finite element method for solution of Maxwell Equations in inhomogeneous magnetoactive plasma, Diploma Work, in Czech].

[58] **Řípa M., Weinzettl V., Mlynář J., Žáček F.:** *Řízená termojaderná syntéza pro každého.* 1. vydání. ISBN: 80-902724-7-9. Ústav fyziky plazmatu AV ČR, Praha 2004. 84 s. [BOOK: Controlled thermonuclear fusion for everybody, 1st edition, in Czech]

[59] **Horák J., Krlín L.:** *Vratnost a nevratnostdynamických systémů.* 1. vydání. ISBN: 80-200-1200-1. ACADEMIA, Praha 2004. 148 s. [BOOK: Reversibility and irreversibility of dynamical systems, 1st edition, in Czech].

[60] **Macko P., Bánó G., Hlavenka P., Plašil R., Poterya V., Pysanenko A., Votava O., Johnsen R. , Glosík J.:** Afterglow studies of H_3^+(v=0) recombination using time resolved cw-diode laser cavity ring-down spectroscopy, *International J. Mass Spectrometry* **233** (1-3) (2004) 299-304.

[61] **Hlavenka P., Macko P., Bánó G., Plašil R., Pysanenko A. and Glosík J.:** The D_3^+ Second Overtone Absorption Spectra in Near-IR Region Using cw-Cavity Ring-Down Spectroscopy, *4th Cavity Ring Down User Meeting*, Heeza, The Nederland 7th and 8th of October 2004, (2004) abstract pp17.

[62] **Mikosch J., Kreckel H., Wester R., Plašil R., Glosík J., Gerlich D., Schwalm D., Wolf A.:** Action spectroscopy and temperature diagnostics of H_3^+ by chemical probing, *J. Chem. Phys.* **121**, No 22, December 2004.

[63] **Macko P., Bánó G., Hlavenka P., Plašil R., Poterya V., Pysanenko A., Glosík J.:** Decay of H_3^+ dominated low-temperature plasma, *Acta Phys. Slov.* **54** (2004) 263.

[64] **Herman Z.:** Surface collisions of small cluster ions at incident energies 10-10^2 eV. *Int. J. Mass Spectrom.* **233,** 361 (2004)

[65] **Qayyum A., Herman Z., Tepnual T., Mair C., Matt-Leubner S., Scheier P., Märk T.D.:** Surface induced dissociation of polyatomic hydrocarbon projectile ions with different initial internal energy content. *J. Phys. Chem.* **108,** 1-8 (2004).

[66] **Kalal M., Borodziuk S., Demchenko N.N., Gus'kov S.Yu., Kasperczuk A., Kondrashov V.N., Limpouch J., Pisarczyk P., Pisarczyk T., Rohlena K., Rozanov V.B., Skala J., Ullschmied J.:** High power laser interaction with single and double layer targets, *invited talk* Fr/O1/3/I, *XXVIII ECLIM.* Roma, September 6-10, 2004

[67] **Limpouch J., Demchenko N.N., Gus'kov S.Yu., Gromov A.I., Kalal M., Kasperczuk A., Kondrashov V.N., Krousky E., Masek K., Pisarczyk P., Pisarczyk T., Rozanov V. B.:** PALS Laser Interactions with foam targets. *31st EPS Conference on Plasma Phys.* London, 2004, ECA Vol. 28G, P-2.031 (2004).

# 1 EDGE PLASMA AND MAGNETIC CONFINEMENT PHYSICS

2D structure of convective cells in the scrape-off layer of CASTOR
J. Stöckel, J. Brotánková, R. Dejarnac, I. Ďuran, M. Hron, V. Svoboda

In collaboration with:
P. Devynck, J. Gunn, (CEA Cadarache), E. Martines (ENEA RFX Padova), G. Bonhomme (University of Nancy), G. Van Oost, T. Hansen (Ghent University), T. Görler (University of Ulm)

Recent experiments performed on the CASTOR tokamak [1] have demonstrated formation of toroidally elongated and poloidally localized structures of potential, if a biased electrode is immersed into the SOL. These structures, called convective cells were identified by a poloidal ring of Langmuir probes located in the SOL. Recently, a new diagnostic tool, a two-dimensional matrix of Langmuir probes (see Fig. 1 left panel) was employed to visualize the 2D structure of the convective cells.
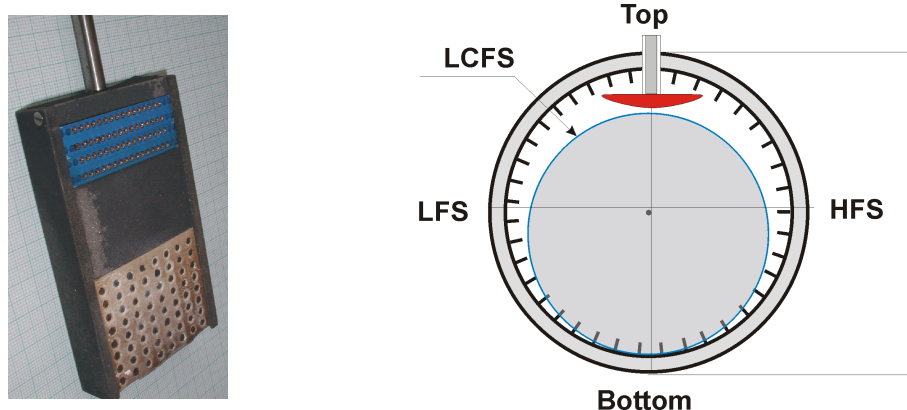
Fig. 1 *Left - Picture* of the *2D matrix of 64 Langmuir probes.* **Right** - *Schematic picture of the poloidal cross-section of the CASTOR tokamak showing the respective position of the biasing electrode, the plasma column and the poloidal limiter.*

The magnetic configuration, employed for the formation of convective cells in the SOL is schematically depicted in the right panel of Fig. 1, from which the respective position of the plasma column and of the poloidal limiter is evident. It is seen that the biasing electrode is immersed into the SOL from the top of the torus, where the connection length is much longer than the toroidal circumference of the torus.

If the electrode is biased positively, the biasing current flows predominantly parallel to the magnetic field lines in the upstream and downstream direction and terminates on the electron and ion side of the bottom part of the poloidal limiter. This is apparent from the schematic picture, shown in Fig. 2, where an unfolded magnetic surface associated with the biasing electrode is depicted. These current tubes appear to be biased, as demonstrated in [1].
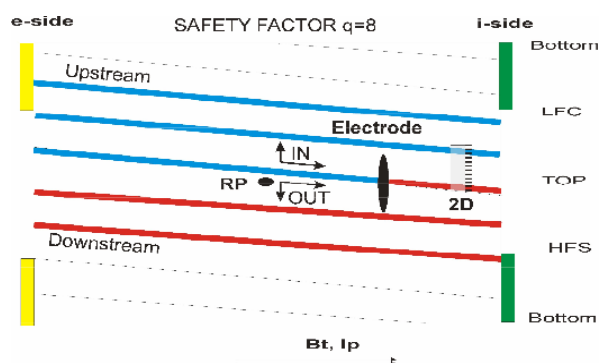
Fig. 2.
Biased flux tube originating at the electrode is shown schematically on an unfolded magnetic surface in the SOL for $q_{edge} \sim 8$. The toroidal location of the rake probe and of the 2D matrix is marked.

To observe directly the biased flux tube, which originates at the electrode and extends along the helical magnetic field line, the 2D matrix is inserted into the SOL from the top, 40° toroidally away from the electrode, as shown in Fig. 2. Its active surface (equipped with probes) is oriented downstream to the toroidal magnetic field lines.
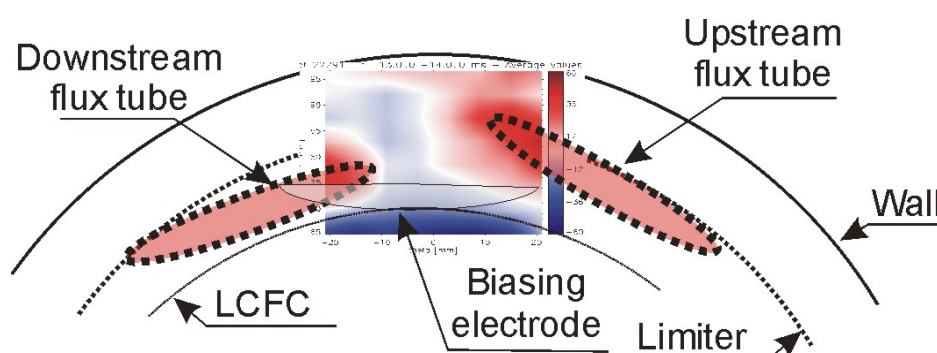
Fig. 3. *Poloidal projection of the biased flux tube as measured by the 2D matrix of Langmuir probes. The lengths of the downstream and upstream tubes are ~30 cm and 220 cm, respectively.*

Projection of the biased flux tube on the 2D matrix (marked by red-colour patterns) is shown in Fig. 3. It is evident that for this particular orientation the probe array "sees" both the downstream and the upstream biased flux tube simultaneously. The poloidal distance of the patterns of the potential corresponds to the angle of the rotational transform for $q_{edge} \sim 8$. It is also evident that the resulting perpendicular electric field, E_{perp}, is two-dimensional, having both radial and poloidal component. A consequence of this is the occurrence of a convective motion of the SOL plasma around the convective cell because of the $E_{perp} \times B_t$ drift.

The amplitude and even the sign of the poloidal component E_{pol} changes with the poloidal angle. A consequence of this is an inward or outward convective motion of the SOL plasma according the sign of the $E_{pol} \times B_t$ drift, which substantially modifies the radial profiles of plasma density in the SOL [1]. On the other hand, the radial component of the electric field is also amplified. This causes sheared poloidal convection, which may reduce the plasma turbulence. If the biasing electrode is located in the proximity of the Last Closed Magnetic Surface (LCMS), such sheared flows appear inside the LCMS. Such biasing scheme (called "separatrix biasing") is discussed in [2]. Formation of an edge transport barrier and improved particle confinement is documented there.

[1]   J. Stockel et al, Plasma Phys. Contr. Fusion, 47, 2005, 635-643
[2]   G Van Oost et al, Plasma Phys. Contr. Fusion, 45, 2003, 621-643

Plasma Interaction with Solid Targets

V. Weinzettl, J. Matejíček, V. Piffl, E. Dufková, J. Ryszawy

In collaboration with:

A. Burdakov, S. Polosatkin, Budker Institute, Novosibirsk, Russia

Y. Koza, EURATOM Association FZJ, Forschungszentrum Juelich, Germany

Intensity radial profiles of VUV line radiation near the solid targets in a hot plasma

The experiments on interaction of hot plasma with solid targets were carried out in the tokamak CASTOR. The edge plasma is similar to that proposed in the divertor of the next generation fusion devices with exception of fast high-power wall loads. The Imaging Seya-Namioka Spectrometer has been installed for monitoring the radial profiles of the low-Z impurity line intensities in the spectral range from 60 to 200 nm. The solid target surface becomes a source of the hydrogen and low-Z atoms, due to the recombination of the plasma ions. The radial profiles of chord-integrated intensity of Lyα and chosen lines of CIII, NV and OVI were determined, see Fig.1 and Fig. 2.
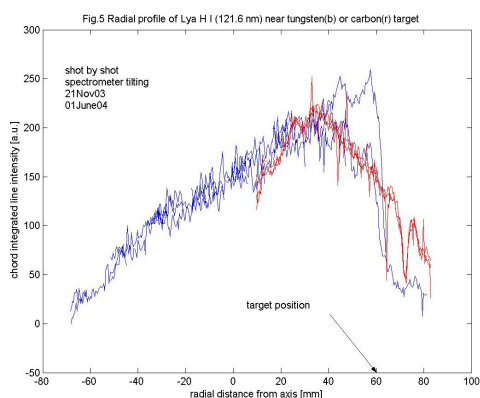
Tests of plasma-sprayed tungsten specimens on CASTOR tokamak discharges

Selection of a wall surface material is an important design issue for tokamaks and other fusion devices. The use of plasma-sprayed tungsten-based coatings in a divertor leg of ITER comes into consideration. Several different plasma-sprayed tungsten-based specimens have been manufactured at IPP Prague, and tested under high heat fluxes by electron beam at Forschungszentrum Juelich and in small-size tokamak CASTOR plasmas at IPP Prague. A special movable holder has been constructed (CASTOR, see Fig. 3), the influence of different insertion depth on main plasma parameters changes was studied. A critical radius, above which no significant influence on the discharge occurred, was determined to be $r_{crit} \sim 55$ mm ($T_e \sim 20$ eV) for Cu+W specimens and $r_{crit} \sim 32$ mm ($T_e \sim 50\text{-}100$ eV) for pure W targets. Plasma current was partially absorbed by a tungsten surface, what was accompanied by line averaged electron density increase. The energy deposition was 10-30 J per discharge. The spatial chord-integrated profiles of VUV line radiation clearly show shielding effect (radiance decrease at the specimen position), and radiance increase in front of the specimen as a result of particle bombardment, ion recombination and re-emission from a solid surface. After specimen removal from the vacuum vessel, a strong surface oxidation resulting in a surface colour change was observed. Small bright "branches" were observed on all irradiated plasma sprayed specimens as a result of unipolar arcing leading to oxidic layer removal (Fig. 4). No traces of deep erosion or local melting were observed. However, few isolated microscopic surface holes and cracks on the irradiated W+Cu specimen were detected. Compositional changes were measured by Rutherford Backscattering Spectrometry (RBS) and Elastic Recoil Detection Analysis (ERDA) at Institute of Nuclear Physics in Rez. Results for pure W coating show hydrogen implantation into the surface for both inserted specimens. Nevertheless, content of oxygen decreases for irradiated one. Carbon content shows no clear trend.

References:

[1] V. Piffl, V. Weinzettl, A. Burdakov, S. Polosatkin, „ Intensity radial profiles of VUV line radiation near the solid target in a hot plasma", 21st Symposium on Plasma Physics and Technology, Prague, 2004, Czechoslovak Journal of Physics, Vol. 54 (2004), Suppl. C, p. C89-94

[2] V. Piffl, V. Weinzettl, A. Burdakov, S. Polosatkin, „Intensity radial profiles of VUV lines near the carbon target in the CASTOR tokamak", 31st EPS Conference on Plasma Phys. London, 2004, ECA Vol.28B, P-5.138 (2004)

[3] V. Weinzettl, J. Matějíček, V. Piffl, S. Polosatkin, „First tests of plasma-sprayed tungsten specimens in CASTOR tokamak discharges", 31st EPS Conference on Plasma Phys. London, 2004 ECA Vol.28B, P-5.139 (2004)

[4] J. Matejicek, Y. Koza, V. Weinzettl, "Plasma Sprayed Tungsten-based Coatings and their Performance under Fusion Relevant Conditions", 23rd Symposium on Fusion Technology, Venice, Italy, P4C-F162, Book of Abstracts, p.271

[5] V. Arzannikov, A. Burdakov, V. Weinzettl, I. Ivanov, V. Kojdan, V. Piffl, S. Polosatkin, V. Postupaev, A. Rovenskich, S. Sinickij, "High-Temperature Plasma-Surface Interaction Using VUV and Visible Spectroscopy", 31st Zvenigorod Conference on Plasma Physics, 2004, Zvenigorod, Russia, contrib. PS-1-9, p. 203
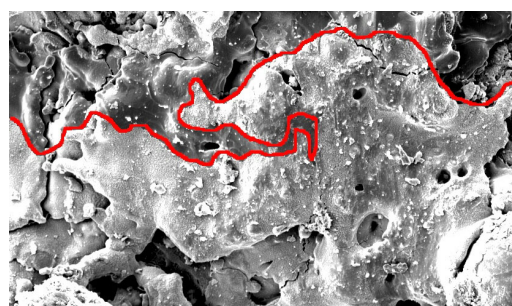
Fig. 1. *Radial profile of H I Lyα 121.6 nm near tungsten (blue) and carbon (red) targets.*
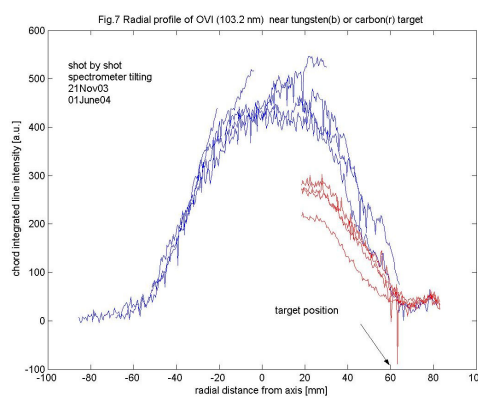
Fig. 2. *Radial profile of O VI 103.2 nm near tungsten (blue) and carbon (red) targets.*
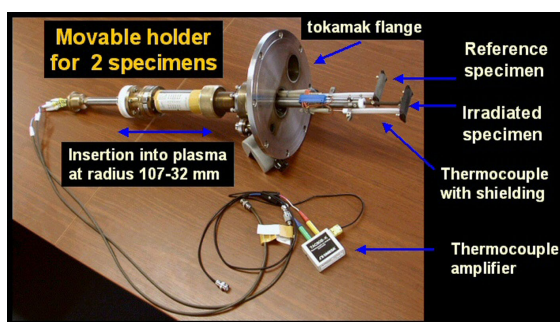
Fig. 3. *The movable holder for the insertion of two plasma-sprayed tungsten specimens into a tokamak chamber.*

Fig. 4. *The detail of the irradiated tungsten surface (SEM image, magnification 500x). The smooth metallic surface of the bright "branch" (without oxides) is on the top.*

2   Diagnostics Development

Carbon impurity transport studies in the TCV tokamak

V. Piffl

In collaboration with:
A. Zabolotsky, H. Weisen and TCV Team, CRPP Lausanne, Switzerland

The transport coefficients could be evaluated by measuring and modelling of the spatial and temporal behaviour of the emission line profiles in different confinement regimes. It is well known, the radial distribution of the line emission density is influenced by the transport phenomena and differs from those calculated using a pure coronal equilibrium. In some tokamak plasma regimes, the ion recombination time is comparable to the characteristic time of the particle transport. This fact leads to a distribution of ionised states, which are not in equilibrium with the electron temperature, as it would be expected according to the coronal model. The broadening of the radial profile for each ionised species is the typical effect of transport phenomena and can be examined by radial profile measurements of the intensity of the selected line.

Carbon transport studies using spatially resolved ultrasoft X-ray spectroscopy [1]

The TCV tokamak is equipped with a 4-channel ultrasoft X-ray (USX) multimonochromator based on use of multilayer mirrors. Recently the instrument was refurbished and new oriented to allow measurements of radial profiles of the CV (308 eV) or CVI (368 eV) line intensities in specially designed discharges. In the usual TCV plasma configurations, the four channels of the USX monochromator span only 40 % of the plasma radius at the outboard side and there is normally no chord passing just inside the plasma edge where the line radiation profile depends most strongly on position.

Fortunately, the shaping capabilities of the TCV tokamak allows us to slowly compress a plasma towards the HFS inner wall, thereby sweeping the low field side flux surfaces across the USX viewing lines with good spatial resolution in a single discharge. Such experiments were performed in several Ohmic L-mode limited discharges with plasma currents I_p ranging between 130kA and 300kA, line averaged electron densities in the range $2.10^{19} \leq <n> \leq 4.3 \cdot 10^{19} m^{-3}$, central electron temperatures about 700-1100 eV, average elongation $\kappa \sim 1.25$ and average triangularity $\delta \sim 0.25$. All four channels measured CV radiation at 308 eV. During the 300 ms of compression, each channel scans about 4 cm in the radial direction, resulting for the four channels in 80% coverage of the distance from the plasma centre to the low field side edge. At the end of the compression the plasma edge is resolved up to the LCFS and the signal of the detector closest to the edge drops practically to zero.

In order to derive a steady state profile of line emission, the main plasma parameters such as profile of the density and plasma safety factor at the edge were kept constant during the compression. It was assumed that current changes during the compression do not significantly affect the impurity transport parameters as long as edge safety factor remains constant **[2].**

In **Fig.1** (left) the experimental profile of integrated line emission measured by USX (dots) is plotted together with the STRAHL simulated one (line) showing a good agreement between experiment and simulation. The examples of radial profiles of the diffusion coefficients used in simulations are shown in **Fig.1** on the right. It was found that there is a range of profiles of the diffusion coefficient, which give a good fit to the final profile of integrated line emission.

The results show that the line integrated radial emission profiles provide a significant constraint for determining the diffusion coefficient in the outer part $\rho_{pol}>0.6$ of the discharge. A series of discharges in different conditions show that there is no simple proportionality between the Carbon ion diffusion coefficient and the effective heat diffusivity**.** The currently used instrument was only intended as a feasibility demonstration and is not adapted for routine measurements of ionisation balance **[3]**.

References:

[1] V. Piffl, A. Zabolotsky, H. Weisen and TCV Team: „Carbon impurity transport studies in the TCV tokamak using spatially resolved ultrasoft X-ray spectroscopy", 31st EPS Conference on Plasma Phys. London, 28 June - 2 July 2004 ECA Vol.**28**B, P-2.142 (2004)

[2] A. Zabolotsky, H. Weisen, TCV Team, *Plasma Phys. Control. Fusion* 45 (2003) 735

[3] V. Piffl, H. Weisen, A. Zabolotsky: „Ultra-soft X-ray spectroscopy using multilayer mirrors on TCV", Plasma Physics and Controlled Fusion 46, (2004), 1659 - 1674
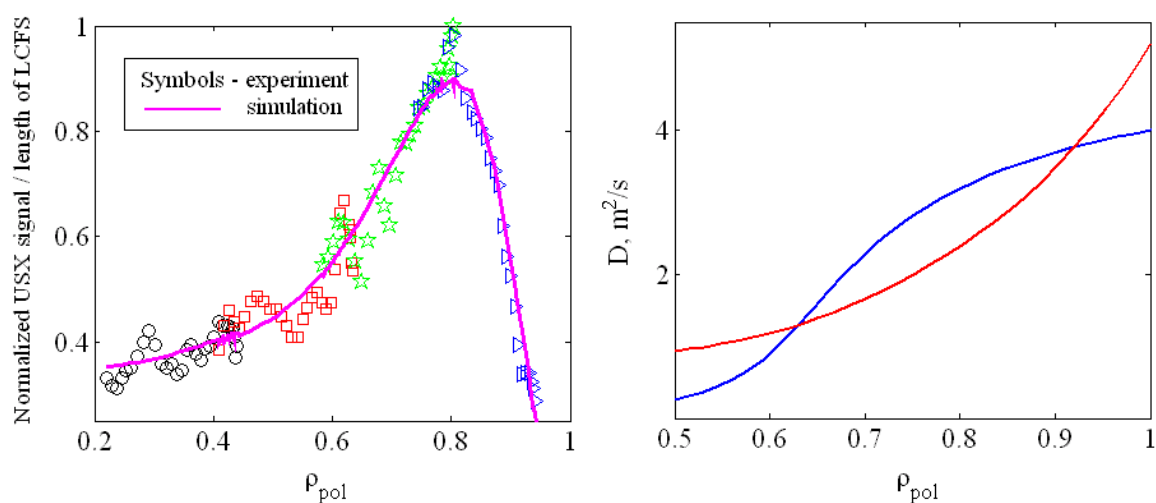
Fig. 1. *The experimental profile measured by USX is plotted together with the simulated one. The same result is obtained by both profiles of diffusion coefficients on the right.*

A novel approach to direct measurement of the plasma potential

J. Adámek, J. Stöckel, M. Hron, J. Ryszawy

In collaboration with:

R. Schrittwieser, C. Ionita, P. Balan, EURATOM-ÖAW, Innsbruck, Austria

M. Tichý, Faculty of Mathematics and Physics, Charles University, Prague, Czech Republic

E. Martines, Consorzio RFX, EURATOM–ENEA, Padova, Italy

G. Van Oost, Department of Applied Physics, Ghent University, Gent, Belgium

Direct measurement of the plasma potential in tokamaks

Up to now, emissive probes [1] and heavy ion beam probes [2] are used for direct measurements of the plasma potential in tokamaks. However, the more widespread use of these techniques is hampered by various technical problems and peculiarities in the interpretation of the measured data. Directly heated emissive probes are rather fragile and of limited lifetime and their exploitation on large tokamak experiments is questionable. Indirectly heated emissive probes [3] are more robust, but they are still under development. The heavy ion beam probe is a complex diagnostic, suitable for the measurement of the plasma potential in the core plasma. Moreover, its spatial resolution is limited. In practice, a simple Langmuir probe is routinely used at the plasma edge for this purpose and the plasma potential Φ is deduced from the formula:

$$V_{fl} = \Phi - \left(\frac{kT_e}{e} \right) \ln(R) \,, \tag{1}$$

where the floating potential V_{fl} and the electron temperature T_e are determined from the *I-V* characteristic of the single Langmuir probe, k and e denote the Boltzmann constant and elementary charge, respectively. The quantity $R = I^-_{sat}/I^+_{sat}$ represents the ratio of the electron to the ion saturation current which is not routinely measured. The main reason is that the magnitude of the electron saturation current is typically rather large, even at the plasma edge of tokamaks. When operating in this mode, the Langmuir probe is exposed to high power loads and can even be destroyed. Furthermore, as the determination of T_e requires measurements of full *I-V* characteristics, this technique is not suitable for measurements with time resolutions in the range of 10^{-6} s, which are usually required to study the plasma turbulence in tokamaks. It has to be also noted that the theory of the electron branch of the *I-V* characteristic in magnetized plasmas is not yet fully developed, and measurements of the electron saturation current are still questionable. Therefore, the ratio R is usually estimated from the Langmuir probe theory of non-magnetized plasmas and its value is taken as $\ln(R) \sim$ 2.5-3 for hydrogen.

The basic idea of direct plasma potential measurements by means of electric probes, however, by avoiding the above-mentioned problems, is to adjust R to be equal to one by a proper experimental set-up of the probe. If this is achieved, the floating potential of the probe is equal to the plasma potential, as evident from Eq. (1).

A possible approach, which can be used only in magnetized plasmas, is the concept of the ball-pen probe (BPP) [4]. The probe is designed so that the ratio R can be modified by changing the collecting areas for electrons and ions, taking advantage of the fact that the Larmor radii of electrons and ions are strongly different. The design of the BPP is shown in the schematic picture of Fig. 1. The probe consists of a conically shaped collector, which is shielded by an insulating tube made of boron nitride.

The collector, which is movable inside the tube, is either completely shielded or partially exposed to the plasma. In the ideal case, when the collector is hidden inside the tube, only ions with sufficiently large Larmor radii can reach the collector surface and the collecting area for electrons is zero. Consequently, the ratio $R = 0$. When the collector is shifted outwards the electron current as well as R increase. At a certain collector position, the electron and ion currents are expected to be balanced (i.e., $R = 1$). When the collector is fully outside the shielding tube, the probe operates as conventional single Langmuir probe and measures the floating potential V_{fl}. Indeed, we have demonstrated in [4] that the ratio R can be significantly modified by moving the collector into the shielding tube. As it is seen from Fig. 2, this ratio can be adjusted close to unity ($R \cong 1.1$) if the tip of the conical collector is located slightly inside the shielding tube at the position h $\cong -0.5$ mm. At this particular position, the floating probe potential $V_{probe} = \Phi^{ball-pen}$ is significantly higher than the floating potential V_{fl}, which is determined with the collector fully exposed to the plasma ($h \cong +1.0$ - 1.7 mm). The normalized difference $\Delta = \ln(R) = (\Phi^{ball-pen} - V_{fl})e/kT_e \cong 2.3$ approaches the value predicted by the theory. Consequently, the potential $\Phi^{ball-pen}$ measured at the position where R is minimum, is expected to be close to the plasma potential.

It should be noted that some experimental observations are not yet fully understood. One of the unexpected feature observed with the collector hidden within the tube is that the probe potential $\Phi^{ball-pen}$ is practically independent of the collector position for $h < 0$ mm. On the other hand, such findings would be beneficial for the practical use of the BPP in future, because a precise positioning of the collector inside the tube will not be required.

References:

[1] R. Schrittwieser, J. Adámek, P. Balan, M. Hron, C. Ionita, K. Jakubka, L. Kryška, E. Martines, J. Stöckel, M. Tichý, G. Van Oost: Plasma Phys. and Control. Fusion, Vol. 44 (2002), p.567-578.

[2] A.V. Melnikov, L.G. Eliseev: Czech. J. Phys., Vol. 49/S3 (1999), p.35-40.

[3] R. Madani, C. Ionita, R. Schrittwieser, T. Klinger: First result on a laser-heated emissive probe, In Proc of 12th International Congress on Plasma Physics, Nice 2004, P2-077, http://hal.ccsd.cnrs.fr/ccsd-00001996

[4] J. Adámek, P. Balan, M. Hron, C. Ionita, E. Martines, J. Ryszawy, R. Schrittwieser, J. Stöckel, M. Tichý, G. Van Oost: Czech. J. Phys., Vol. 54/C95 (2004).
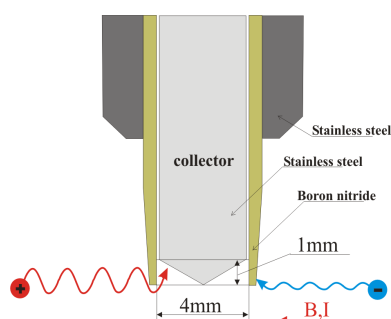
Fig. 1. *Schematic picture of the ball-pen probe.*
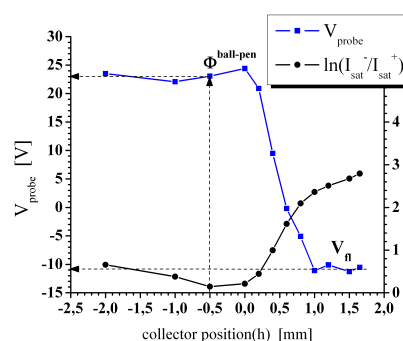
Fig. 2. *Dependence of the BPP signals on the collector position. The probe potential (V_{probe}) and ln(R).*

VUV Spectroscopy and Bolometry on the CASTOR Tokamak

V. Piffl, V. Weinzettl, E. Dufkova, J. Ryszawy

In collaboration with:
A. Burdakov, S. Polosatkin, Budker Institute, Novosibirsk, Russia
D. Sarychev, Kurchatov Institute, Moscow, Russia

The Imaging VUV Spectrometer

The Imaging VUV Spectrometer was assembled according to the Seya-Namioka scheme. The spherical dispersion grating with gold cover, radius of curvature 0.5 m, 1200 grooves per mm, was installed in this instrument. The incident radiation after the diffraction is focused on the output window displaced near to the Rowland circle. The two-dimensional detector system consists of set of two channel-plates of the working area diameter, 38 mm. The image is recorded by a CCD camera optically coupled to the lightguide output. The CCD element contents 165×192 pixels of rectangular form.

Effect of biasing on radial shape of the chord-integrated VUV lines intensity

The radial profiles of the chord-integrated line intensity of the lithium-like oxygen ions O^{5+}(103.2 nm and 103.7 nm), Fig.1-2, were measured by tilting of the Imaging VUV Spectrometer. The spatial resolution is found to be better than 5 mm. Optical enlargement of the system is 2.93, so the viewed part of the plasma is 70 mm in height. The shapes of the radial profiles were investigated basically in two different discharge regimes: ohmic heating regime and plasma polarized regime (biasing). In ohmic heating discharge regime without polarization, the radial profile is axially symmetric, Fig.1. The maximum profile value achieves around 25 mm apart from the centre, where the local minimum of intensity is usually located. In Fig.2, the radial profile of the chord-integrated intensity of oxygen ion line O^{5+} is shown, if the biasing electrode is positioned inside the last closed magnetic surface at radius of 50 mm, and applied potential is +150V. The emission radial profile does displace from the polarization electrode, consequently the intensity falls almost to zero near to the polarization electrode.

The effect of transport can be deduced from the chordal measurements of the line intensity radial profiles. The radial profile shape of the O^{5+}(103.2 nm) and O^{4+}(63.0 nm) lines were also modelled by emission/transport code STRAHL. The result of such modelling is shown in Fig. 3. The calculated radial profile shape seems to be broader as measured one, like as the real diffusion coefficient of the oxygen impurity be lower than fitted, $D_\perp \sim 2$ m2/s and constant at radius.

Fast bolometry

The bolometric system, consisting of the AXUV-20EL silicon photodiode linear array from IRD Inc., was installed on the CASTOR tokamak in cooperation with KI Moscow. Its main features are a fast response time (20 µs with standard data acquisition system, 1 µs with fast data acquisition system), a spatial resolution of 12 mm on a plasma column and an improved signal-to-noise ratio achieved owing to utilization of semiconductor detectors with wide-band spectral sensitivity. The system ensures 16-channel measurements, which allow obtaining of radial profiles of the radiation losses and its behaviour, see Fig. 4. Scans over the main plasma parameters (I_p, n_e, B_T) in L-mode OH discharges were performed. The poloidal

reconstruction of the radiation profile can be computed using the asymmetrical Abel inversion at each time step. The estimation of the plasma radiation centre, FWHM and their temporal behaviour can be done. Fast transitions from centric to hollow profiles and slow relaxations back (0.2-3 ms) to the stable configuration were observed in shots with edge plasma biasing.

References:
[1] V. Piffl, V. Weinzettl, A. Burdakov, S. Polosatkin, "Line Intensity Radial Profiles Evolution in VUV & XUV Spectral Range", 30th EPS Conference on Contr. Fusion and Plasma Phys., St. Petersburg, 2003, ECA Vol. 27A, P-1.61

[2] M. Hron, V. Weinzettl, E. Dufkova, C. Hidalgo, I. Duran, J. Stockel, "Relaxation of potential, flows, and density in the edge plasma of CASTOR tokamak", 12th International Congress on Plasma Physics, Nice, France, 2004, P1-083
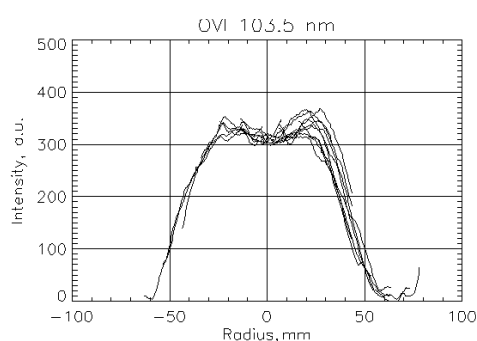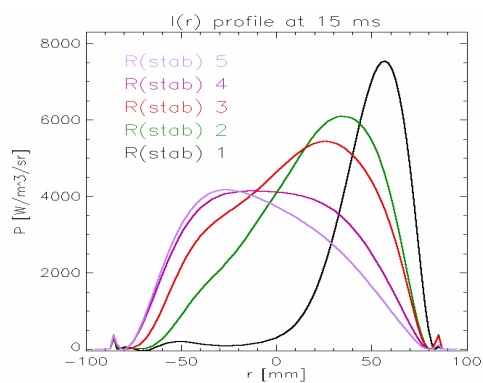
Fig. 1. *O5+ radial profile in OH regime without biasing.*
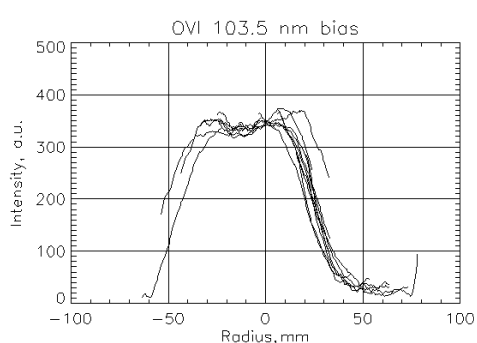
Fig. 2. *O5+ radial profile in OH regime with biasing.*
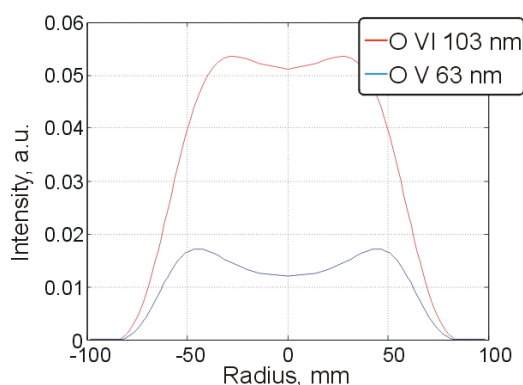
Fig. 3. *Computed radial profiles of O^{4+} and O^{5+} lines.*

Fig. 4. *A bolometrically measured radial distribution of the radiated power for 5 different settings of the horizontal stabilization system of the CASTOR tokamak at 15 ms.*

Emissive Probe Diagnostics Development
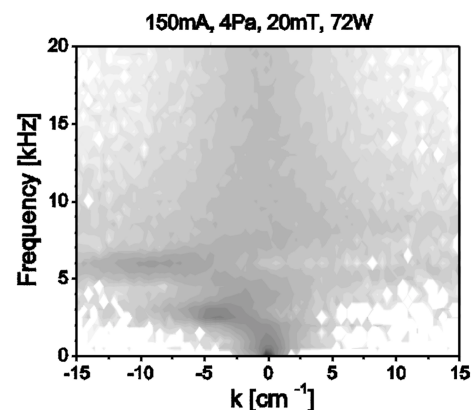## M. Tichý, P. Kudrna (FMP)

In collaboration with:

*R. Schrittwieser, Codrina Ionita-Schrittwieser, OAW, Innsbruck University*
E. Martines, Consorzio RFX, Padova

Fig. 1. *Frequency wave number histogram of the fluctuations observed in DC discharge in cylindrical magnetron. From [2].*

Following the work by Martines et al. [1], who investigated fluctuations of magnetized plasma in planar magnetron we attempted to study fluctuations of DC discharge in cylindrical magnetron. We developed similar data acquisition system as described in [1] and performed extensive study over broad range of experimental conditions (argon pressure, magnetic field strength, discharge current). We investigated power density spectra as well as frequency-wave number histograms (dispersion properties). Sample of the latter data is given in Fig. 1. Within certain intervals of discharge parameters we found fluctuation "modes" as observed in [1], however, due to different geometry of our system the frequency of modes lay roughly one order of magnitude below those found in [1] - around 10 kHz. The phase velocity calculated from experimental data was, however, in the range of km/s, i.e. very similar to that found in [1]. The physical mechanism is therefore probably also the E×B/density gradient instability as described in [1]. Results of the investigations were published in [2].

The emissive probe has been developed in collaboration with the Innsbruck University, Austria. Principle based on direct heating of the probe wire loop by stabilized DC current was exploited. As the probe wire tungsten in diameters of 72 and 120 μm was used. The probe system consisted of GPIB controlled measuring instruments - power supply for heating, probe bias voltage supply and digital ammeter. Preliminary measurements of the plasma potential by the emissive probe were performed in the cylindrical magnetron system in DC discharge in argon, see Fig. 2.
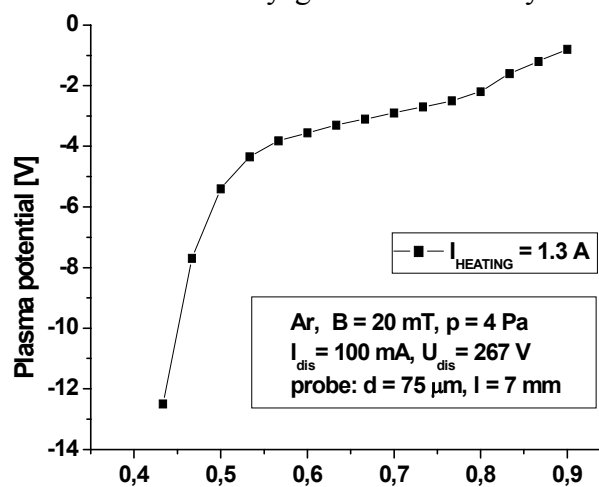
Fig. 2. *Radial profile of plasma potential obtained by emissive probe in magnetron.*

References:
[1] E. Martines, R. Cavazzana, G. Serianni, M. Spolaore, L. Tramontin, M. Zuin, V. Antoni, *Phys. of Plasmas* **8** (2001) 3042.
[2] O. Bilyk, P. Kudrna, M. Holík, A. Marek, M. Tichý, J.F. Behnke, Czech. J Phys. **54** (2004), Suppl. C, pp. C735-C741.

Multi-dimensional Codes for Particle Modelling in High-Temperature Plasmas

O. Barina, R. Hrach, J. Simek (FMP)

We studied methodology of self-consistent particle modelling of plasma-solid interaction in one and more dimensions. The study is based on the analysis of time requirements of principal parts of several algorithms used in the course of simulation. The programs analyzed were one-dimensional (*1d2v* and *1d3v*), two-dimensional (*2d3v*) a three-dimensional (*3d3v*), where *d* denotes spatial and *v* velocity coordinates, and they use different algorithms for force calculations and in molecular dynamics part of programs.

The particle simulation codes are extremely ineffective, especially in higher dimensions and in the presence of magnetic field. In order to prepare practically usable code for the simulation of probe diagnostics in high-temperature plasma, it is necessary to improve the performance of the model by optimizations of crucial subroutines that are the most time consuming [3], [4].
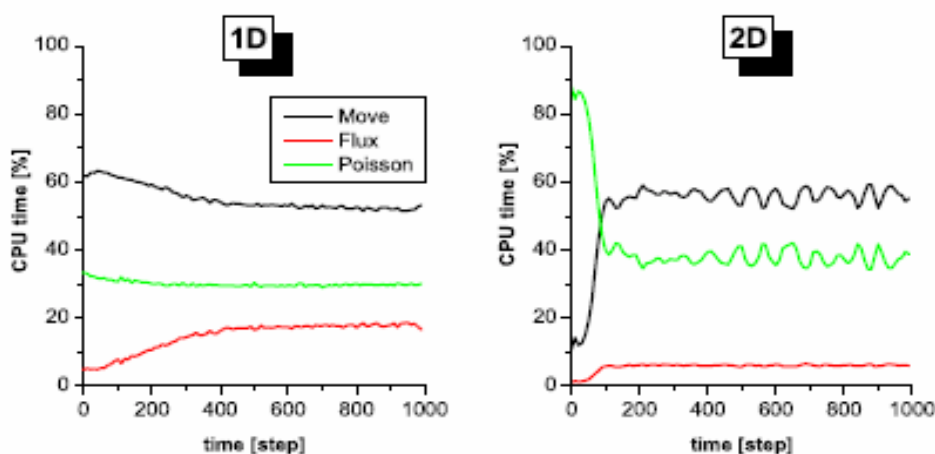

Fig. 1. *Time evolution of time requirements for one- and two-dimensional models.*

Main Results

Attention was devoted to three main parts of the model – source of particles (subroutine *Flux*), executing molecular dynamics part (subroutine *Move*) and force calculations (subroutine *Poisson*). From Fig. 1 [1] it can be seen, that while in 1D the time requirements of all three parts of program are equivalent, in 2D the influence of source of particles decreases. The same analysis performed in 3D proved, that the force calculation is the most time consuming part of the code (over 99 %). Therefore, in order to obtain practically usable code, this part of program must be optimized above all. First attempt to derive more efficient code in the presence magnetic field was made in [2] and the work continues with application of fast Fourier Transform on the problem of calculation of forces acting between charged particles in edge plasma of tokamak.

References:
[1] J. Simek, R. Hrach, O. Barina, Algorithms for Self-Consistent Particle Modelling in Plasmas, SPPT 2004, Prague, 2004.
[2] O. Barina, R. Hrach, J. Simek, Multi-dimensional Codes for Particle Modelling in Low-Temperature and High-Temperature Plasmas, Czech. J. Phys, Vol. 54 (2004), p.C654-C658.

3   Wave Interactions in Plasmas

Simulation of electron cyclotron emission and Bernstein modes
J. Preinhaelter, J. Urban, P. Pavlo

In collaboration with:
V. Shevchenko, M. Valovic, UKAEA, Culham, England
G. Taylor, L. Vahala, G. Vahala, NSTX, Princeton, USA

Simulations on MAST

We built, in cooperation with people from EURATOM/UKAEA Association, Culham, a code simulating the electron cyclotron emission (ECE) from spherical tokamak MAST. In order to interpret the experimental results, we have developed a realistic 3D model of the MAST plasma. The instantaneous magnetic field and its spatial derivatives are reconstructed by a 2D spline of two potentials determined by the EFIT equilibrium reconstruction code, assuming toroidal symmetry. Boundary problem of the wave propagation in cold collision plasma is solved by our finite element method with adaptive mesh. The absorbed power in UHR than represents the power of EBW to which the X-mode would be converted in warm plasma. To determine the radiative temperature we must study the propagation of EBW in 3D. For this purpose, we adopt the standard ray tracing. We found good agreement between the simulation of EBW emission and the detected signals for L-modes and ELMy H-modes. On the other hand the emission from ELM free H-modes in MAST suggests that the magnetic field in the transport barrier as determined by EFIT is too low. Typically the detected signal in the 16-60 GHz band has five peaks, each corresponding to the emission from subsequent electron cyclotron harmonics (see Fig. 1). The gaps between the peaks correspond to the frequencies at which the upper hybrid frequency coincides with some of the electron cyclotron harmonics. From the position of the gaps in the spectrum of the detected signal we can determine the magnitude of the magnetic field. The corresponding R position occurs where the upper hybrid frequency coincides with the frequency of the electron cyclotron harmonics (we investigate the shot where the detected signal originates in the equatorial plane). We assume that only the poloidal magnetic field is influenced at the transport barrier. The magnetic configuration in the rest of the plasma is assumed to be that determined by EFIT. So with the help of ECE simulation and the detected signal we can obtain some insight into the structure of the transport barrier.

Simulations on NSTX

One of the most important results deduced from EBW emission measurements on NSTX is the time development of the radiation plasma temperature. The obliquely viewing EBW radiometer on NSTX detects signals polarized parallel and perpendicular to the magnetic field at the EBW mode conversion layer. Since the outgoing O-mode at oblique incidence is approximately circularly polarized, the sum of these signals can be interpreted as a radiation temperature. We have performed simulations of the time development of ECE in interval $0.09s < t < 0.6s$. In Fig. 2, the time evolution of the sum of the EBW radiometer signals is plotted along with the maximum temperature detected by Thomson scattering (this independent measurement for $0.1s < t < 0.5s$ corresponds well to the temperature at $R = 1.007\,m$) and the theoretical simulation of EBW radiometer signals of Gaussian beams

corresponding to actual antenna orientation (angles $\phi_{dev} = 23.3\S$, $\phi_{long} = 31\S$) as well as to orientations that are optimal for $EBW - X - O$ mode conversion (angles $\phi_{dev} = 24.01\S$, $\phi_{long} = 24.89\S$). The signal is proportional to the central temperature only for $t > 0.3s$ when the plasma current and the poloidal magnetic field reach their stationary values. For $t < 0.3s$, EBW is emitted from the 2nd electron cyclotron harmonic at the plasma periphery, where the plasma temperature is low. The simulation shows that the conversion efficiency for EBW-X-O is optimal and practically constant for $t \in (0.2s, 05s)$. Simulations also clarify the relationship between the central temperature derived from the EBW signal and the temperature determined from Thomson scattering. We can state that the EBW temperature is always less than the actual temperature.

References:
[1] Preinhaelter J., Shevchenko V., Valovic M., Pavlo P., Vahala L., Vahala G., Urban J. and the MAST team, "ECE from MAST- Gaussian beams and antenna problem", Czech. J. Phys. 54, Suppl. C (2004), C116-C122
[2] Urban J., Preinhaelter J., "Adaptive finite elements method for the solution of the Maxwell equations in inhomogeneous magnetized plasma", Czech. J. Phys. 54, Suppl. C (2004), C109-C115
[3] Preinhaelter J., Urban J., Pavlo P., Shevchenko V., Valovic M., Vahala L., Vahala G., "Influence of antenna aiming on ECE in MAST", 15th Topical Conference on High Temperature Plasma Diagnostic, San Diego 19-22 April 2004. Review of Scientific Instruments 75 (2004) 3804
[4] Preinhaelter J., Shevchenko V., Valovic M., Wilson H., Urban J., Pavlo P., Vahala L., Vahala G., "The role of magnetic equilibria in determining ECE in MAST", 46th APS Meeting of Division of Plasma Physics, Savannah Nov 16-20, 2004, GA, USA, Bull. Am. Phys. Soc. 49, No.11 (2004)
[5] Preinhaelter J., Shevchenko V., Valovic M., Wilson H., Urban J., Pavlo P., Vahala L., Vahala G., and the MAST team, "The sensitivity of ECE simulations in MAST to different magnetic equilibria models", 31th EPS Conference on Contr. Fusion and Plasma Physics, London, UK, 28 June – 2 July, 2004, ECA Vol. 28G, P-4.184
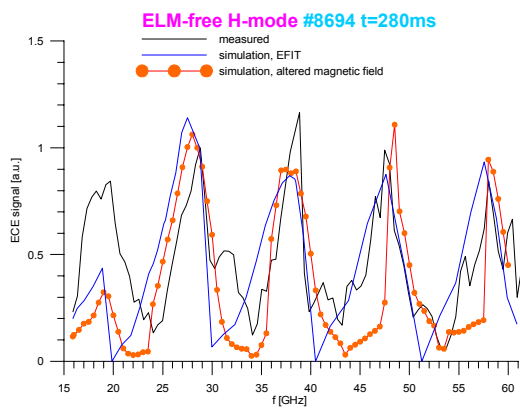
Fig. 1. *Comparison of the detected ECE signal and two simulations: EFIT magnetic equilibrium and the equilibrium with a bump in the magnetic field profile at the transport barrier.*
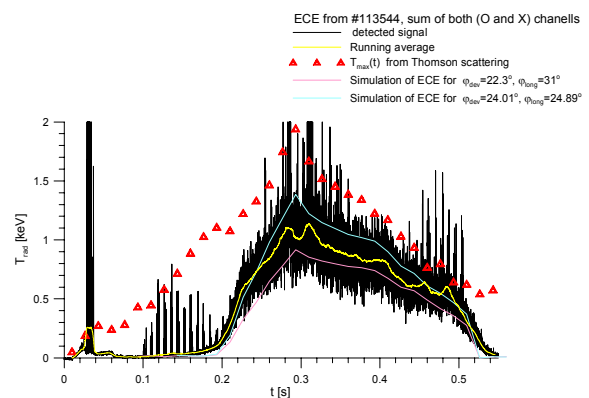
Fig. 2. *The time development of EBW signal (sum of O and X channels) detected by the NSTX antenna operating at 16.5 GHz. #113544.*

Effect of lower hybrid grill electric field on tokamak edge plasma
V. Fuchs, V. Petržílka, L. Krlín

In collaboration with:
J.P. Gunn, M. Goniche, P. Devynck, Association Euratom/CEA, Cadarache, France
K.M. Rantamäki, Association Euratom/TEKES, Helsinki, Finland

The principal activity in 2004 was the theoretical and numerical study of the behaviour of electrons and ions flowing along magnetic field lines near a lower hybrid antenna. The Landau interaction of electrons resonant with the grill spectrum [1] is the cause of all other related plasma effects, particularly then of the self-consistent ion response via the generated space charge [2]. Incorporating the ion dynamics requires a self-consistent description of the antenna-plasma interaction. We opted for a numerical treatment using a particle-in-cell (PIC) code. The simulation proceeds on the ion transit time along the simulation region which is of the order of meters. Since the plasma edge Debye length is of the order of 10^{-5} m, and the electron plasma frequency is of the order of the LH frequency, 3.7 GHZ, the simulation problem even in one dimension is enormous. We therefore developed a quasi-neutral PIC code (QPIC), where the self-consistent electric field is determined from the electron fluid momentum equation rather than from the Poisson equation. First results from the code were reported in [3]. As expected, electrons are strongly heated along the grill while experiencing a density depression. The ions without volumetric sources react very weakly. Quasi-neutrality is maintained throughout very well. There is excellent agreement with PIC code results while the QPIC calculation is about 2 orders of magnitude faster. A particular problem we had to deal with is developing a suitable accurate, simple and stable integration method of particle equations of motion for velocity dependent forces [4]. Furthermore, we participated in the preparation and planning of experiments on LH – generated fast particles in Tore Supra and JET [5-7]. Finally, we initiated work on incorporating wall effects in QPIC [8].

References:
[1] V. Fuchs, J.P. Gunn, M. Goniche, V. Petržílka, *Tokamak edge electron diffusion and distribution function in the lower hybrid electric field*, Nucl. Fusion **43** (2003) 341.
[2] V. Petržílka, V. Fuchs, M. Goniche, J.P. Gunn, R. Klíma, et al., *Electron acceleration in front of LH grills and ensuing plasma flows, density perturbations and charge separation fields*, 29th EPS Conf. On Control. Fusion and Plasma Phys. (Montreux, 17-21 June 2002).
[3] V. Fuchs, J.P. Gunn, V. Petržílka, M. Goniche , *Quasineutral simulations of plasma response to the lower hybrid antenna electric field,* 31st EPS Conf. on Contr. Fusion and Plasma Physics, London, 28 June–2 July, 2004.
[4] V. Fuchs and J.P. Gunn, *Numerical stability of 2ⁿᵈ order Runge-Kutta integration algorithms for use in particle-in-cell codes*, Czech J. Phys. **54**, 2004, Suppl. C, C100.
[5] K.M. Rantamäki, V. Petržílka, V. Fuchs, F. Žáček et al, *Bright spots generated by lower hybrid waves on JET*, submitted to Plasma Physics Controlled Fusion.
[6] M. Goniche, V. Petržílka, P. Devynck, J.P. Gunn, et al, *Exploration of fast particle generation and density fluctuations in front of the lower hybrid grill,* 31st EPS Conf. on Contr. Fusion and Plasma Physics, London, 28 June–2 July, 2004.
[7] V. Petržílka, V. Fuchs, M. Goniche, L. Krlín and F. Žáček, *Modelling of the effects of Random fields in front of LH grills on the local fast particle production,* 31st EPS Conf. on Contr. Fusion and Plasma Physics, London, 28 June–2 July, 2004.
[8] J.P. Gunn and V. Fuchs, *Simulations of LH-generated fast particles in the tokamak scrape-off layer,* Workshop on LH generated fast particles, IPP Prague, 16-17 Dec., 2004.

Nonlinear Effects in Front of LH Grills – Numerical Modelling

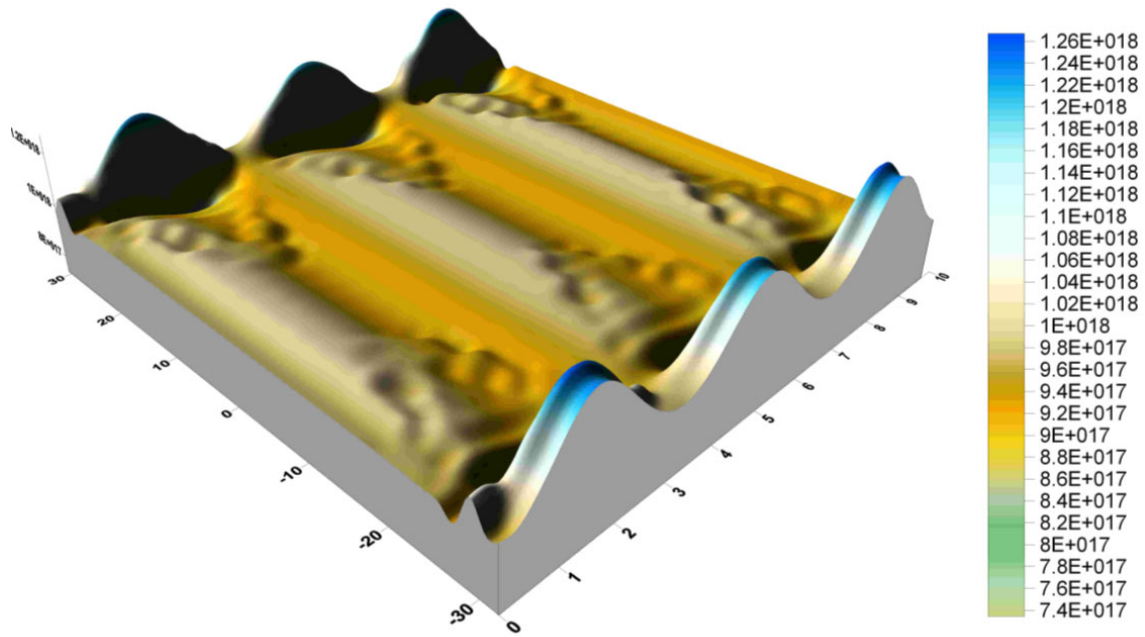*V. Fuchs, L. Krlín, V. Petržílka, F. Žáček*

In collaboration with:

M. Goniche, P. Devynck, J. Gunn, J. Achard, E. Gauthier, A. Ekedahl, J.Y. Pascal, Association Euratom-CEA Cadarache, France

We further developed [1] our theoretical model of the self-consistent dynamic LH wave-plasma interaction in front of LH grills. In order to assess the predictive capability of our 3-d two fluid numerical code, a more detailed numerical study of the dependence of the nonlinear development of the plasma density in front of the LH grill (which determines the LH wave reflection coefficient R), including the study of the poloidal, toroidal and radial dependence, was undertaken. For this, we prepared an advanced version of our 3-d numerical two-fluid code. We concentrated on the LH power dependence of the vortex in front of the grill (the plasma density of the vortex determines the reflection coefficient R) and on the dependence of the vortex on the plasma sources in front of the grill. A typical profile of the plasma density given by the numerical simulations is illustrated in Fig. 1., which shows the plasma density just in front of three wave-guide rows for the case of low LH power density and low plasma sources. Efforts were undertaken to optimize the profile of the expelling force arising due to electron acceleration, in order to amend the stability of computational runs, and in order to obtain the density profiles growing with the power in the middle of the wave-guide rows, and decreasing near the row boundaries. A density profile of this form agrees with the experimental measurements of the reflection coefficient R, which show growing R with the LH power at the wave-guide row boundaries, and decreasing R for the central modules of the row. These results will be also part of our future publication.

We also modelled random field effects using random fields values based on recent tokamak CASTOR measurements [2]. It is well known that thermal electrons can be accelerated in front of a lower hybrid (LH) wave-guide array by the electric field of the slow LH wave. They may cause high thermal loads and erosion observed on parts of the grill and tokamak vessel. This generation of fast electrons in front of LH frequency antennas is known to be caused by Landau damping of high $N_{//}$ components of the launched spectrum. Therefore, advanced LH wave launchers, like the PAM launcher for ITER, are being developed to reduce the energy contained in the high $N_{//}$ components. However, according to theoretical estimates, the electron acceleration in front of the grill may be significantly enhanced by random fields spontaneously generated near the antenna. Therefore, we explored fast electron generation in front of LH grills, taking into account presence of random fields. The model of random fields is based on recent measurements of fluctuating toroidal electric fields in front of the CASTOR tokamak LH grill mouth. In each numerical experiment, five thousand of test electrons are injected in front of the grill, and their trajectories are computed. The content of high $N_{//}$ components in the LH spectrum is varied in the numerical model. Using a random field representation in agreement with the CASTOR measurements, we demonstrate that the enhancement of electron acceleration by the random fluctuating fields can lead to a significantly high fast particle production, even if the content of high $N_{//}$ components in the LH grill spectrum is low, Fig. 2. The higher spatial harmonics $N_{//}$ of the launched LH wave field are artificially reduced in the computations by the parameter "reduce", while keeping the LH wave energy density constant.

[1] V. Petržílka, V. Fuchs, M. Goniche, L. Krlín, and F. Žáček, 31th EPS Conference, London, June 2004, P-1.41.

[2] M. Goniche, V. Petržílka, P. Devynck, J. Gunn, F. Žáček, J. Achard, E. Gauthier, A. Ekedahl, V. Fuchs , J.Y. Pascal, 31th EPS Conference, London, June 2004, P-4.110.

Fig. 1. *Dependence of the plasma density in front of three wave-guide rows of a LH grill launcher, the parameters correspond to the Tore Supra C3 launcher.*
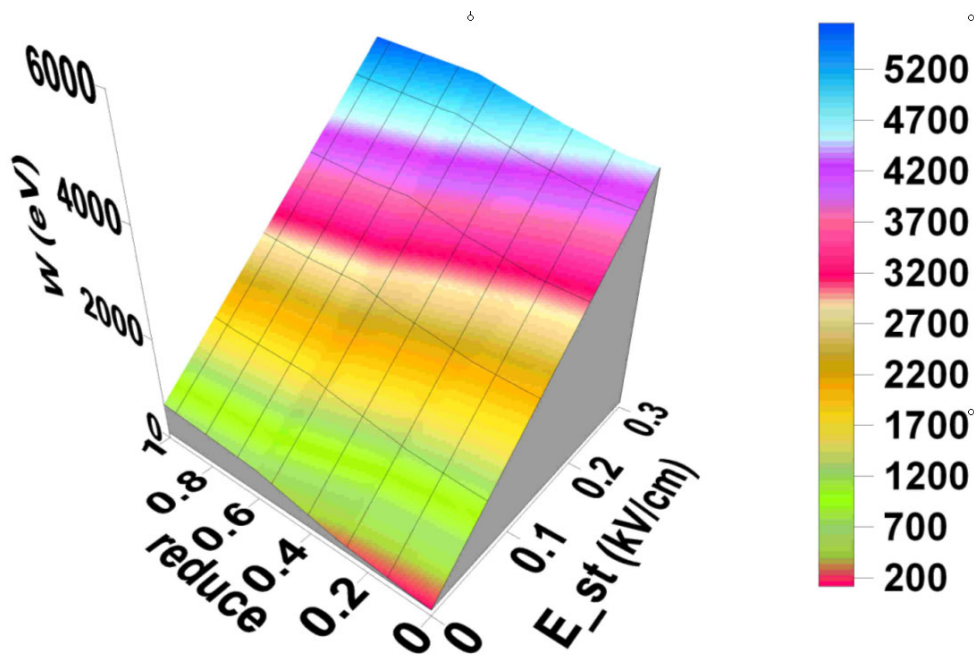
Fig. 2. *The maximum accelerated electron energy W (eV) as a function of the parameter "reduce" and as a function of the varying random field amplitudes E_{st} .*

# RF Probe and RFA Measurements in LHCD Tore Supra Experiments
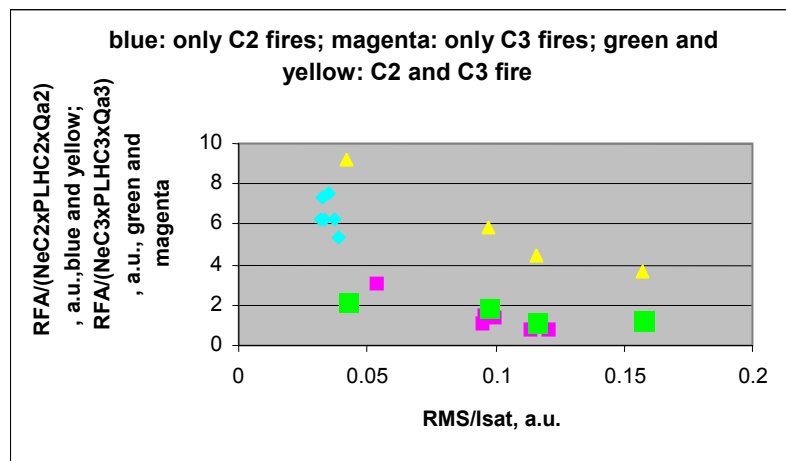
V. Petržílka, F. Žáček

In collaboration with:
M. Goniche, P.Devynck, J. Gunn, J. Achard, E. Gauthier, A. Ekedahl, J.Y. Pascal, A. Ekedahl, Association Euratom-CEA Cadarache, France

New low safety factor q value Lower Hybrid Current Drive (LHCD) Tore Supra experiments, enlarged the turbulence measurement database by RF (Radio Frequency) probe by RF probe, mounted on the grill for the purpose of these measurements, and magnetically connected to the locations in front of an active LH C3 grill wave-guide row. For the first time, a second RF probe mounted on the grill (unconnected) was operational, too. The fast acquisition system of the RF probes was again used, and we continued our study of the intensity of the fast particle generation, of the thermal loads due to fast particle effects and, in the same time, of the turbulence level. In Fig. 1, the normalized RMS of the saturation currents of probes 1 (unconnected – magenta) and 2 (connected – green) are plotted. The decrease of the fluctuation level in the connected probe is clearly seen. According to our numerical modelling, this decrease may be due to the additional fast particle generation by fluctuation energy absorption by the fast particles. The probe 2 begins to be connected for the safety factor Qpsi less than about 3.9. For larger Qpsi, when both probes are unconnected, the difference in the normalized RMS is probably due to the different gains in the electronic channels 1 and 2. Therefore, the RMS values can be further normalized, by shifting the magenta curve (and points), as indicated by the red arrow. Because of the dependence of the signal on the plasma density in front of the launchers, and namely on the safety factor q, there is a large dispersion in the measured signal plotted as a function of the LH power. RFA (Retarding Field Analyzer) data were analyzed in another series of shots (with shot numbers between # 31252 and #31291), when the beam of the fast particles from the C2 and C3 launchers was directed into the slit of the RFA. In this case, the q value was larger than in the RF probe measurements just described, and both RF probes mounted at the top of the C3 launcher were unconnected. The RFA was set in order to collect electrons with energy larger than 100eV, and it was reciprocated in ~250ms up to 1cm behind the last closed flux surface. The spatial resolution (~ 5mm) allows to assess that the radial width of the collected fast electron beam is less than 1 cm. To evaluate the measurements, we ascribed to each shot a number called "quality of area connection" between zero and one, Qa2 or Qa3, according to how much of the wave-guide row area of the launcher C2 and C3 is accelerating the particles. Then we were able to normalize the RFA signal to the LH power, to the plasma density and to the "connection quality". Fig. 2 shows the dependence of the RFA signal on the fluctuations intensity as given by the RMS of the RF probe saturation current Isat. It can be seen that the normalized number of the accelerated electrons (given by the normalized RFA signal) is lower, when the fluctuation level in locations magnetically connected to the waveguide rows is higher. This could indicate dissipation of the random fields by accelerated particles. However, it is difficult to assess the role of fluctuations in the acceleration process, as the fluctuation level depends in turn on the LH power, Fig. 3. As it is demonstrated in Fig. 3, there are no shots with significantly different fluctuation level, but with about the same LH power. For several shots, when only one of the LH launchers fires, we also evaluated the temperature variations of the C2 LH grill guard limiter as a function of the LH power. The temperature of the guard limiter grows with the power, even if the normalized (to power) number of the fast particles decreases with the power.

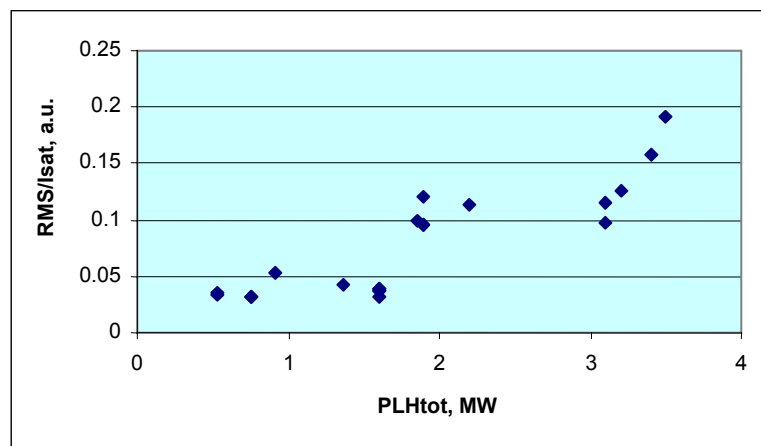[1] M. Goniche, V. Petržílka, P. Devynck, J. Gunn, F. Žácek, J. Achard, E. Gauthier, A. Ekedahl, V. Fuchs , J.Y. Pascal, 31th EPS Conference, London, June 2004, P-4.110.
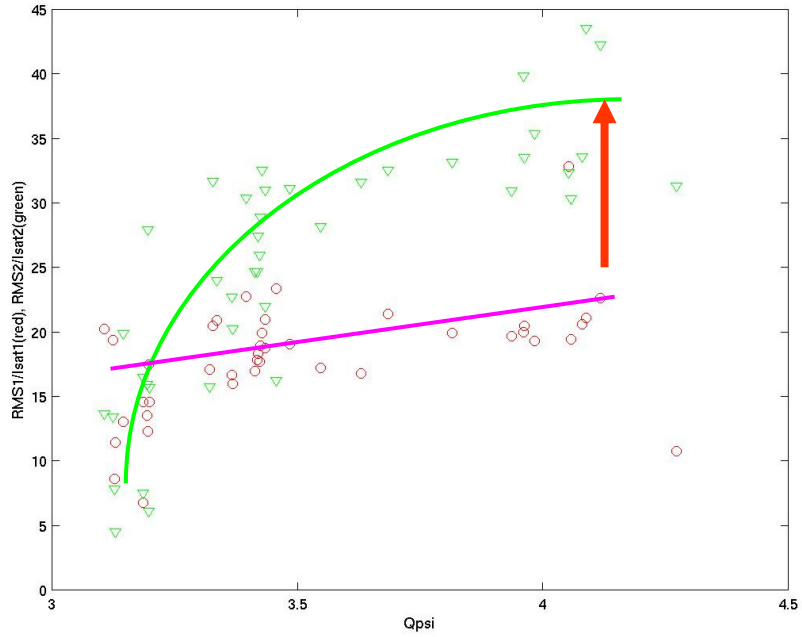
Fig. 1. *Normalized RMS, in dependence on the safety factor Qpsi.*

Fig. 2. *Normalized RFA signal in dependence on the intensity of fluctuations.*

Fig. 3. *Dependence of the fluctuation level on the LH power*

Positive biasing of plasma in front of LH antennas

F. Žáček, V. Petržílka

In collaboration with:
M. Goniche, Association Euratom/CEA, Cadarache, France

New experimental data, concerning the character of the interaction between the LHW and the plasma periphery in front of the LH antennas, have been obtained by using cold and emissive Langmuir probes [1]. The results of the measurements can be summarized as follows:

1. The measurements with the non-emissive cold probe confirmed the formation of a "well" on the profile of floating potential during LH discharge phase, observed already on CASTOR tokamak before [2] and explained by the existence of a group of electrons accelerated to the corresponding supra-thermal energies.

2. The radial width of this "well" is less than 4 mm, and its minimum is localized about 2 mm in front of the grill mouth.

3. On the other hand, the floating potential of the probe heated to the temperature over $2500^{o}C$ (i.e. when the probe becomes to be emissive) exhibits near to the grill an expressive   increase, if the LHW is applied.

4. This increase of the emissive probe floating potential is localized still closer to the grill mouth than the "well" of the cold probe floating potential. It starts to be observable at a distance 2-3 mm from the grill and it increases till the grill mouth itself.

5. If we consider this measured potential to be the plasma potential, a strong radial electric field of nearly 30 kV/m will appear in this radially very narrow layer just in front of the CASTOR grill at the LHW power 20 kW. The shear velocity layer, formed under such electric field, can result in substantial changes in the transport coefficients in this region due to the **ExB** drifts (improvement of the global particle confinement is routinely observed in CASTOR during LHW application, see [3]).

6. The dependence of the effect on the LHW power, characterized as the difference of the floating potentials of the heated and of the cold probe in the LH and OH plasmas, seems to have a linear character, i.e. still much higher radial electric fields can be expected in front of antennas launching the power up to several MW.

The results obtained can be considered as a direct experimental confirmation of the presence of the locally accelerated electrons in front of LH antennas, already predicted by the theory [4]. The escape of these electrons along the magnetic field lines results in the positive plasma biasing with a possible successive acceleration of plasma ions by the positive charge of the Coulomb separation. These ions might then contribute to the observed erosion of the parts of the first tokamak wall, connected directly by magnetic field lines with the interaction region in front of the LH antenna (as observed already in tokamaks with the LH power of the MW order, where the energy of accelerated particles can reach values up to several keV).

References:

[1] F. Zacek, V. Petrzilka, J. Adamek, M. Goniche, *Positive plasma biasing in front of the LH grill of CASTOR tokamak*, 12th International Congress on Plasma Physics, P1-70, 2004, Nice, France.

[2] F. Zacek et al., Toroidal electric field in front of the lower hybrid grill of the CASTOR tokamak, 30th EPS Conf. on CFPP, St. Petersburg 2003, ECA Vol. **27A**, P-1.196

[3] F. Zacek et al. 2001, Plasma edge biasing on CASTOR tokamak using LHCD, Czech. J. Phys. **51** (2001) 1129-1138

[4] V. Fuchs et al., Acceleration of electrons in the vicinity of a lower hybrid waveguide array, Phys. Plasmas **3** (1996) 4023

4 Atomic Physics and Data for Edge Plasma and Plasma–Wall Interactions

Spectroscopy and temperature diagnostics of H_3^+

R. Plašil, J. Glosík, M.Tichý, P. Kudrna

In collaboration with:
J. Mikosch, R. Wester, Physikalisches Institut, Universitat Freiburg, Germany
D. Schwalm, A. Wolf, H. Kreckel,max-Planck-Institut fuer Kernphysik, Heidelberg, Germany
D. Gerlich, Institut fuer Physik, Technische Universitat Chemnitz, Germany
G. Bano, Res. Inst. for Solid State Phys. and Optics, Budapest, Hungary
P. Macko, Comenius University, Bratislava, Slovensko

Abstract
Spectroscopy and temperature diagnostics of H_3^+ using cavity ring-down IR absorption spectroscopy and laser induce reactions technique.

Experiments
We have build new cavity ring-down spectrometer (CRDS) with IR diode laser to study absorption of $H_3^+(v=0)$ ions in hydrogen containing plasma. The new system was first tested on residual H_2O vapours remaining in the discharge chamber and data taken from the HITRAN 96 database were used to calibrate the laser wavelength and lambdameter, then the discharge tube was filled with high purity hydrogen and absorption spectra of $H_3^+(v=0)$ was measured. The experimental set-up is given in Fig 1. Example of obtained absorption line together with traces of H_2O line is plotted in Fig. 2.

Results and Discussion
The recombination of spectroscopically identified $H_3^+(v=0)$ ions with thermal electrons has been studied in pulsed afterglow plasma by means of IR CRDS. Time -resolved measurements of the $H_3^+(v=0)$ ions density were carried out in helium buffer gas with a small admixture of argon and hydrogen to optimize the kinetics of the formation of $H_3^+(v=0)$ ions. The CRDS signal was monitored as a function of time during the discharge afterglow. Since the absorption cross-section is known, the decay of $H_3^+(v=0)$ ions density and hence, the recombination coefficient can be deduced. At hydrogen number density $[H_2] = 1\times10^{14}$ to 8×10^{14} cm^{-3} the measured recombination rate was found to be $\alpha = (1.6\pm0.6) \times10^{-7}$ cm^{3}s^{-1}. Our experiments clearly demonstrate the feasibility of observing the concentration of $H_3^+(v=0)$ ions in rapidly decaying plasma by the cavity ring-down technique. Details of our study are given in our recent publication [1]. We have started similar studies of $D_3^+(v=0)$ ions in deuterium containing plasma [2].

Obtained spectra of $H_3^+(v=0)$ ions were used to characterize an ion source for test storage ring in Heidelberg (TSR). In the ion source, ions are trapped by combination of RF and electrostatic field in the ion trap and they are cooled by collisions with buffer gas atoms. The ions are injected to the acceleration segment and than to the storage ring after the cooling. The STR is used to study recombination of ions with electrons. In this experiment IR absorption spectroscopy was used in combination with laser induce reactions with argon atoms (LIR) technique to measure effective translational and rotational temperature of stored

ions. Obtained spectrum is plotted in Fig. 3. Details of this study are given in our recent publication [3].

References:

[1] P. Macko, G. Bánó, P. Hlavenka, R. Plašil, V. Poterya, A. Pysanenko, O. Votava, R. Johnsen, J. Glosík, Afterglow studies of $H_3^+(v=0)$ recombination using time resolved cw-diode laser cavity ring-down spectroscopy, International J. Mass Spectrometry, 233 (1-3) (2004) 299-304.

[2] P. Hlavenka, P. Macko, G. Bánó, R. Plašil, A. Pysanenko and J. Glosík: The D_3^+ Second Overtone Absorption Spectra in Near-IR Region Using cw-Cavity Ring-Down Spectroscopy, 4th Cavity Ring Down User Meeting, Heeza, The Nederland 7th and 8th of October 2004, (2004) abstract pp17.

[3] J. Mikosch, H. Kreckel, R. Wester, R. Plašil, J. Glosík, D. Gerlich, D. Schwalm, A. Wolf: Action spectroscopy and temperature diagnostics of H_3^+ by chemical probing, J. Chem. Phys., Vol. 121, No 22, December 2004.
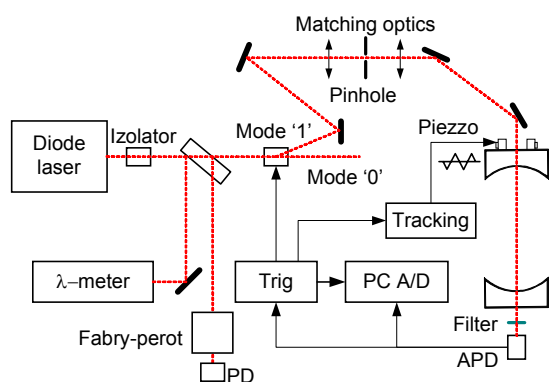
Fig. 1. *The experimental set-up.*
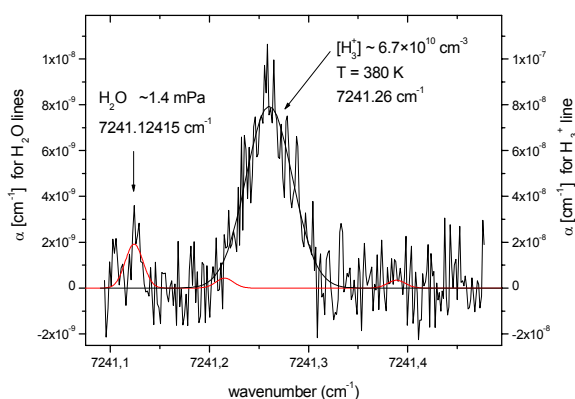
Fig. 2. *The absorption spectra of $H_3^+(v=0)$ obtained in a continuous microwave discharge in He with admixture of hydrogen.*
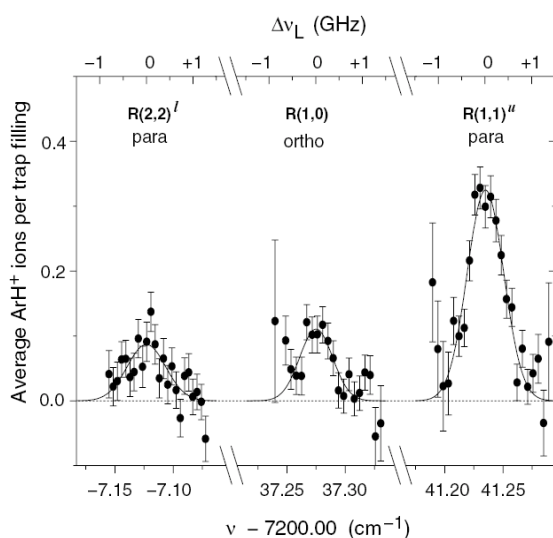
Fig. 3. *Measured absorption profiles for the three observed transitions in the $(0,3^1)\leftarrow(0,0^0)$ vibrational overtone band. The employed chemical probing technique yields an ArH^+ ion per absorbed infrared photon. The signal is derived by averaging over 500 trap fillings, interleaved by 500 background measurements. The absolute accuracy of the frequency scale is ±0.017 cm^{-1}.*

Collisions of slow hydrocarbon ions $C_3H_n^+$ and $C_3D_n^+$ (n=2-8) with room temperature carbon surfaces

Z. Herman, J. Žabka, A. Pysanenko

In collaboration with

T. D. Märk, L. Feketeová, Association EURATOM-ÖAW, Innsbruck, Austria

In response to a recent quest for data on interaction of molecular ionic species in collisions with surfaces of relevance to fusion devices, we started earlier a series of scattering experiments on collisions of slow (10-50 eV) simple diatomic and polyatomic ions with carbon surfaces. Ion-surface collisions can provide important information relevant to plasma-wall interactions in electrical discharges and fusion systems [1]. In fusion devices carbon is widely used as the material exposed to plasma and the outcome of collisions between ions and carbon surfaces is of considerable interest.

The experimental method used is the recently developed scattering method, in which the projectile ion reactant beam of a well-specified incident energy is directed under a pre-determined angle towards a carbon surface, and mass spectra of product ions as well as translational and angular distributions of the product ions are measured. The data offer information on ion survival probability of the projectile ions in ion-surface collisions, on surface-induced dissociation processes and on chemical reactions with the surface material. The data can also serve in determining the mechanism of reactions at surfaces, to elucidate energy transfer in collisions with surfaces, the extent of inelasticity of the collisions and the degree of incident-to-internal energy transfer for ions of increasing complexity. The surface used in these experiments was a sample of highly oriented pyrolytic carbon (HOPG), shown earlier to behave very similarly as samples of tokamak carbon bricks [2]. This surfaces could be studied either at room temperature, when it was covered -as shown earlier- by a layer of hydrocarbons, or at a temperature of about 1000 K, when this hydrocarbon layer was effectively removed [3,4].

In this part we report on the ion-surface interactions of polyatomic hydrocarbon ions $C_3X_n^+$ (X=H, D; n = 2-8) and thus we complement our earlier studies in which simpler hydrocarbon projectile ions CX_n^+ and $C_2X_n^+$ were investigated [3,4]. We report here on results of collisions with room temperature HOPG surfaces.

Mass Spectra of product ions.

Collisions of projectile ions $C_3H_8^+$, $C_3H_7^+$, $C_3H_6^+$, $C_3H_5^+$ $C_3H_4^+$, $C_3H_3^+$, $C_3H_2^+$ and their deuterated variants $C_3D_8^+$, $C_3D_7^+$, $C_3D_6^+$, $C_3D_5^+$ of energies 14.6 − 46.6 eV with room-temperature (covered by hydrocarbons) carbon (highly-oriented pyrolytic graphite) surfaces were studied using the scattering method. In these projectiles, ions of different structures may exist. Nevertheless, mass spectra of product ions do not indicate major differences in fragmentation patterns that would point clearly to different is $C_3H_n^+$ projectile ions. All minor differences observed could be related to a different initial internal energy content of the projectiles. The spectra show, as expected, an increasing extent of fragmentation with increasing incident energy of the projectiles (Fig. 1, results for $C_3H_8^+$ and $C_3H_7^+$).

Chemical reactions at surfaces.

The radical cations (e.g., $C_3H_8^+$, $C_3H_6^+$, $C_3H_4^+$) show a certain tendency to form protonated projectiles in H-transfer processes with the hydrocarbons on the surface and their mass spectra are then an overlap of fragmentation of the projectile and protonated projectile. However, the tendency to form protonated projectiles (as judged from the presence of H-containing fragments after an impact of fully deuterated projectile ions) seems to be substantially smaller than with $C_2H_n^+$ and CH_n^+ radical ion projectiles studied earlier [3,4]. Also, chemical reactions of carbon chain build-up, observed earlier with CH_n^+ (formation of C_2-hydrocarbons) and $C_2H_n^+$ (formation of C_3-hydrocarbons) in reactions with the surface

hydrocarbons, appears to be significantly less probable. In fact, no measurable amounts of C_4-hydrocarbons, formed in putative reactions of $C_3H_n^+$ projectile ions with the surface hydrocarbons could be detected.

Ion survival probability.

Data on absolute survival probability of $C_3H_n^+$ ions (i.e. sum of intensities of all product ions leaving the surface to intensity of projectile ions striking the surface in %) show that there is some difference between the radical cation projectiles and the closed shell ions: the survival probability of radical cations is close to 1% or somewhat below it, while for the closed shell ions it is 3-9 % at collision energies 15-46 eV and the incident angle of 30^0 with respect to the surface. The difference between these two types of ions persists, but it is smaller than observed for the earlier studied $C_2H_n^+$ and CH_n^+ projectile ions [3,4]. Because the survival probability of closed-shell ions remains approximately the same, the decreasing difference is due the increasing survival probability of the radical cations. This in turn may be connected with the decreasing recombination energy of the larger polyatomic hydrocarbon cations.

Translational energy and angular distributions of product ions.

 Preliminary results on translational energy distributions of product ions show, similarly as in the earlier studies, that the collision of C_3-hydrocarbon ions with carbon surfaces covered with hydrocarbons are inelastic. The product ions dissociate in the unimolecular way (the velocity distributions of the scattered projectile ion and of the so far measured fragment ions formed from it peak at the same velocity) after the interaction with the surface and their equivalent kinetic energy is about 45-50% of the energy of the incident projectile ion. Angular distributions of the scattered product ions are very similar: they peak at this incident angle (30^0) at a slightly sub-specular scattering angle (about 20^0 with respect to the surface) and the angular width of the distributions is $18-19^0$ (full width at half maximum). Further measurements of these parameters are under way.

References

[1] Hofer, W.O.; Roth, J. Eds. *Physical Processes of the Interaction of Fusion Plasmas with Solids;* Academic Press, San Diego, CA, 1996.

[2] J. Žabka, Z. Dolejšek, J. Roithová, V. Grill, T.D. Märk, Z. Herman, Int. J. Mass Spectrom. 213 (2002) 145.

[3] J. Roithová, J. Žabka, Z. Dolejšek, Z. Herman, J. Phys. Chem. B, 106 (2002) 8293-8301.

[4] J. Jašík, J. Žabka, L. Feketeová, I. Ipolyi, T.D. Märk, Z. Herman, J. Phys. Chem. A (prepared for submission)

Figure 1: *Mass spectra of product ions from collisions of the projectiles $C_3H_8^+$ and $C_3H_7^+$ at three different collision energies*
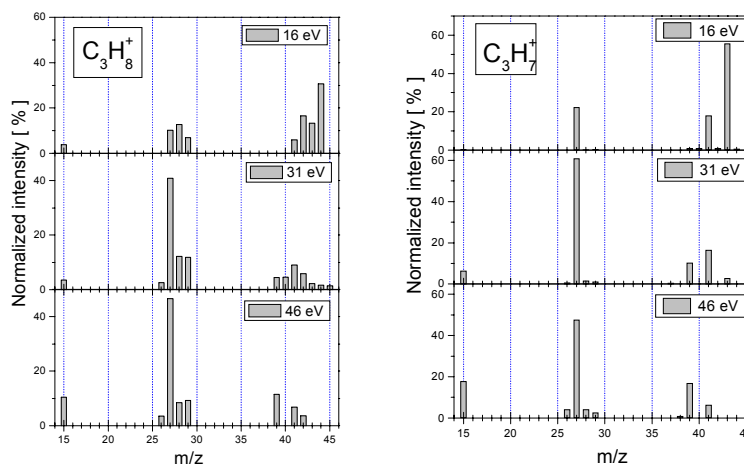
5   JET Collaboration

First Results of Minimum Fisher Regularisation as Unfolding Method in JET Neutron Spectrometry
J. Mlynář

In collaboration with:

J.F. Adams, Association EURATOM-UKAEA Fusion, Culham Science Centre, Abingdon, Oxfordshire, OX14 3DB, UK

L. Bertalot, Association EURATOM-ENEA sulla Fusione, Frascati, C.P. 65, 00044-Frascati, Italy

S. Conroy, Association EURATOM-VR, Uppsala University, SE-751 05 Uppsala, Sweden

and EFDA-JET contributors

Introduction
At JET, the NE213 liquid scintillator is being validated as a diagnostic tool for spectral measurements of neutrons emitted from the plasma. Neutron spectra have to be unfolded from the measured pulse-height spectra, which is an ill-conditioned problem. Therefore, use of two independent unfolding methods allows far less ambiguity on the interpretation of the data. In parallel to the routine algorithm MAXED based on the Maximum Entropy method, the Minimum Fisher Regularisation (MFR) method has been introduced at JET [1].

Advantages of MFR
The algorithm, modified from its 2D SXR tomography version [2], [3], provides solution to the 1D inversion task of spectra deconvolution in a simple form of a matrix. One time-averaged matrix can be, in principle, applied to a set of similar data (e.g. on time evolution). The individual terms of residual misfit can help to determine corrupted spectral channels or elements in the response matrix. Being fully based on matrix operations, MFR is relatively rapid. Last, but not least, the Minimum Fisher information provides a solution with the highest variance within the expected data error bars.

First results and conclusions
An example of the first results is in the figures below, which show neutron data from a JET discharge from Trace Tritium Experiment with 1.4 MW ICRH Tritium minority heating. Fig. 1 shows data (pulse height light spectrum) and the retrofit of the reconstructed neutron spectrum, Fig. 2 shows the reconstructed neutron spectrum for two slightly different response functions, and the expected position and shape of the D-T peak. The FWHM of 2 MeV corresponds to the expected values due to ICRH heating and agrees with the MAXED reconstruction.

MFR proved to be an efficient method in 1D spectra unfolding. MFR validated MAXED results within expected errors, namely it confirmed high energies of alpha particles accelerated by ICRH, see [1]. The significant role of detailed knowledge of the response matrix has been demonstrated. In suppressing the artefacts, energy shifts and other systematic errors the primary challenge is now in consolidating the response matrix, while ambiguities in

the unfolding procedure will play secondary role. The MFR method, thanks to its transparency, can help in tracing these systematic errors.

In future it is desirable to implement in MFR an automated procedure for finding the optimal smoothing level, probably based on the L-curve method [4]. Following this, it can be used for a routine post-discharge spectra unfolding at JET.

References:

[1] Mlynář J., Adams J., Bertalot L., Conroy S.: First Results of Minimum Fisher Regularisation as Unfolding Method in JET Neutron Spectrometry. . 23rd Symposium on Fusion Technology, Venice, Sep 20-24, 2004, Fusion Engineering and Design, in press

[2] M. Anton et al., X-ray tomography on the TCV tokamak, Plasma Phys. Control. Fusion 38 (1996) 1849-1878.

[3] J. Mlynar et al., Investigation of the consistency of magnetic and soft x-ray plasma position (...), Plasma Phys. Control. Fusion 45 (2003) 169-180

[4] P.C. Hansen, Numerical tools for analysis and solution of Fredholm integral equations of the first kind, Inverse Problems 8 (1992) 849-872
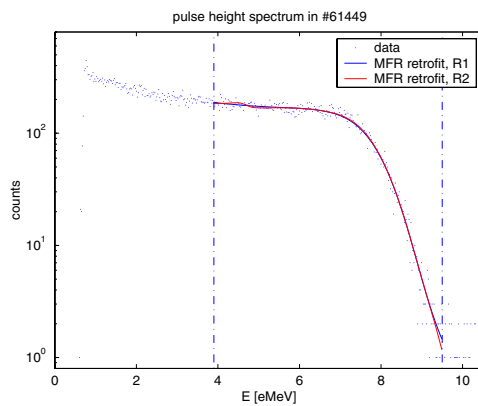
Fig. 1. *Pulse height spectrum from NE213.*
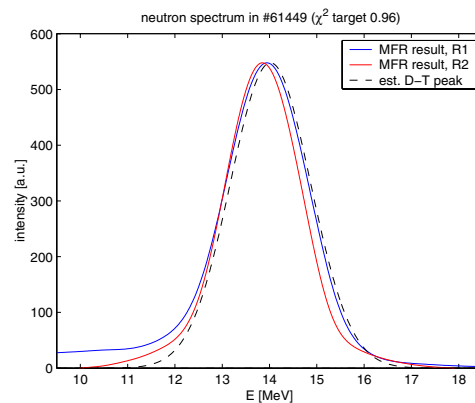
Fig. 2. *MFR reconstructed neutron spectrum.*

III TECHNOLOGY

1 Technology Tasks

OVERVIEW OF TECHNOLOGY TASKS

Most of the technology tasks within Association EURATOM/IPP.CR deal with study of tritium breeding and properties of various diagnostic and structural elements of future thermonuclear reactors, before and under neutron irradiation. For this purpose two irradiation sites are utilized: light water experimental fission reactor LVR-15 (operated by NRI plc), and the isochronous cyclotron U-120M with the maximum proton energy of 37 MeV (operated by NPI ASCR). Both devices are located in Řež about 20 km from Prague and they are integrated within the Association EURATOM/IPP.CR.

The structure of the technology research of the Association EURATOM/IPP.CR is following:

Contracts under Article 5.1a:

- **Tritium Breeding and Materials**
    - ❖ **Breeding Blanket** (1 task, 1 deliverable)
    - ❖ **Materials Development** (5 tasks, 7 deliverables)
- **Vessel/In Vessel**
    - ❖ **Blanket** (1 task, 1 deliverable)

Contracts under Article 5.1b:

- **Vessel/In Vessel**
    - ❖ **Blanket** (1 task)
- **Physics Integration**
    - ❖ **TPD Diagnostics** (sub-contractor of 1 task)

Generally, the technology programme in Association EURATOM/IPP.CR continued in 2004 along the same lines as in previous periods with the total effort of 14 ppy and 900 kEuro. The specific feature of this year was a delivery of several tasks that were delayed due to severe flooding of the NRI and NPI sites in Řež in August 2002. The recovery lasted approximately till mid-2003 and as a result, progress in many technology tasks was slowed down significantly.

1. Tritium Breeding and Materials: Breeding Blanket

Task TW2-TTBC-004 - Helium Cooled Lithium Lead: Processes and Components
(coordinated by NRI Řež; staff: M.Zmítko, P.Hájek, K.Šplíchal, P.Vachtfeidl, V.Richter)

<u>Deliverable 4</u>: Pb-17Li Auxiliary and purification systems.

> 4a: Design of the Auxiliary PbLi loop
> 4b: Design of the Purification system of PbLi (e.g. from Bi) and evaluation of impact on Po production

Status: delivered, see page 48 for more details.

2. Tritium Breeding and Materials: Materials Development

Task TW2-TTMS-001b - RAFM Steels: Irradiation Performance
(coordinated by NRI Řež; staff: P.Novosad, K.Šplíchal, W.Soukupová)
<u>Deliverable 3</u>: Static and dynamic toughness testing at the transition temperature. Neutron irradiation of plates and weldments after up to 2.5 dpa at 200-250°C and post irradiation examination.
Status: in progress, see page 50 for more details.

Task TW2-TTMS-003a - RAFM Steels: Compatibility with Hydrogen and Liquids
(coordinated by NRI Řež; staff: M.Zmítko, K.Šplíchal, V.Masařík, V.Švarc, P.Chvátal)

<u>Deliverable 7</u>: Water corrosion effect inside Eurofer tube under PWR conditions.

<u>Deliverable 12</u>: Water corrosion test under PWR conditions on Eurofer tube/tube and tube/plate weldments.
<u>Deliverable 15</u>: Testing of Eurofer tube under flowing PbLi.
Status: delivered, see page 51 for more details.

Task TW2-TTMS-003b - RAFM Steels: Compatibility with Hydrogen and Liquids
(coordinated by NRI Řež; staff: M.Zmítko, K.Šplíchal, V.Masařík, P.Hájek, J.Berka, J.Zmítková)
<u>Deliverable 4</u>: In-pile PbLi corrosion testing of TBM´s weldments (stiffeners and bottom plate relevant), up to 2 dpa.
Status: in progress, see page 55 for more details.

Task TW3-TTMS-003 - RAFM Steels: Compatibility with Hydrogen and Liquids
(coordinated by NRI Řež; staff: M.Zmítko, K.Šplíchal, V.Masařík, P.Hájek, J.Berka, J.Zmítková)

<u>Deliverable 1</u>: Crack growth kinetic and fracture toughness on EUROFER 97 in presence of hydrogen (up to 10 wppm) at RT, 250° C
Status: in progress, see page 56 for more details.

Task TW4-TTMN-002. Experiments for the validation of cross-sections up to 55 MeV in an IFMIF-like neutron spectrum (coordinated by NPI Řež, P. Bém)
<u>Deliverable 6</u>: Activation experiment on W.
Status: delivered, see page 57 for more details

3. Physics Integration - TPD Diagnostics – Article 5.b

Sub-contractor of Task TW3-TPDS-DIASUP: Support to the ITER Diagnostic Design: Visible and UV impurity monitors (divertor). (IPP Prague, V. Piffl)
Deliverable: Assess techniques for in-situ calibration of the system in connection with deterioration of optical components.
Status: in progress, see page 58 for more details.

4. Vessel/In Vessel – Blanket – Article 5.a

Task TW3-TVB-INPILE: In-pile experiment on PFW Mock-ups. (coordinated by NRI Řež; staff: M.Zmítko, J.Bohatá, T.Klabik, P.Hájek)
Deliverable D3: Perform in-pile testing of Be protected PFW mock-ups under heat flux.
Status: in progress, see page 59 for more details

5. Vessel/In Vessel - Blanket – Article 5.b

Task TW3-TVB-FWPAMT: Mechanical testing of a panel to shield block attachment system. (coordinated by FNSPE Praha, V. Oliva)
Status: in progress, see page 60 for more details.

Tritium Breeding and Materials: Breeding Blanket

Helium Cooled Lithium Lead: Processes and Components
Task TW2-TTBC-004 (coordinated by NRI Řež)

Deliverable 4a: Pb-17Li Auxiliary and purification systems - Design of the Auxiliary PbLi loop for HCLL TBM
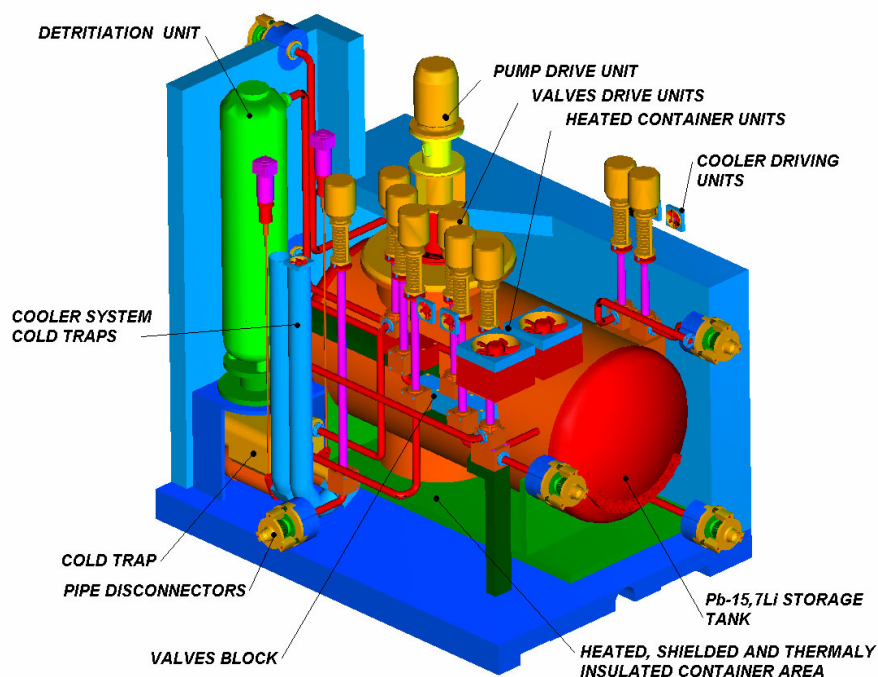
Achievements:
The Helium Cooled Lithium Lead (HCLL) Test Blanket Module (TBM) will be installed and tested in the ITER. For this reason a dedicated auxiliary Pb-17Li system for the HCLL TBM needs to be developed with the aim: (i) to ensure circulation of Pb-17Li liquid metal in this breeding blanket, (ii) to remove tritium produced by a nuclear reaction in the TBM, (iii) to purify and remove impurities from Pb-17Li, and (iv) to ensure the Pb-17Li system feeding, sampling, draining, monitoring etc. In the frame of this deliverable, a design study of the Pb-17Li auxiliary system for TBM was performed and the system layout was proposed (see figure 1).
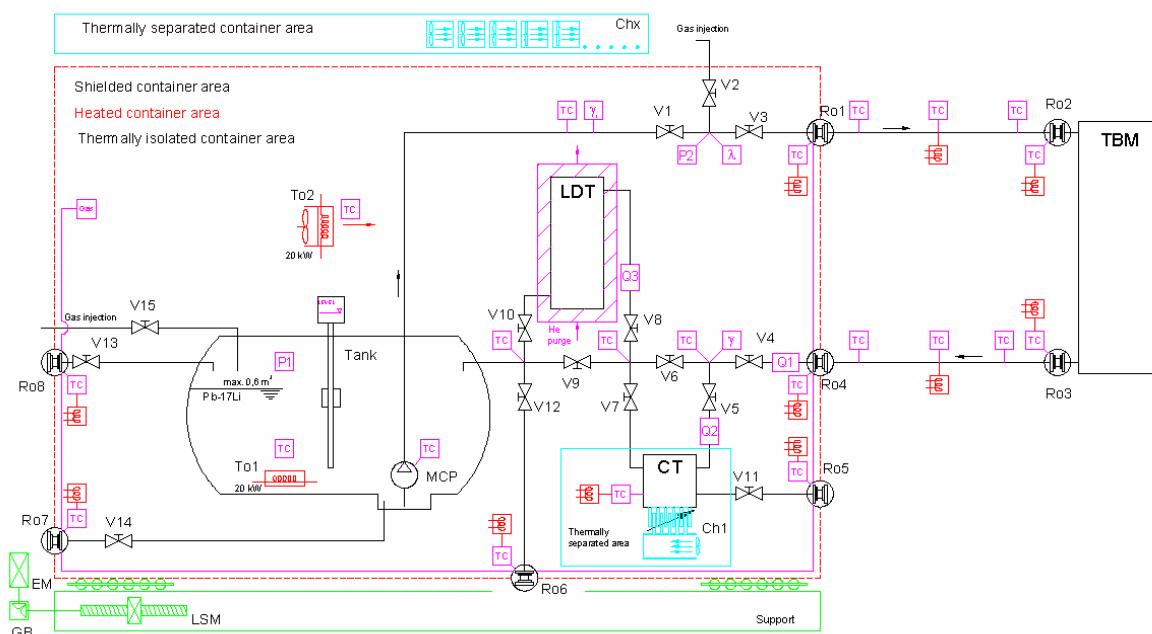
Fig. 1. *Schematic layout of the Pb-17Li auxiliary system for the HCLL TBM*

The Pb-17Li auxiliary system will be situated in a special container with dimensions of 2.315 m (height) x 2.19 m (length) x 1.6 m (width) that will be placed as close as possible to the TBM to prevent tritium permeation from the connection piping. The system is from the functional point of view divided into the following parts: main circuit, detritiation unit, cold trap, dosing and sampling systems, heating and cooling systems, and shielding and insulation. The Pb-17Li circuit is a closed loop with a forced circulation of Pb-17Li. From the tank that, at the same time, is a Pb-17Li storage tank, liquid metal is pumped into the TBM where tritium is produced. The flow velocity in the Pb-17Li system will be controlled in the range of 0.1 to 1 kg/s. Pb-17Li outlet temperature from the TBM is 550°C. Tritium is removed from Pb-17Li in a detritiation unit. Corrosion products and impurities are removed from Pb-17Li in

a cold trap. Design of the whole system (see figure 2), description of the key system components, operation modes, operational parameters control and monitoring, the structure material used, as well as the assembly, testing, installation and maintenance requirements are described in the technical report submitted to EFDA. Also, recommendations for further developments of the Pb-17Li auxiliary system are proposed, focused mainly on detailed development and testing of selected key components (e.g. cold trap, mechanical pump, flanges, etc.).

Fig. 2. *View of the Pb-17Li auxiliary system for ITER HCLL TBM*

<u>Deliverable 4b: Pb-17Li Auxiliary and purification systems - Design of the Purification system of PbLi (e.g. from Bi) and evaluation of impact on Po production</u>

Achievements:
In the frame of this deliverable, the available literature information on behaviour and purification of liquid metal Pb-17Li from corrosion products and impurities like bismuth, thallium, polonium and mercury was summarized. It involves results of experiments that were performed for the purpose offinding the best method of removal of corrosion products, bismuth and other heavy metals from the eutectic mixture Pb-17Li. Three types of purification devices were tested: i) mechanical filter, ii) cold traps, and iii) magnetic traps. The cold traps use the fact that corrosion products and many compounds including bismuth have lower solubility in Pb-Li at lower temperature. At lower temperatures they precipitate and can be removed. These procedures are controlled by the rate of impurity removal and the capacity for retaining impurities. It was demonstrated that cold traps are effective for corrosion product and other impurity removal.

During the Helium Cooled Lithium Lead (HCLL) blanket operation of a fusion reactor a number of radionuclides will be formed from the Pb-17Li breeder. Of special concern for safety questions is the polonium radioisotope [210]Po that is formed by β-decay from the

bismuth radioisotope [209]Bi. With regard to the most worrying radioisotope [210]Po, to achieve desired polonium content in the breeder blanket it is necessary to keep the bismuth concentration in the Pb-17Li eutectic mixture below 8 appm that corresponds to temperature of 250°C (see figure 3). For bismuth removal adiffusion cold trap was also suggested. The assessment of purification procedures shows that different kinds of cold traps trapped more than 50 % corrosion products particles. It was shown that purification devices were also effective for the deposition of the intermetallic compound PbLi or (PbLi + Pb-15.8Li) mixture. It can be concluded from the experimental observations that the cold trap shows the best Pb-17Li purification performance from corrosion products and impurities like bismuth and polonium.
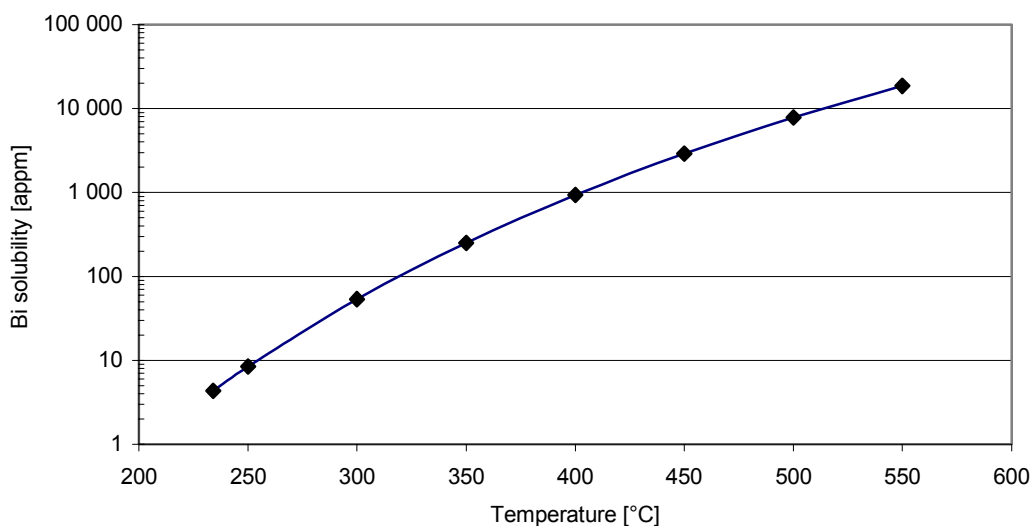
Fig. 3. *Temperature dependence of Bi solubility in Pb-17Li*

Tritium Breeding and Materials: Materials Development

RAFM Steels: Irradiation Performance
Task TW2-TTMS-001b (coordinated by NRI Řež)

Deliverable 3: Static and dynamic toughness testing at the transition temperature. Neutron irradiation of plates and weldments after up to 2.5 dpa at 200-250°C and post irradiation examination. – in progress

Achievements:
Reduced activation ferritic and martensitic (RAFM) steels are considered as structural materials for fusion reactor applications. Investigations of radiation damage of EUROFER 97 steels have been carried out on materials irradiated at temperature higher than 350°C. At the present time some experimental studies are also focused on effects of neutron irradiation on static and dynamic fracture toughness at lower temperature 200 – 250°C.

Plates of EUROFER 97 steel were manufactured by Böhler Bleche GMBH works. EUROFER segments delivered by Forschungs-zentrum Karlsruhe were used. Weld joins were prepared in CEA Saclay by TIG procedure. Static and dynamic fracture toughness will be measured with microspecimens. Mikrospecimen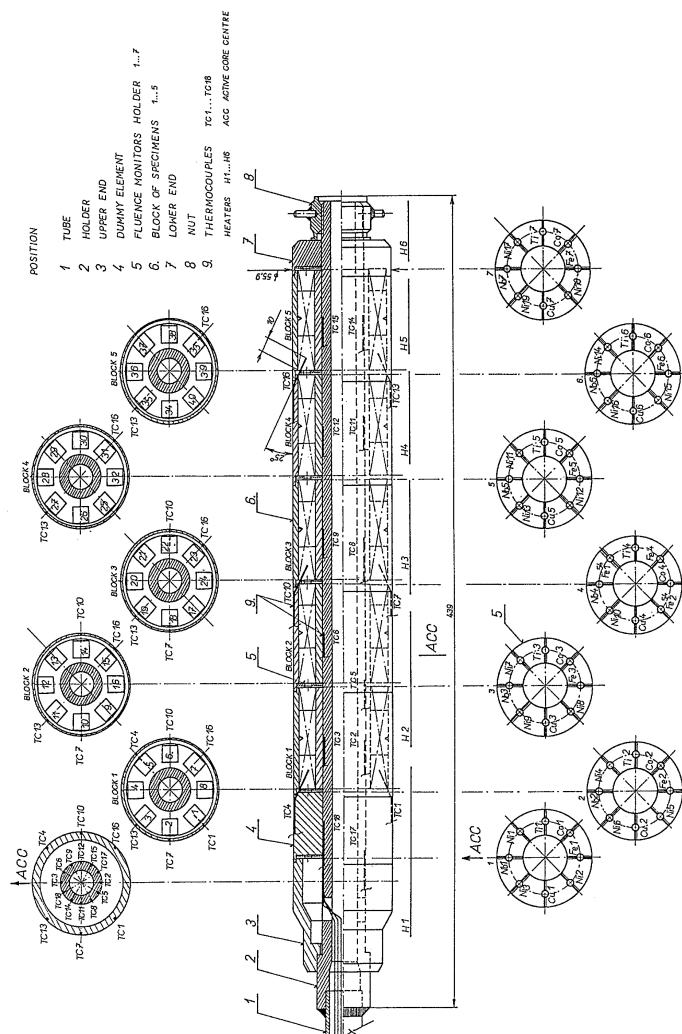s K.L.S.T were machined from base metal and welds. Notch preparing and fatigue pre-crack cycling were carried out before irradiation. A Chouca rig (see figure 4) was used for the irradiation experiment. Specimens were placed in the holder of the Chouca rig and out of pile testing was performed. Rig irradiation in the core of research reactor LVR 15 started in September 2003 and the experiment is running at a temperature of approximately 235°C with a fast neutron flux about 4×10^{13} cm^{-2} s^{-1} in He atmosphere. Total irradiation time from the beginning of the experiment is 4425 hours which represents about 1 dpa.

The irradiation experiment continues to the end of 2005. A method of fracture toughness measurement was developed and should be applied for testing of K.L.S.T. specimens under hot cell conditions. Fracture toughness of irradiated and un-irradiated microspecimens will be measured in the temperature range – 150°- 250° C and the ductile to brittle transition temperature will be evaluated.

Fig. 4. *Chouca rig*

RAFM Steels: Compatibility with Hydrogen and Liquids
Task TW2-TTMS-003a (coordinated by NRI Řež)

Deliverable 7   Water corrosion effect inside EUROFER tube under PWR conditions
Deliverable 12 Corrosion behaviour of base and weld metals EUROFER 97 under primary water PWR conditions

Achievements:
Reduced Activation Ferritic-Martensitic (RAFM) steels were developed as potential structural materials for the fusion reactor blanket. EUROFER 97 steel is a main candidate material for first wall and structural components. In the frame of the water cooled liquid led-lithium blanket concept (WCLL) corrosion behaviour of EUROFER was investigated under Pressurized Water Reactor (PWR) conditions. EUROFER base and weld metal and tube

specimens were exposed in the reactor water loop RVS 3 under primary water parameters at 320°C and 2000 hours. The susceptibility of base and weld metals to stress corrosion cracking and the crack growth initiation were evaluated, see e.g. figs. 5, 6.. General and local corrosion were investigated after the exposure of tube specimens.

The tested specimens of the base metal as well as the weld metal did not show stress corrosion cracking at aload of four levels K_I in the range of 22 to 34 $[MPa.m^{1/2}]$.
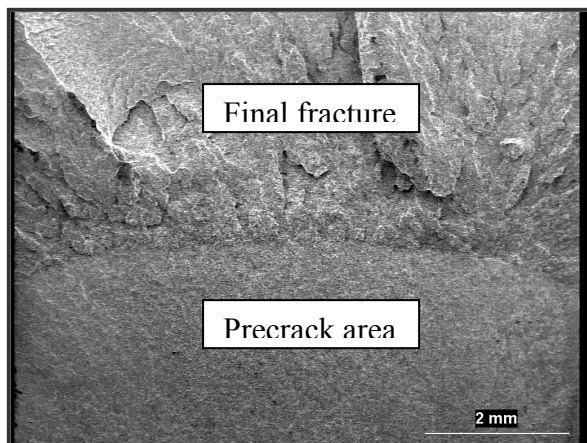
Fig. 5. *Crack tip of weld metals, no crack growth covered with oxide initiation was indicated.*
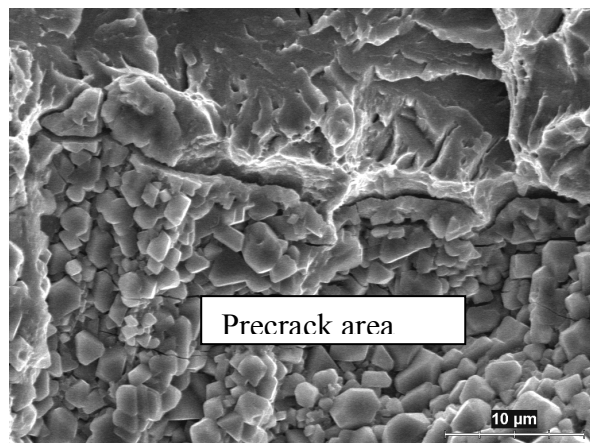
Fig. 6. *Fatigue fracture surface deposit layers.*

The level, over which the initiation of corrosion cracking should take place, will be higher than the given range of applied load values. After exposure of tube specimens, the appearance of sample surface was uniform and compact, and did not show any sign of pitting or traces of other local attack. The surface layers correspond to the creation of passive protection films and are formed by magnetite or spinel type of oxides, the presence of which was proved by SEM investigations and EDX analyses. The character of surface layers corresponds to the creation of passive protection films on similar type of stainless steels. Interaction with the corrosive environment manifests itself by decreased sample weight with increasing exposure time and this relationship is parabolic (see figure 7).

Fig. 7. *EUROFER tube specimens weight loss under PWR conditions*

These results are consistent with the evaluation of corrosion susceptibility of stainless steels investigated under similar water chemistry parameters. The experimental results proved, although for a limited period of time, that EUROFER 97 steel has sufficient resistance to local and general corrosion.
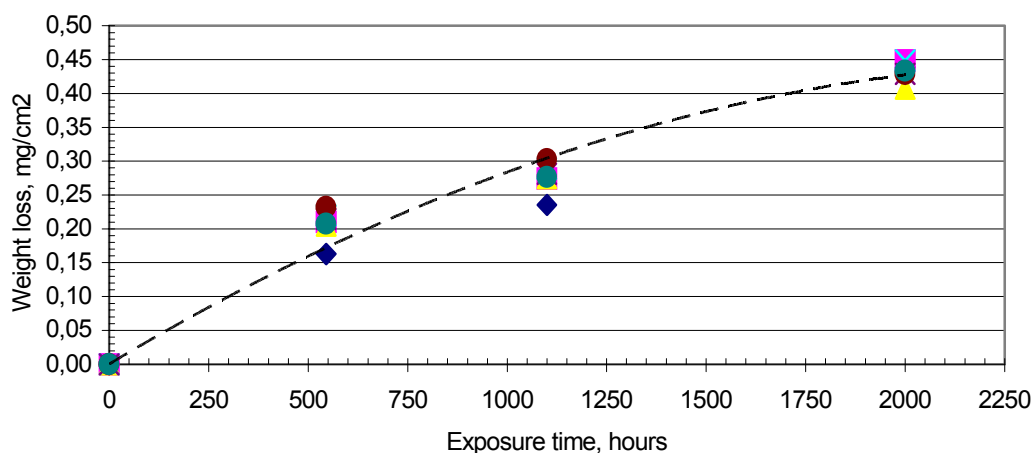
Reports:

[1] Final report: K.Splíchal, P.Chvátal, M.Zmítko: *Corrosion behaviour of base and weld metals of EUROFER 97 in primary water PWR conditions*, NRI Rez report No.12058, April 2004.

[2] Final report: K.Splíchal, V.Masarík, V.Svarc, M.Zmítko: *Corrosion behaviour of EUROFER 97 tube in primary water conditions*, NRI Rez report No.12038, March 2004.

Deliverable 15 Testing of EUROFER tube under flowing Pb-Li

Achievements:

Liquid Pb-Li alloys are investigated as potential coolants and tritium breading fluids for fusion reactor concepts. Various studies have been carried out to examine the compatibility of structural steels with liquid metals. Reduced Activation Ferritic-Martensitic (RAFM) 8 – 10 % Cr steels were investigated as structural material for the fusion reactor DEMO. EUROFER 97 represents main potential material of this steel type for a fusion reactor blanket. In this work the corrosion behaviour of EUROFER 97 was tested in flowing Pb-17Li at the temperature 500° C for the period up to 2500 hours. Surface morphology, weight changes and chemical composition profile were investigated. Melt interaction with tube steel specimens result in its dissolution, which is demonstrated by surface morphology and specimen weight changes. After exposures up to 1000 hrs, corrosion attack is non-uniform. Both unaffected and affected areas of the specimen surfaces were observed. This is probably due to the presence of protective layers with different behaviour in melt and also successive wetting of the specimen surface.

Fig. 8.

After 2500 hrs exposition, corrosive attack took place practically along the whole surface and a noticeable weight decrease of specimens was observed. The experiments have shown that during a certain incubation period the surface layers are relatively stable. In the course of subsequent exposure time those layers are not more resistant and cannot influenced the dissolutions of metal.

A noticeable weight decrease and calculated loss of metal were observed after 2500 hrs of testing. The weight decrease of approximately 1 mg/cm^2 after 2500 hrs can be compared with data of Fe-12Cr-1MoVW steel after 3000 hrs under similar test conditions with the flow rate of 25 mm/s [2].

Concentration profiles of steel components near the steel surface were examined by EDX line-scan and point analyses. Under the experimental conditions no considerable decrease of Cr and Fe was observed. After 2000 and 2500 hrs, a slight decrease of Cr and Fe could be observed in a few microns layers, see fig. 9. The content of W and V near the surface does not decrease, on the contrary, there is an increase of the W content compared to the matrix composition. The increased W content corresponds to EDX results [1] for similar F82H steel tested for 2000 hrs at 480°C.

Thus, the main mechanism of Pb-17Li corrosive attack is dissolution of steel, which takes place after some incubation period needed for removing the surface protective layers. At longer exposure times, those layers are not more resistant and do not prevent dissolutions of steel components. The attack results in the dissolution of Cr and Fe as components with higher solubility in Pb-Li. The increase of W relative content, as a component with lower solubility in liquid metals, was observed near the steel surface.
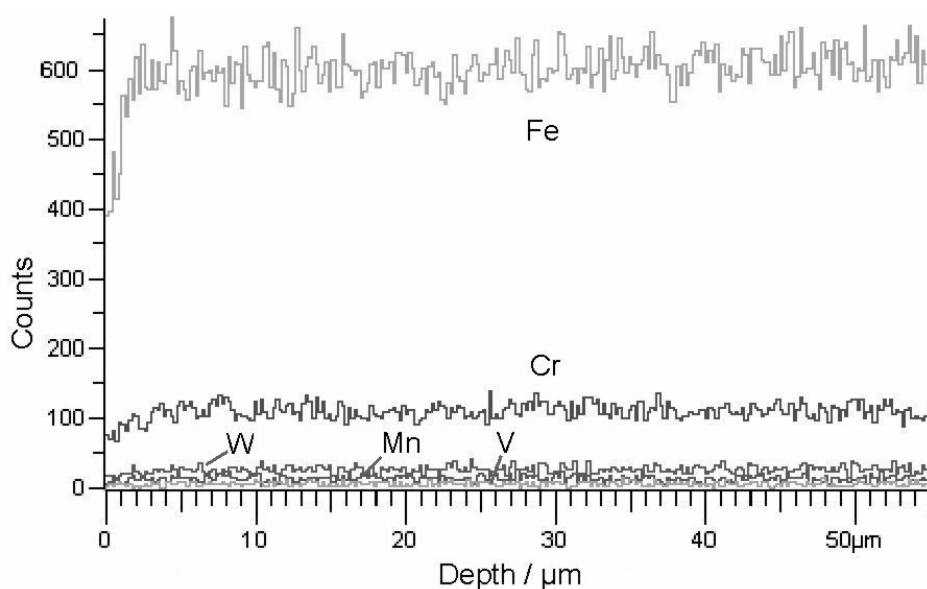
Fig. 9. *EDX line scan of specimen cross-section after 2000 hrs exposure in Pb-17Li at 500°C.*

Reports:
[1] Final report: M.Zmítko, K.Splíchal, V.Masarík: Corrosion and surface conditions of EUROFER 97 steel in Pb-17Li at 500°C, NRI Rez report No.12016, January 2004.
[2] K.Splíchal, M.Zmítko: Corrosion behaviour of EUROFER in Pb-17Li at 500°C, J. Nucl. Mat., 329-333 (2004) 1384-1387.

## RAFM Steels: Compatibility with Hydrogen and Liquids
Task TW2-TTMS-003b - (coordinated by NRI Řež)

Deliverable 4: In-pile PbLi corrosion testing of TBM´s weldments (stiffeners and bottom plate relevant), up to 2 dpa. - in progress

Achievements:
The long term development program of fusion power reactor DEMO is focused on structural material which can withstand neutron loading, heat fluxes and environment conditions. The relevant materials of the ITER Test Blanket Modules (TBMs) involve Reduced Activation Ferritic-Martensitic steel EUROFER 97 as structural material and Pb-17Li as a breeder and neutron multiplier material. Compatibility of EUROFER 97 with Pb-17Li melt is to be therefore investigated under neutron irradiation (up to 2 dpa) and temperatures up to 550°C. A special irradiation in-pile rig has been designed and manufactured with the aim to perform in-pile corrosion testing. The main part of the in pile rig (see figure 10) consists of a capsule filled with Pb-Li eutectic alloy and EUROFER 97 specimens. Nuclear heating and dedicated cooler of the capsule are to ensure the required test temperature about 500-550°C in the hot part and about 350-400°C in the cold part giving a corresponding temperature difference of 100-150° C. Flow of the molten Pb-Li eutectic is driven by natural convection in the range of few mm/s.

Mock-up Pb-Li in-pile sets were designed, manufactured and tested in research reactor LVR-15 with the aim of verifing the irradiation rig thermal performance and temperature distribution. The finite elements code COSMOSFloWorks was used for the in-pile rig design optimisation, e.g. capsule dimensions, cooler design, number of specimens etc.
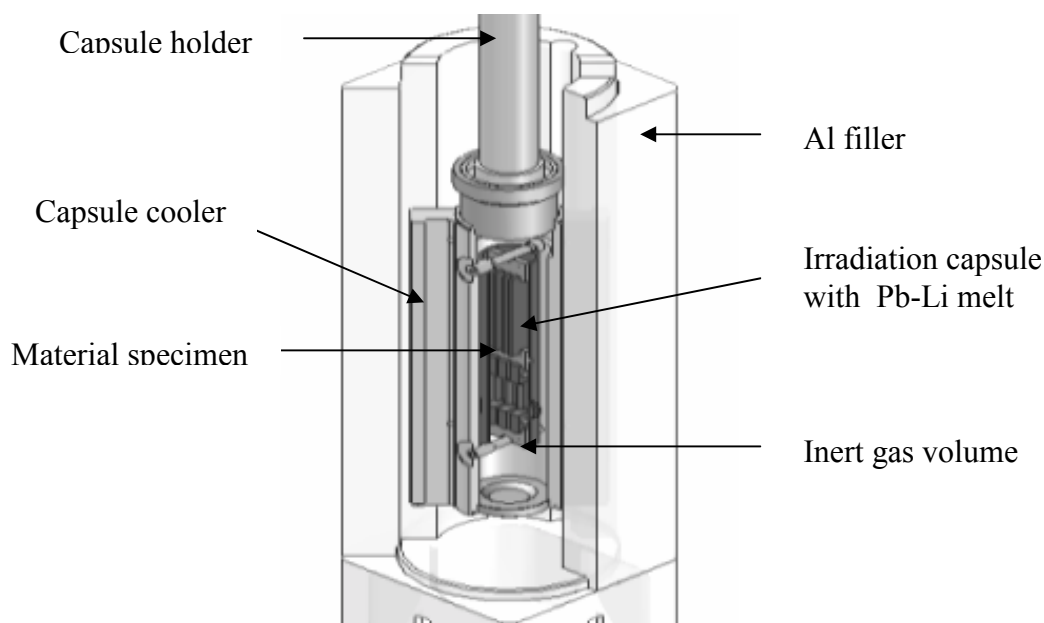
Fig. 10. *Design of Pb-17Li in-pile rig.*

The input data for the finite elements model were corrected regarding the results of the previous mock up test, which was not successful due to the irradiation capsule overheating. The subsequent mock-up test was performed and results indicate good agreement between measured

and required target temperatures in the hot and cold parts at the operation reactor power of 9 MW (see figure 11). After this mock-up test, the in-pile rig has been loaded into the active core of the reactor LVR 15 and irradiation has been launched.
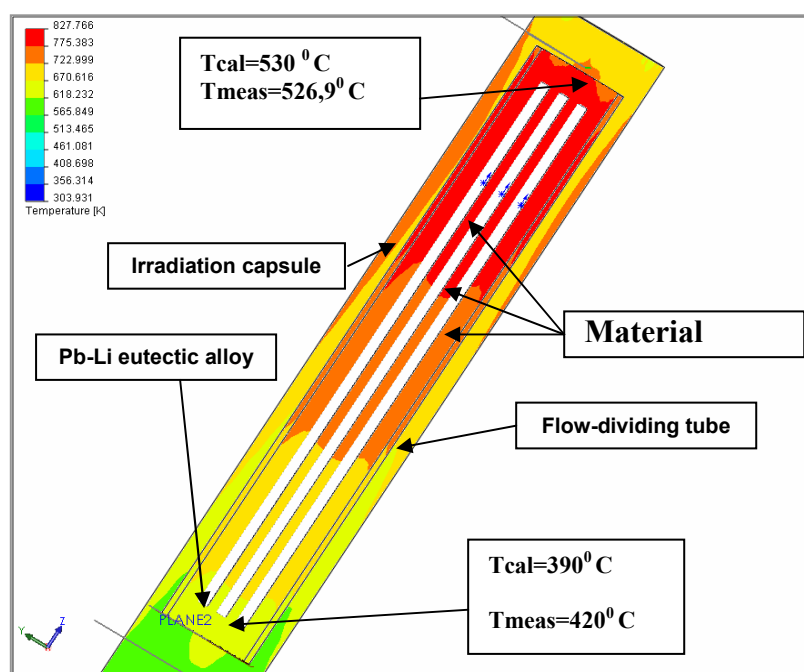
Fig. 11. *Comparison of calculated and measured temperatures in the Pb-17Li in-pile rig at reactor power 9 MW*

RAFM Steels: Compatibility with Hydrogen and Liquids

Task TW3-TTMS-003 (coordinated by NRI Řež)

Deliverable 1: Crack growth kinetic and fracture toughness on EUROFER 97 in presence of hydrogen (up to 10 wppm) at RT, 250° C - in progress

Achievements:

Low activation martensitic steel Eurofer 97 is investigated as structural material for first wall and blanket structure of a future fusion reactor. Diffusivity and solubility of hydrogen and its isotopes in this material is crucial issue, which can introduce hydrogen embrittlement damage. Such susceptibility under fusion reactor conditions is to be evaluated with respect to several hydrogen sources mainly generation by (n,p) reaction, adsorption from plasma.
Examination of EUROFER base metal and weld metal was suggested to evaluate the impact of hydrogen on corrosion, mechanical and fractural properties regarding hydrogen induced cracking and changes of fracture toughness characteristics.

The methods for hydrogen charging and hydrogen induced embrittlement testing were evaluated. Fracture toughness measurements are performed by 3-point bend method and crack growth rate is determined by the Slow Strain Rate Test (SSRT) method. Gaseous hydrogen and cathodic hydrogen charging experiments were evaluated. Hydrogen contents after gaseous charging at temperature 150° - 300°C do not exceed about 2 wppm. Hydrogen contents after cathodic hydrogen charging reached 4 to 6 wppm. It was therefore chosen for hydrogen embrittlement testing. The EUROFER base metal plate was delivered from FZ Karlsruhe. Two separate plates were manufactured in NRI and welded in CEA Saclay by TIG procedure. SSRT

experiments were performed at room temperature and at higher temperature 250°C in demineralised water saturated with hydrogen under a pressure of 2 MPa. SSRT does not show changes of total elongation, uniform elongation and reduction of area of hydrogen charged specimens. Hydrogen charging of EUROFER base and weld metal did not influence specimen crack growth under slow strain rate testing and ductile and strength tensile properties correspond to values of hydrogen uncharged materials.

Fracture toughness testing was started.

Experiments for the validation of cross-sections up to 55 MeV in an IFMIF-like neutron spectrum

Task TW4-TTMN-002. (coordinated by NPI Řež)

Deliverable 6: : Activation experiment on W.- delivered

Achievements:

Nuclear heating calculations of the IFMIF Test Cell (Ref. [1], see Fig. 12) need validation of tools and evaluated data for neutron activation for the set of materials/elements relevant to the test-cell design. As a part of experimental benchmarking of the IFMIF neutron calculations, the activation experiment on tungsten has been carried out at NPI. Tungsten was selected for an investigation as it poses a considerable source of gamma-emitting radionuclide constituent of the Eurofer-97 steel [2]. Besides that, knowledge of dominated γ-dose rate inventories from W-moderator of the IFMIF Test Cell is of great importance.

Fig. 12.

The arrangement of activation experiment has been described previously [3]. In the present measurement, the W disks (tungsten 99.95%, 12 mm diameter, GoodFellow product) were activated at a neutron flux density of about 1.2×10^{11} cm^{-2} s^{-1} of the NPI neutron source based on the p(37MeV)-D$_2$O reaction. The investigated samples were sandwiched by Al and Au foils for monitoring the neutron flux and irradiated at different overall neutron flux and different source-to-sample distances to prove consistency of measurement. The time profile of the neutron source strength during the irradiations was monitored by the proton beam current on the neutron-source target, recorded by a calibrated

Fig. 13.

current-to-frequency converter and scaler on a PC. Irradiated samples were investigated by gamma-spectrometry utilizing calibrated HpGe detectors repeatedly, after different cooling time intervals up to 95 days. Evaluation of gamma spectra was performed utilizing the NPI code DEIMOS. By analyzing the spectra, the resulting specific activities A$_{sp}$ in Becquerels
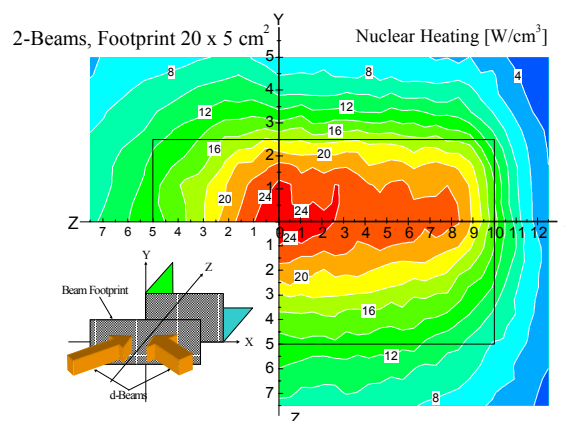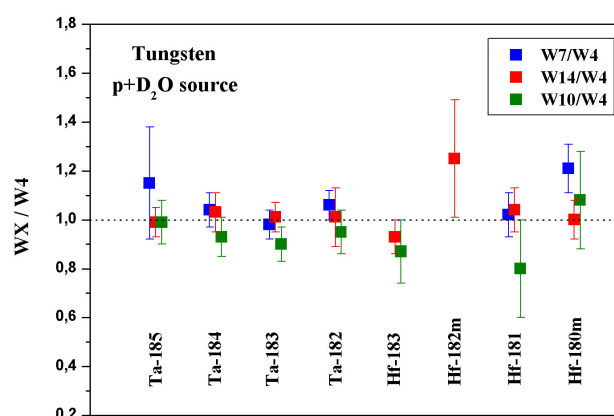
per kilogram to the end of irradiation were obtained. To prove the consistency of experiment, the activities determined simultaneously from different runs and different source-to-sample distances were compared in the form of reaction-rate ratios. The data were found to be consistent within statistical uncertainty of measurement (see Fig. 13).

In summary, the 12 activation products were determined from irradiation of a W sample in the $p+D_2O$ neutron field. The experiment presents the first benchmark for ^{185}Ta, ^{180m}Hf and ^{182m}Hf production in Tungsten (no cross section measurements exists for the ^{182m}Hf nuclide).

Reports:

[1] S.P. Simakov, U. Fischer, U. von Möllendorff, P. Bém, V. Burjan, M. Götz, M.Honusek, V. Kroha, J. Novák, E. Šimečková, *Pre-analysis of the validation experiment on Eurofer up to 55 MeV in an IFMIF-like neutron spectrum, Benchmark,* EFF-DOC-875

[2] S.P.Simakov, U. Fischer, U.von Mollendorff, P. Bém, V. Burjan, M. Götz, M. Honusek, V. Kroha, J. Novák, E. Šimečková, *The analysis of the validation experiment on Eurofer up to 55 MeV in an IFMIF-like neutron spectrum, Benchmark,* EFF-DOC-900 (2004)

[3] P. Bém, V. Burjan, M. Götz, M. Honusek, U. Fischer, V. Kroha, U. v. Möllendorff , J. Novák, S.P. Simakov, E. Šimečková, *Activation of EUROFER in an IFMIF like neutron field,* Proc. 23rd Symposium on Fusion Technology (SOFT), 20-24 September 2004, Venice, It., to appear in Fusion Eng. and Design.

Physics Integration - TPD Diagnostics

In-situ calibration of the system in connection with deterioration of optical components

(IPP.CR activity related to Art.5.1b Contract No EFDA/03-1114 EFDA Ref.: TW3-TPDS-DIASUP
"Support to the ITER Diagnostic Design: Visible and UV impurity monitors (divertor)"

ENEA-RFX Research Unit acquired the Contract TW3-TPDS-DIASUP No EFDA/03-1114: **"Support to the ITER Diagnostic Design: Visible and UV impurity monitors (divertor)".** In November 2004, on the basis of previous negotiation, it was agreed that IPP.CR Prague would perform this part of the contractual activity.

IPP.CR experience in this field

The CASTOR tokamak is equipped with an imaging VUV spectrometer of the Seya-Namioka type with a spherical diffraction grating and a two-dimensional detection system. Its purpose is to monitor the spectrum of highly ionised low-Z impurities (Carbon, Nitrogen and Oxygen) in 50-200 nm wavelength range and the emission from selected lines with a high spatial and temporal resolution in the radial direction. The emission and radial profiles of lines are also modelled by the emission/transport code STRAHL. A long-term collaboration in USX diagnostics with the Association EURATOM/CRPP Lausanne and in a VUV monitor research & design with Budker Institute in Novosibirsk, Russia confirms the ability to solve the actual problems in edge-plasma impurity monitoring.

Rewieved problems

In the hard environmental conditions during the long burn discharge in ITER, the deterioration of the optical components in the Diverter Impurity Monitor give rise to disbelief

on output issues. The measures like a running in-situ recalibration of the monitor system performance and an axis optical alignment of elements guarantee a preservation of credibility of the spectroscopy data.

In our opinion, the design of the Divertor Impurity Monitor is in starting stadium, which allows considering some extra amendments beneficial for in-situ monitoring of system performance.

An arrangement of the integrated calibration beam line as a common line of sight for visible and VUV spectrometers in Diverter Impurity Monitor and more with a blind line ("dead end") equipped with a shutter in front of first mirror, permits implantation of the proven calibration methods using thermal emission of a black body in the visible range and branching ratio cross calibration method in the VUV range.

In addition, the development of actual in-situ and remote calibration techniques should be completed by the new methods appearing nowadays or expecting in the next future. An installation of the diagnostic neutral beam injector in the divertor port for in-situ monitoring of the changes in transmission of line of sight by Beam Emission Spectroscopy of the He-doped energetic neutral beam is very promising and should be considered now.

Also the injection of an exact amount of impurity in divertor space: hot pellet black body source or gas target, need attention.

Our judgement of in-situ calibration techniques will be continued. We prefer to apply the present trends of in-situ calibration techniques in the final design of the Divertor Impurity Monitor for ITER.

Vessel/In Vessel – Blanket

In-pile experiment of PFW mock-ups
Task TW3-TVB-INPILE (coordinated by NRI Řež)
Deliverable 3: Perform in-pile testing of Be protected PFW mock-ups under surface heat flux
- in progress

Achievements:
The objective of this task deliverable is to perform in-pile thermal fatigue testing of actively cooled Primary First Wall (PFW) mock-up specimens (see figure 14) to check the effect of neutron irradiation on the Be/CuCrZr joints under representative PFW operation conditions.
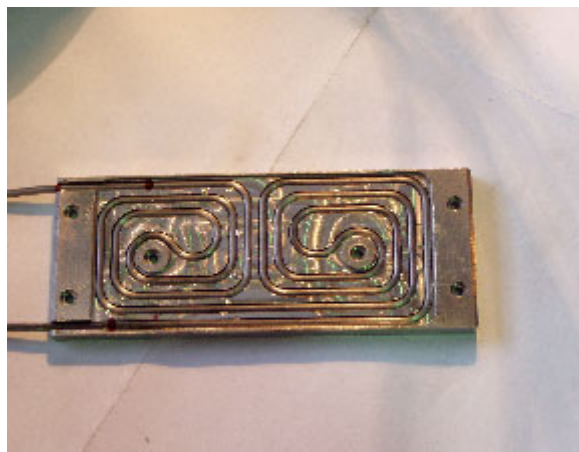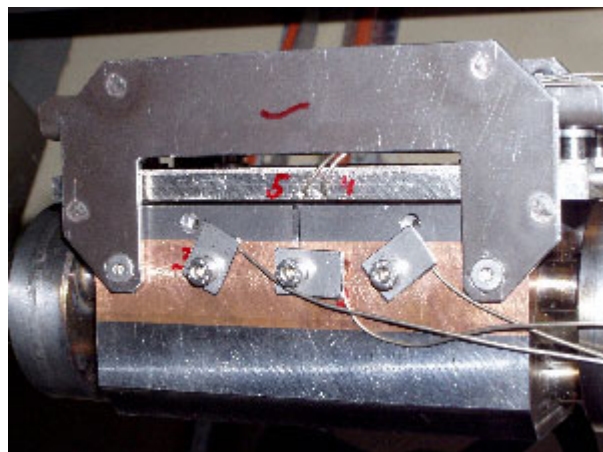

Fig. 14. *View of the Primary First Wall mock-up specimen*

The PFW mock-ups should be irradiated at 0.6 dpa with parallel thermal fatigue testing at 0.5 MW/m^2 heat flux for 20,000 cycles.

The design of the test in-pile facility has been developed and designed. The irradiation rig occupying two reactor cells (71.5x143 mm) will be located in the core of LVR-15 test reactor. The rig will contain up to three PFW mock-ups situated in axial position and will be filled with He gas. Electrically heated panels situated in small distance (gap 1-2 mm) parallel to the Be surface will be used to produce the required heat flux. Heat flux on the PFW surface will consist of radiation heat flux and, as well as, of He gap convection and conductivity. Three individually controlled heating wires will be used to heat-up the panels. Nickel will be used as a material of the heating panel.

Based on the design, thermal-hydraulic and thermo-mechanic calculations have been performed to model and verify the test rig performance, especially with regards of temperatures, heat flux and deformations. Requirement for performance of 20,000 thermal cycles will be met during the irradiation campaign. Specified neutron dose of 0.6 dpa will be achieved in LVR-15 reactor in approx. 105 effective full power days (EFPD). Duration of one thermal cycle is derived from the irradiation time and will last approx. 7 minutes. One heating cycle will consist of approx. 1 minute heat-up period, followed by 2 minutes steady state heat flux period at 0.5 MW/m^2 and temperature of 850-900°C and then followed by a cool-down period of at least 3 minutes. The PFW mock-ups will be connected in series and actively cooled using reactor primary coolant water with inlet temperature of 35-40°C. Flow rate of the cooling water of approx. 4 m/s will be controlled to achieve specified Be/CuCrZr joint temperature range.

For an adjustment of the heating parameters and the heating panels qualification a special out-of-pile test has been designed (see figures 15, 16).

Fig. 15. *Instrumented Primary First Wall mock-up specimen prepared for out-of-pile test* **Fig. 16.** *Nickel heating panel with Thermocoax heating wire*

Mechanical Testing of a Panel to Shield Block Attachment System
Task: TW3-TVB-FWPAMT (FNSPE)

The innermost part of the planned fusion reactor ITER is the blanket-shield system, directly exposed to the plasma. So called Primary First Wall (PFW) modules consist of shielding block and separable PFW panels, mechanically attached onto the block. To verify the rigidity, strength, and durability of the panel to block attachment system of a "key - key way" type, EFDA formulated the Task TW4-TVB-FWPMAT. The Czech Technical University in Prague, Faculty of Nuclear Sciences and Physical Engineering - Dept. of Materials has been assigned to solve this task along with cooperating Czech companies ŠKODA RESEARCH, Ltd., and VÍTKOVICE – Research and Development, Ltd. The objective of the research project is to design simplified mock-ups of the PFW panel and the shield block, their manufacturing, and long term cyclic thermal and mechanical testing of the panel to block attachment system, which would best approximate the behaviour of the system under loading by poloidal moment, radial moment, radial pulling force, and poloidal force in the reactor.

At the beginning of the year 2004, simplified geometry of the panel and supporting plate (during experiments, the supporting plate will act as the shielding block) has been proposed. Before the start of manufacturing of the test objects and the final design of the tests, EFDA requested preliminary finite element simulations of all tests under an "ideal" distribution of forces on the panel surface and ideal fixation of the supporting plate. The objective of the simulations was especially:

- to assess the influence of smaller thickness of the supporting plate (100 mm) as against the real thickness of the shield block (300 mm). The austenitic steel supporting plate produced by VÍTKOVICE Research and Development, Ltd. cannot be made thicker than 100 mm,
- to propose adjustments which would minimize this influence,
- to obtain the first notion of the behaviour of the whole attachment system under prescribed loading (state of stress, deformation, clearance, etc.) and thus gain data for preparation and eecution of the real experiments in ŠKODA RESEARCH, Ltd.
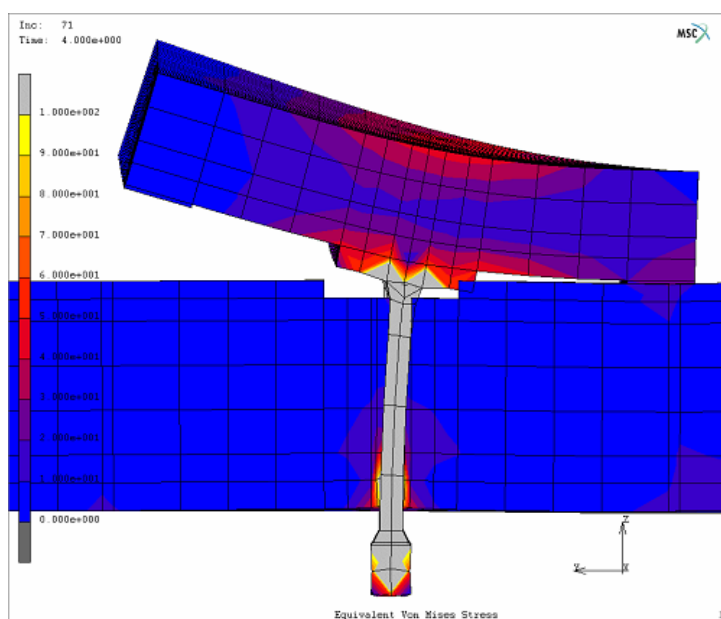
Fig. 17. *Von Mises stress distribution in the PFW panel, supporting plate and attachment stud under prescribed poloidal moment. The deformation of the test objects (magnification factor 200)*

The detailed description of the FEM simulations can be found in [1]. All simulations were performed in the commercial software MSC Marc. The 3D models respect all considered geometric configurations. The contact algorithm has been activated to avoid mutual penetration of the panel, supporting plate, and central studs MJ16 joining the panel and the plate. The effect of friction has been omitted. The loss of the contact between panel and shielding block under loading by poloidal moment is showed in Fig. 1 as an example of the FEM model. The results of computer simulations can be summarised as follows:

1. The influence of small supporting plate thickness on important geometrical quantities does not exceed 10 %. In view of this, the supporting plate 100 mm thick is considered sufficiently rigid.

2. For further increase of supporting plate rigidity with radial force and poloidal moment tests, it is advisable to use additional bolting to fix the supporting plate along its longitudinal axis. However, in the test with the poloidal moment, the additional bolting slightly increases the deviations from 300 mm shielding block in its marginal part.

3. Using the mean values of tolerances in the attachment system, no risk of plastic deformation of the key or the key way has been detected in any of the computed variants.

4. Local plastic deformation under small contact areas of the first few threads of the studs have to be expected. In this manner, the pre-load is transferred to other threads. If the contact in the key way is not lost, no further plastic strains should occur during subsequent cyclic loading. The real behaviour of the threads under cyclic loading has to be revealed by real tests, in particular in cases of alternating load.

5. According to FEM simulations, the tests with radial moment and poloidal force should not cause any problems. The loss of contact does not occur, and a smaller thickness of the supporting plate does not matter.

6. The total loss of contact along the whole key way can be expected in case of poloidal moment loading, and a partial loss of contact will probably occur also in marginal parts of the panel in case of radial force loading. A more reliable contact in the key way could be achieved by increasing of the pre-loading force in the studs and by decreasing the distance between the last stud and panel margin.

Reference:

[1] Denk, T. – Oliva, V. – Materna, A.: Mechanical tests of a panel to shield attachment system for ITER: preliminary FEM simulations. Research report, Department of Materials, CTU in Prague – FNSPE, in print.

2   Underlying Technology Tasks

The following five tasks have been performed as underlying technology tasks to complement the EFDA Work Programme in 2004:

Measurements of activation cross-sections at neutron energies below 35 MeV. M1: Activation tests on tungsten
Task: UT_IPP.CR_1
Field: Tritium breeding and materials
Task Area: IFMIF
Principal investigator :   *Pavel Bém, NPI*

On the basis of the EFDA reviews performed in 2003 of the status of nuclear data in EU neutron activation files, a number of elements, relevant to Tritium Breeding Materials (TBM) and to International Fusion Material Irradiation Facility (IFMIF), were identified for which the data were found inadequate, or incomplete, or not validated or missing. Therefore, new activation cross-section data measurements for pertinent nuclides are requested. The IFMIF relevant data have to be measured at neutron energies above 20 MeV.

The project was aimed to develop the quasi-monoenergetic neutron field for energies between 20 to 35 MeV that will broaden an applicability of white neutron fields presently available from the NPI neutron facility. Such fields will enable to perform the activation cross-section measurements for isotopes selected in accordance with requests of the IFMIF project. The results of a benchmark test of tungsten activation - an important component of the Eurofer-97 steel [1]- was investigated with respect of the priority of this selection.

Development of the monoenergetic neutron source:

The standard $^7Li(p,n)$ reaction on thin lithium target induced by the variable-energy proton beam of NPI cyclotron is used for the production of quasi-monoenergetic neutron field. Carbon backing for the thin Li target is utilized

To prepare thin self-supporting lithium foils for a target, the vacuum stand was completed and proved for reliable operation under argon atmosphere. The Li-foil-target technique was then investigated employing a proton beam of the cyclotron. The versatile chamber-holder for Li-foils and the multipurpose target chamber with cooling system was developed with this aim.

For measurements of neutron fluence from the p-Li source, the proton-recoil telescope (PRT) method with polyethylene radiator and the dE-E detector system together with two-dimensional data output were developed and tested on the cyclotron. The data from the PRT were stored in a list mode of a multichannel pulse-height-analysis on a PC. The PRT-measurement of relative neutron flux was combined with the activation-foil method. The activity of irradiated dosimetry foils were analyzed by gamma spectrometry method employing the calibrated HPGe detectors [2].

Several foil/backing configurations and cooling were investigated at different proton current under experimental investigation of a working lifetime of the Li target. At present, the stable operation of the source was achieved under separate cooling of the foil and carbon

backing. For the 24 MeV proton beam of 2 μA current, the system permits to produce a neutron fluence of about 1.5 x10^8 n/sr/s.

Activation cross-section test on tungsten:

The database for a production of radioactive nuclides from the irradiation of tungsten was tested in a benchmark experiment, carried out in a separate task [3,4]. In this experiment, the IFMIF-like white-spectrum neutron field of the NPI p-D2O source was employed. Present work has dealt with the analysis of measured activation products compared with the prediction of the IEAF-2001 library (the calculations were performed under the NPI -FZ Karlsruhe collaboration [5]). Reasonable agreement of data with predictions was found for generated isotopes ^{179m}Hf and ^{181,182,187}W. However, large disagreements were determined for ^{180m,181,182m,183}Hf and ^{182,183,184,185}Ta. Therefore, the updating of the specific cross sections for tungsten in the IEAF-2001 library above 15 MeV neutron energy is approved as a first priority programme.

Reports:

[1] P.Bém, V.Burjan, M.Götz, M.Honusek, U.Fischer, V.Kroha, J.Novák, S.P.Simakov and E.Šimečková, Activation of Eurofer in an IFMIF-like neutron field, 23-rd Symposium on Fusion Technology (SOFT-23), Venice, 18.-23. 09., 2004

[2] P. Bém, V. Burjan, M. Götz, M. Honusek, U. Fischer [+], V. Kroha, J. Novák, S.P. Simakov [+] and E. Šimečková, The NPI Fast Neutron Facility: Development of mono-energetic neutron field I, Report NPI ASCR Řež , EXP(EFDA)-08/2004

[3] P.Bém, V.Burjan, U. Fischer, M.Götz, M.Honusek, V.Kroha, J.Novák, S.P. Simakov, and E.Šimečková, Activation benchmark tests at the NPI fast neutron facility, EFF/EAF Fusion Nuclear Data and Neutronics Meeting, NEA Data Bank, Paris, 24-26 November 2004, EFF-DOC-910

[4] P. Bém, V. Burjan, M. Götz, M. Honusek, U. Fischer [+], V. Kroha, J. Novák, S.P. Simakov [+] and E. Šimečková, Activation experiment on tungsten in the NPI p-D$_2$O neutron field,   Report NPI ASCR Řež , EXP(EFDA)-09/2004

[5] S.P. Simakov, U. Fischer, P.Bém, V.Burjan, M.Götz, M.Honusek, V.Kroha, J.Novák, and E.Šimečková, Analysis of the NPI validation experiment for tungsten activation cross section in an IFMIF like neutron spectrum, EFF/EAF Fusion Nuclear Data and Neutronics Meeting, NEA Data Bank, Paris, 24-26 November 2004, EFF-DOC-913

Characterization of ITER related materials by nuclear analytical methods

Task: UT_IPP.CR_2
Field: *Vessel/in Vessel*
Task Area: *TVM-materials*
Principal investigator :   *V. Hnatowicz, NPI*

The aim of the work was to analyze the Si distribution in the silicon doped CFC samples by Particle Induced X-Ray Emission (PIXE), Rutherford Back-Scattering (RBS) and and Proton Induced Gamma-ray Emission (PIGE) methods. Additionally, a content and distribution of trace element impurities in the CFC samples can be studied by the above-mentioned methods. The work was a part of the broader task TW3-TVM-CFCQ within which the study of the ITER construction materials important for the Fusion Technology Program is being performed. The PIXE method, based on detection of characteristic X-rays induced by MeV protons, is suitable for determination of concentrations of different trace elements down to ppm concentration level. The RBS method, based on detection of elastically scattered protons or alpha particles, can be used for the determination of concentration and depth profiles of different elements with a depth resolution of about 10 – 20 nm. PIGE method makes use of proton induced gamma-ray emission. The measurements of CFC samples were accomplished

on the Van de Graaff accelerator of Nuclear Physics Institute (NPI) in Rez near Prague. The accelerator delivers proton and alpha particle beams with energies up to 3 MeV and beam intensities up to 1μA. The analyses were performed in a target chamber allowing simultaneous analyses by PIXE, RBS and PIGE methods. The PIXE, RBS and PIGE spectra evaluation was performed using standard computer codes available at NPI.

The CFC samples (B6-8f) from the block no.38 designated for ion beam analyses (IBA) have been prepared according to a cutting plan and delivered to NPI for analysis on the beginning of January 2004. The cut samples have dimensions of 12x50x1mm, which was an optimal size to be fitted in our experimental set-up. All three samples were analyzed by simultaneous PIXE, RBS and PIGE (Proton Induced Gamma-ray Emission) analytical techniques in a recently designed target chamber. The 2.95 MeV proton beam, collimated into 3mm circular beam spot, was used in this case. Next, several sample scans with the 2.95 MeV protons beam 1mm in diameter were done in order to determine lateral distribution of Si in samples. The sample B7f was also separately analysed at five spots by RBS technique in special designed RBS chamber using 2.35MeV protons and 1mm beam diameter. The aim of this analysis was to determine the depth profile of Si.

Because of nonstandard sample form and sample heterogeneity, several calibrations of the PIXE-RBS device was performed in order to optimize analytical procedure and to obtain reliable analytical results. The results of CFC sample analyses were summarized in a final report, which was submitted in Nov. 2004.

The Si concentration was found to be lateraly homogeneous on a large scale (broad ion beam), but large variations in Si concentration were observed on a mm scale. The average Si concentration in the samples was about 12 wt.%. Pronounced variations in the sample composition on mm lateral scale are obviously connected with CFC intrinsic structure. The CFC samples at hand were found unsuitable for ERDA (Elastic Recoil detection Analyses) analyses because of their too rough surface and porous structure, so that it was impossible to determine hydrogen content.

The observed depth distribution of Si was constant in all measured spots over the visible (analytical) depth, which is about 5μm in our case. Concentrations of Si and selected trace elements determined by RBS and PIXE methods are summarized in the Final report of the Contract EFDA/02-698, November 2004.

When a broad proton beam is used, the observed concentration of trace elements does not vary significantly among the samples. The only exception is Zn and Cu where rather large differences in concentrations are found. Also the PIXE and RBS results for the Si concentrations in different samples are in good agreement. There is a completely different picture on the mm scale. Large variations in elemental concentrations are observed in measurements performed with sufficiently narrow proton beam. No significant correlation between Si concentration and concentrations of other trace elements was found.

The PIGE spectra have also been collected during the simultaneous analysis with the 2.95MeV proton beam, however potentially determinable light elements were found to be below the detection limit (fluorine) or the analytical signal cannot be separated from background signal due to the Na and Al admixtures. Anyway, we can state the upper limit for the fluorine concentration in the samples, which was about 10-20μg/g F for all measured samples.

Reports:
V. Havranek, V. Hnatowicz, A. Macková, Assessment of the Si content of Si impregnated Carbon-Carbon Fibre Composite, Final report of the Contract EFDA/02-698, November 2004

Recovery effect on stainless steel strain hardening during welding
__Task: UT_IPP.CR_3__
Field: Vessel/in Vessel
Principal investigator :   J. Junek

The main objective of this task was the determination of the SS recovery effect and the implementation of the phenomenon into numerical simulation of welding on simple models.

A new material model with viscoplastic behavior has been applied. Up to now, the conventional plastic models with isotropic, kinematic or combined strain hardening have been used for almost all types of the welding analysis. The prevailing model used is the isotropic and then kinematic hardening. However, conventional models of the strain hardening are valid only up to 400°C. Above this temperature, the viscoplatic effect should be considered. The new version of the SYSWELD Code uses the viscoplastic model.

The objective of this work was to find the appropriate input parameters for analysis with the viscoplastic model for the steel 316 L. The measurements supplied from EFDA, as well as those performed in the Vitkovice laboratory have been used. The parameters supplied from ESI have been also taken into account.

The complete analysis is divided into several parts. The first part, the necessary viscoplastic input parameters were found on the basis of the experimental measurements. The second part, the creep tests have been numerically simulated with the found viscoplastic parameters. The comparison between the calculated and the measured total strain has been done, and on the basis of the results, the viscoplastic parameters have been modified. When the comparison between the calculated and measured total strain is satisfactory, the viscoplastic parameters are prepared for a real analysis. The third part, the numerical analysis of the real welding joints have been done with several types of the material behaviour, with conventional plastic strain hardening models and with viscoplastic material behaviour. The calculated results have been compared.

Full account of the results can be found in the report [1].

Reports:

Slovacek M.: Recovery effect of stainless steel strain hardening during welding, report of IAM Brno, number 3586/04, November 2004

Helium Cooled Lithium-Lead: Processes and components
__Task: UT_IPP.CR_4__

Field: Tritium Breeding and Materials
Task Area: Breeding Blanket
Principal investigator :   V. Masarík, NRI

The scope of this UT activity was to support development of relevant technical infrastructure to perform testing of selected sub-component for Pb-Li ancillary system of HCLL TBM under relevant conditions. An upgrade of the existing Pb-Li testing facility has been proposed including modifications in the instrumentation, measurements and liquid melt sampling. On this basis a detailed design has been developed.

Based on a literature review and available practical experience obtained in various

laboratories, various purification units have been evaluated (e.g. cold traps, metallic filters, magnetic traps). The selected purification unit of cold trap type will be installed into the upgraded Pb-Li testing facility for subsequent testing. The Pb-Li testing facility has been modified to be able to assess the purification efficiency of these units (e.g. a new Pb-Li sampling design was suggested). Possible techniques for controlled injection of corrosion products (intermetallic compounds, Fe, Ni, Cr) and impurities (e.g. Bi), and appropriate analytical methods have been evaluated and proposed.

Reports:
P.Vachtfeidl, J.Berka, K.Splichal, *"Pb-Li auxiliary and purification systems: Design of the purification system of Pb-17Li"*, NRI Rez report No. 12067, December 2004

Structure materials: compatibility with hydrogen and liquids
Task: UT_IPP.CR_5

Field: Tritium Breeding and Materials
Task Area: Materials Development
Principal investigator : K. Splichal

The main objective of this sub-task was to develop and verify a suitable method for controlled hydrogen charging of EUROFER specimens. Such specimens will be subsequently used for evaluation of the effect of hydrogen on EUROFER embrittlement.

Two hydrogen charging methods have been tested: i) electro-chemical (cathodic) charging and ii) hydrogen charging in gaseous environment. Hydrogen charging devices have been designed and fabricated. The KLST specimens made of EUROFER were used for the testing. Hydrogen content in the material specimens was determined by the LECCO hydrogen analyser. Using the gaseous hydrogen charging at different hydrogen pressures (15-20 MPa) and different temperatures (in the range of 200-320ºC) a hydrogen content of only 2.5 wppm has been achieved in the material. Using cathodic charging at a solution temperature of 75ºC and varying charging time and current density, a 3-5.5 wppm hydrogen level has been achieved. A charging curve, i.e. the dependence between current density and hydrogen content in EUROFER, has been established for given temperature and charging time (2 hours).

IV Keep-in-Touch Activities on Inertial Confinement Fusion

Activities in the field of the inertial confinement are performed on the Prague Asterix Laser System (PALS) in close collaboration with the Institute of Plasma Physics and Laser Microfusion, Warsaw, Poland. The experimental work was focused on the interferometric measurement of the laser plasma and its dynamics on the PALS by using a unique 3-frame interferometer developed at IPPLM.

1. Experimental studies of shock wave generation and crater formation in planar laser targets

Person in Charge: J. Ullschmied, IPP
Participants in the project: K. Jungwirth, B. Kralikova, E. Krousky, K. Masek, M. Pfeifer,
                         K. Rohlena, J. Skala (PALS laboratory, CR)
Collaborators from other laboratories:
T. Pisarczyk (principal investigator), A. Kasperczuk, S. Borodziuk, Z. Patron, P. Pisarczyk
    (Poland)
N. N. Demchenko, S.Yu. Gu'skov, V.N. Kondrashov, V.B. Rozanov (Russia)
J. Limpouch, M. Kalal (Czech Technical University in Prague, CR)

Introduction

Experiments on laser interaction with planar targets of various types represent a starting point for analysis of numerous physical phenomena accompanying implosion of complex spherical targets, on which the idea of laser fusion is based. The experiments utilizing ablatively accelerated planar targets can model large pellet shells in their early implosion phase. Instead of imploding a pellet, a disk target can be accelerated and treated as a section of a sphere (until convergence effects dominate). In planar configuration it is possible to observe also the cold back of the target, which is difficult to access in the experiments with real pellets.

The experiments performed at the PALS laboratory within the keep-in-touch activity context since 2002 were aimed at investigation of energy transfer and shock wave generation in planar targets driven both by direct laser illumination and by laser-driven macroparticles. In another series of experiments the crater creation in massive targets and smoothing of inhomogeneities induced by imperfections of the laser beam by foam layers were investigated. The temporal development of the laser-produced plasma was studied by means of laser interferometry, the crater parameters were obtained from microscopic replicas of the craters. The theoretical part of the work consisted e.g. in elucidating the role of heat transport in the smoothing mechanism inside the dense plasma regions at the double pulse interaction, and in studies of fast electrons and ions production by high-power laser beams.

Laser pulses were delivered by the upgraded PALS facility. Its new auxiliary and diagnostic beam lines and new main beam delivery options made it possible to illuminate and diagnose laser targets by sequences of laser pulses of various colours – at the basic wavelength 1315 nm, and at its red (668 nm) and blue (438 nm) harmonics. Output energy in the main laser beam (pulse duration 0.4 ns) was varied between 100 J and 500 J. Depending on the focusing conditions the focused laser beam intensity at the target were adjusted to values from 10^{14} W/cm^2 up to 10^{16} W/cm^2.

Interferometric measurements of the plasma dynamics

The work performed in 2004 was carried out in close co-operation with physicists from the Polish Institute IPPLM in Warsaw, from the Russian Institutes PIAS in Moscow and TRINITI in Troitsk, and from the Czech Technical University in Prague. Time-resolved interferometry of ablative plasma and shadowgraphy of the foil motion were applied as one of the main diagnostic tools. Density of the laser-produced plasma was measured by means of a 3-frame polari–interferometric system with automated image processing, developed for PALS by T. Pisarczyk and his colleagues from IPPLM Warsaw. A simplified scheme of the interferometer is depicted in Fig. 1.
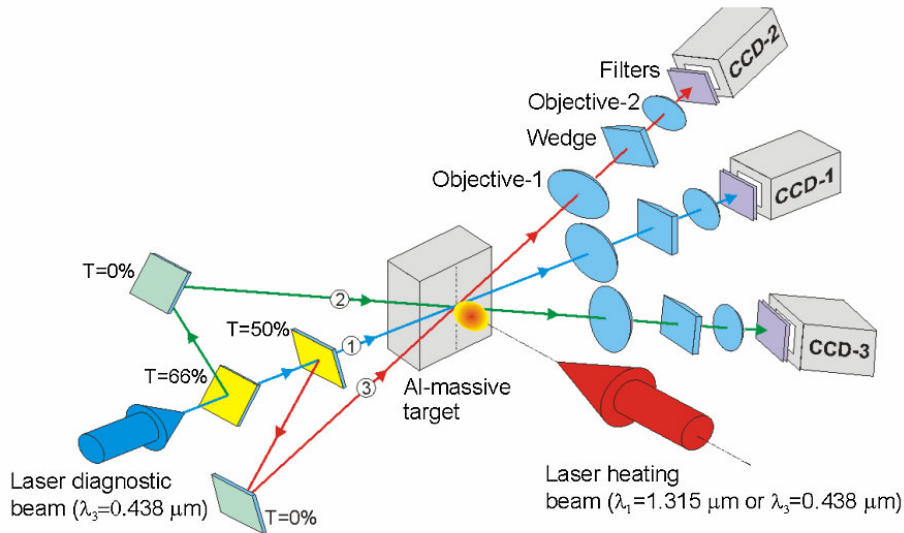

Fig. 1 *Simplified scheme of the 3-frame interferometric system exploited at PALS.*

The interferometer exploits a probing beam at the third harmonic (wavelength 438 nm, energy 2 J, diameter 100 mm) derived from the main laser beam. Its optical delay lines allow the making of three different frames during a single laser shot. The delay between subsequent frames was set at 3 ns, while the probing time of the first channel was varied for individual shots. Each of the interferometric channels is equipped with its own independent interferometer of the folding wave type and a CCD camera Pulnix TM-1300, with the matrix of 1300×1030 pixels. The arrangement of the registration system is shown in Fig. 2.
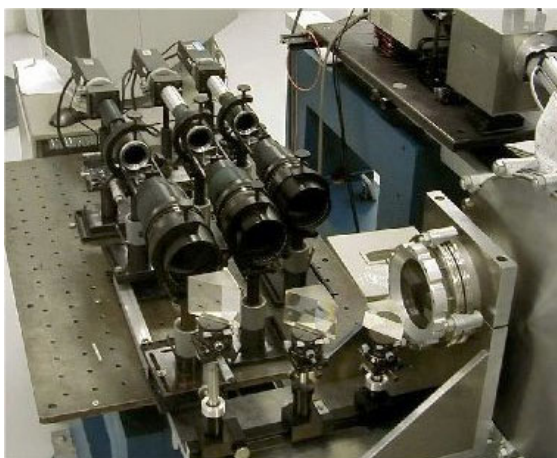

**Fig. 2** *View of the detection part of the 3-frame interferometer.*
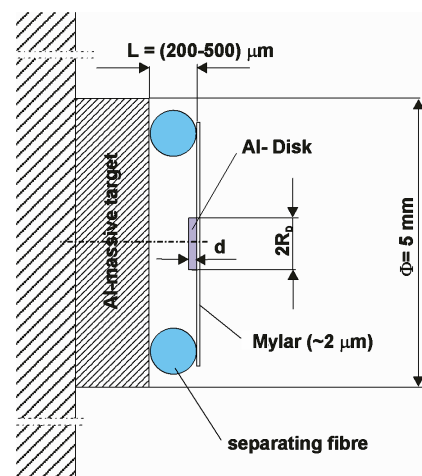
Fig. 3 *The target holder used in the double-target experiments.*

For the space behind the target to be accessible for interferometry, a special target holder has been developed and used. The target arrangement depicted in Fig. 3 made it possible to investigate ablative acceleration and crater formation in various types of double targets, the front part of which consists either of a single foil with attached disk, or of more complex structures covered e.g. by low-density foams. Craters in the massive part of the target were created by a direct laser irradiation, or by impact of the foil fragments and ablatively accelerated disks. The shapes and volumes of the craters were determined by employing wax replica technology and microscopy.

Interferograms of undercritical plasma regions in the corona and at the target rear can be used for reconstructing the plasma density, while denser plasma regions and opaque parts of targets are seen in shadowgraphic parts of the pictures. Processing of the recorded interferograms included parasitic noise filtering, comparison of object and reference interferograms, and subsequent reconstruction of radial electron density distributions. An illustrating sample taken from a sequence of interferograms and resulting densitograms of the plasma generated on a foil target is shown in Fig. 4a,b.
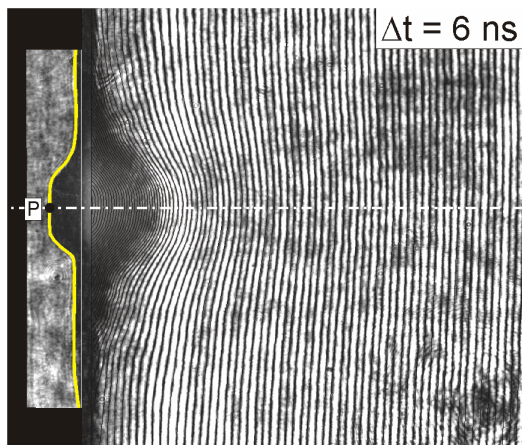
**Fig. 4a** *Interferogram/shadowgram of a laser-exploded foil*
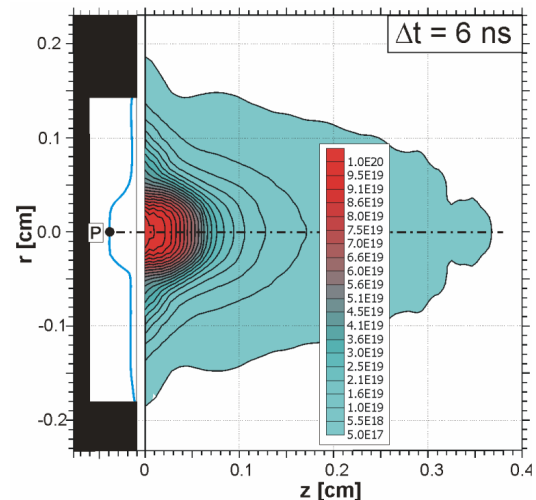
Fig. 4b *Processed densitogram of an exploding-foil plasma*

Different types of multi-layer, cascade and double laser targets were used in the experiments. The targets were made of different materials and their combinations, namely polyethylene, Al and Cu. In order to find optimum conditions for the disk acceleration and crater creation, the foil and disk thickness in the case of double targets was varied from 6 μm to 60 μm, the disk diameter from 300 and 600 μm, and the distance between foil/disk and massive target from 100 μm to 500 μm. The measurements were carried out for fixed irradiation conditions: laser energy 130 J and focal spot diameter 250 μm.

The investigated cascade targets were made of combination of Al, Cu, and polyethylene. They were fabricated in variants with and without a covering polyethylene foil (Fig. 5). They were irradiated at the constant laser energy of 100 J, by using three different irradiation manners as for the position of the beam spot with respect to the central boundary of different target materials.

Based on the interferometric and crater volume data, detailed information on the plasma contour and its expansion, on the spatial distribution of electron density, total electron number and velocity of accelerated macroparticles have been obtained for various parameters (energy, wavelength) of the irradiating laser beam. In addition, the values of laser energy absorption coefficient, ablation loading efficiency and efficiency of energy transfer were determined both in the case of a direct laser beam action and at a laser-driven impact of macroparticles.

a)   **b)**
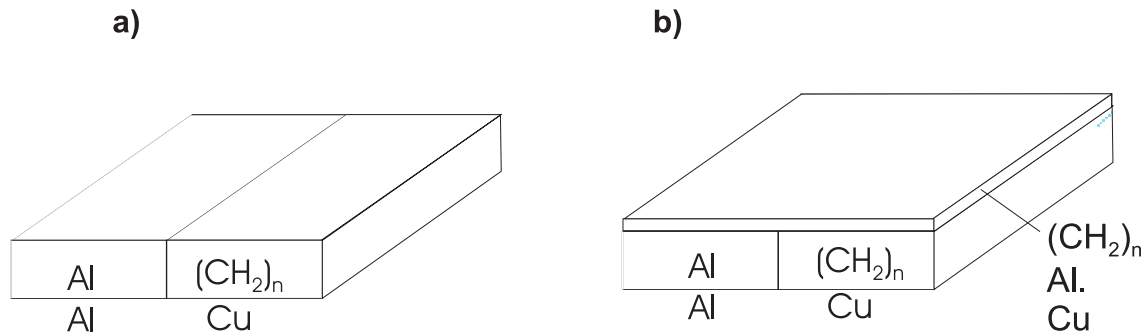
Fig. 5 *Cascade targets without (a) and with (b) a covering polyethylene foil.*

The experimental results were analyzed and interpreted by using a recently developed two-dimensional theoretical model and numerical simulations by means of the two-dimensional Lagrangian hydrodynamic code ATLANT-HE, which includes all the physical phenomena important in the above experiments, such as electron and ion heat conductivity, laser radiation absorption, fast electron generation and transport. The change of the focal spot radius at different laser shots made it possible to test the role of the two-dimensional plasma expansion effect on the shock wave characteristics. For smaller beam radii (<100 μm) the plasma torch expansion has a clearly two-dimensional character. On the contrary, at larger beam radii (>300 μm) it can be reasonably regarded as one-dimensional.

A lot of experimental material has been collected, which is now being processed and analyzed. Some of the results have been already published (see references [1-8]).

Publications

[1] S. Borodziuk, A. Kasperczuk, T. Pisarczyk, S.Yu. Gus'kov, J. Ullschmied, B. Kralikova, K. Rohlena, J. Skala, M. Kalal, P. Pisarczyk: Investigation of plasma ablation and crater formation processes in the Prague Asterix Laser System laser facility, Optica Applicata 34 (2004) 31-42.

[2] M. Kalal, J. Limpouch, S. Borodziuk, A. Kasperczuk, T. Pisarczyk, N. N. Demchenko, S.Yu. Gu'skov, V.B. Rozanov, K. Rohlena, J. Skála, J. Ullschmied, V.N. Kondrashov, and P.Pisarczyk: Investigation of the wavelength influence on the efficiency of macroparticles acceleration and craters creation in the PALS double targets experiment. Czechoslovak J. Phys., 54 (Suppl. C):C415-C420, 2004.

[3] T. Pisarczyk, S. Borodziuk, A. Kasperczuk, N.N. Demchenko, S.Yu. Gus'kov, V.B. Rozanov, M. Kalal, J. Limpouch, K. Jungwirth, B. Králiková, E. Krousky, K. Masek, M. Pfeifer, K. Rohlena, J. Skála, J. Ullschmied, V.N. Kondrashov, and P. Pisarczyk. Experimental and theoretical studies of the crater formation process on PALS experiments. Czechoslovak J. Phys., 54 (Suppl. C):C403-C408, 2004.

[4] A. Kasperczuk, S. Borodziuk, N.N. Demchenko, S.Yu. Gus'kov, M. Kalal, V.N. Kondrashov, J. Limpouch, P. Pisarczyk, T. Pisarczyk, K. Rohlena, V.B. Rozanov, J. Skala, J. Ullschmied: Ablation loading efficiency and shock wave generation driven by powerful laser pulse of different wavelengths, paperTu/P/20, XXVIII ECLIM. Roma, September 6-10, 2004

[5] M. Kalal, S. Borodziuk, N.N. Demchenko, S.Yu. Gus'kov, A. Kasperczuk, V.N. Kondrashov, J. Limpouch, P. Pisarczyk, T. Pisarczyk, K. Rohlena, V.B. Rozanov, J. Skala, J. Ullschmied: High power laser interaction with single and double layer targets, *invited talk* Fr/O1/3/I, XXVIII ECLIM. Roma, September 6-10, 2004.

[6] S.Yu. Gus'kov, S. Borodziuk, M. Kalal, A. Kasperczuk, B. Kralikova, E. Krousky, J. Limpouch, K. Masek, P. Pisarczyk, T. Pisarczyk, M. Pfeifer, K. Rohlena, J. Skala, J. Ullschmied: Shock wave generation and crater formation in solids by a short laser pulse interaction. Quantum Electronic, 34 (11), 989-1003, 2004.

[7] M. Kalal, A. Kasperczuk, V.N. Kondrashov, B. Kralikova, E. Krousky, J. Limpouch, K. Masek, M. Pfeifer, P. Pisarczyk, K. Rohlena, V.B. Rozanov, J. Skala, J. Ullschmied: Experimental and theoretical investigations of the crater formation process by means of double-target technique. 31st EPS Conference on Plasma Phys. London, 2004, ECA Vol. 28G, P- 5.066 (2004).

[8] A. Kasperczuk, S. Borodziuk, N.N. Demchenko, S.Yu. Gus'kov, M. Kalal, V.N. Kondrashov, B. Kralikova, E. Krousky, J. Limpouch, K. Masek, M. Pfeifer, P. Pisarczyk, T. Pisarczyk, K.Rohlena, V.B. Rozanov, J. Skala, J. Ullschmied: Investigation of crater creation efficiency by means of single and double targets in the PALS experiment, 31st EPS Conference on Plasma Phys. London, 2004, ECA Vol. 28G, P- 5.067 (2004).

2. Laser imprint smoothing by low-density foam layers

Person in Charge: J. Ullschmied, IPP
Participants in the project: E. Krousky, K. Masek, M. Pfeifer, K. Rohlena, J. Skála, P.
                             Straka (PALS laboratory)
Collaborators from other laboratories:
J. Limpouch (principal investigator), M. Kalal, J. Kuba, M. Sinor - FNSPE Czech Technical
    University in Prague, CR
N.N. Demchenko, S.Yu. Gus'kov, A.I. Gromov, V.N. Kondrashov, V.B. Rozanov (Russia)
A. Kasperczuk, T. Pisarczyk, P. Pisarczyk (IPPLM Poland)

Introduction

Foam layers are becoming of growing interest as a medium, which can be used for the improvement of the spherical symmetry of direct-drive inertial fusion, for increasing shock wave pressure in equation-of-state experiments, and for laboratory astrophysical simulations of interaction of exploding stars with circumstellar matter. In the experiments performed at the PALS facility we studied the interactions of a high-power laser beam with low-density foam targets, and acceleration of Al foils by the pressure of the heated porous matter. The main goal of the work was to investigate energy transport through the low-density porous matter, to determine the efficiency of thin foil acceleration and to demonstrate the smoothing effect of the low-density foam absorber.

The experiments were conducted at laser irradiances in the range of 10^{14} - 10^{15} W/cm^2 in the laser spot of ≈150 μm in diameter, at the basic wavelength of the iodine laser 1315 nm. Several types of foam target were used. Most of the shots were done with polystyrene foam of density 8 –10 mg/cm^3 and typical pore diameter of 50 –70 μm. In some shots also polystyrene and polyvinylalcohol (PVA) foams of smaller pore diameter and different densities were also used. The foam thickness was varied from 100 μm to 500 μm. An aluminium foil 2 μm or 0.8 μm thick was placed at the foam rear side in the majority of foam targets. A Kentech low-magnification x-ray streak camera, placed in a side view, was used for time -resolved detection of the plasma x-ray emission. The temporal evolution of plasma density and the motion of the solid target parts was recorded by a three-frame interferometer, described in more details in the preceding chapter the Association Euratom-IPP.CR part of the Report.

The results of experiment were compared with numerical simulations and with a simple analytic model of hydrothermal wave propagation. The simulations were performed by the two-dimensional Lagrangian hydrodynamics code ATLANT-HE including an advanced treatment of laser propagation and absorption. The code is based on the one-fluid, two-temperature model of plasma with Spitzer's heat conductivities for electrons and ions. For interpretation of the experimental data also a novel theory of formation of the laser light absorption region and of the ablation pressure generation in porous matter has been developed.

Measurements of efficiency of laser imprint smoothing by low-density foam layers.

In experiments with laser-irradiated polystyrene foam targets an efficient energy transfer and a considerable smoothing effect have been observed [1-6]. As the x-ray emission from polystyrene foam targets was rather low, good streak camera records were obtained just for the foams with the largest pore diameter (50 –70 μm). In the shot shown in Fig. 1 the heat wave propagates inward with the velocity of ~1.4 ×10^7 cm/s, the x-ray emitting zone covering only about two-thirds of the foam thickness. There is no emission near the Al foil at the target rear, the foil remains cold and is accelerated as a whole. The foil acceleration is well seen in

the sequence of interferograms/shadowgrams in Fig. 2. The rear side target boundary remains sharp, with no signs of low-density plasma behind the target. The shape of the accelerated foil is smooth without any detectable small-scale structures. Its central velocity (point P) reaches up to 10^7 cm/s.
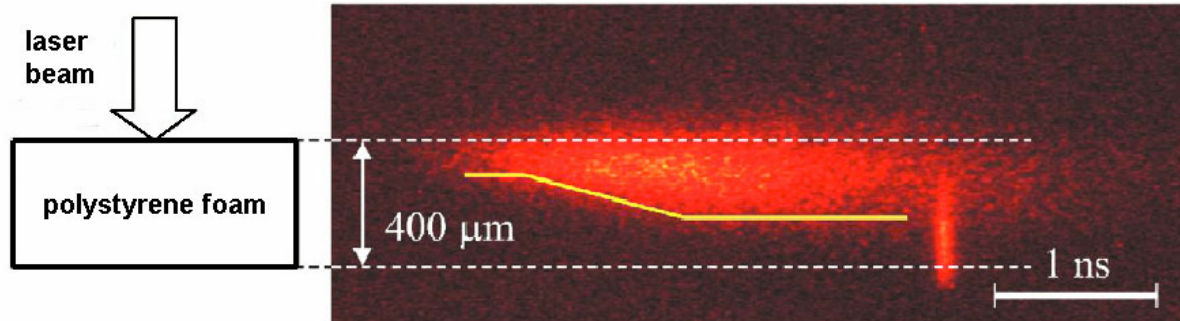
Fig. 1 *X-ray streak record of the thermal wave penetration into the polystyrene foam layer 400 μm thick (foam density 9mg/cm³, pore diameter 50–70 μm).*
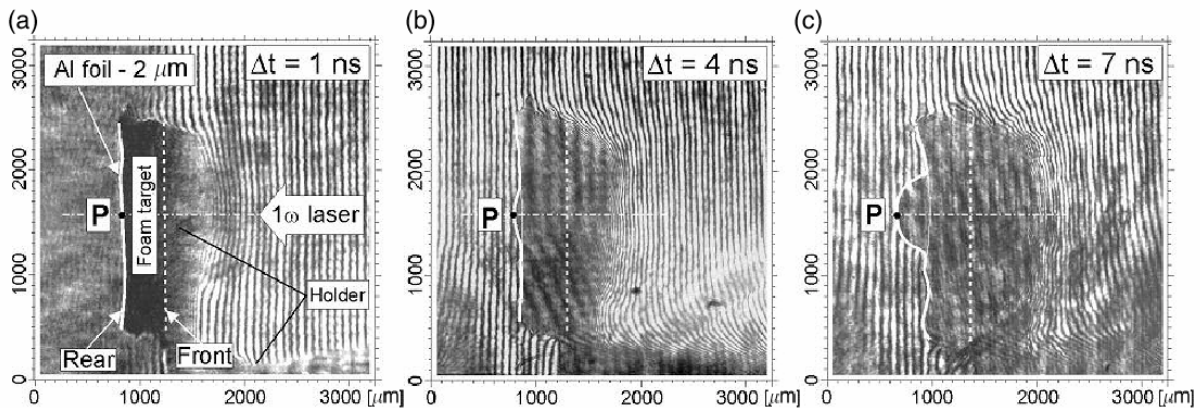
Fig. 2 Sequence of interferograms/shadowgrams showing the acceleration of Al foil attached to the rear side of the 400-μm thick polystyrene foam target.

The recorded interferograms demonstrate good symmetry and smooth propagation of the thermal wave, and absence of any local plasma perturbations at the target rear. The measured velocities of the accelerated foil agree well with two-dimensional hydrodynamic calculations, and with the values obtained from analytical modelling. Hydrodynamic efficiency of the foil acceleration was estimated up to 12 –14%. The experimentally observed delay of the shock wave propagation can be explained by non-equilibrium homogenization processes in the structured foam matter, which were not included in the theoretical model.

Publications

[1] M. Kalal, J. Limpouch, E. Krousky, K. Masek, K. Rohlena, P. Straka, J. Ullschmied, A. Kasperczuk, T. Pisarczyk, S.Yu. Gus'kov, A.I. Gromov, V.B. Rozanov, V.N. Kondrashov:, Thermal Smoothing by Laser-Produced Plasma of Porous Matter, Fus. Sci. & Tech., Vol. 43, No. 3 (2003) 275-281.

[2] J. Limpouch, N. N. Demchenko, S.Yu. Gus'kov, M. Kalal, A. Kasperczuk, V.N. Kondrashov, E. Krousky, K. Masek, P. Pisarczyk, T. Pisarczyk, V. B. Rozanov: Laser interactions with plastic-foam-metallic foil layered targets, Plasma Phys. Control. Fusion 46 (2004), p. 1831-1841.

[3] J. Limpouch, N.N. Demchenko, S.Yu. Gus'kov, A.I. Gromov, M. Kalal, A. Kasperczuk, V.N. Kondrashov, E. Krousky, K. Masek, P. Pisarczyk, T. Pisarczyk, V.B. Rozanov: PALS Laser Interactions with Foam Targets, 31st EPS Conference on Plasma Phys. London, 2004 ECA Vol.28G, P-2.031

[4] J. Limpouch, N.N. Demchenko, S.Yu. Gus'kov, A.I. Gromov, M. Kalal, A. Kasperczuk, V.N. Kondrashov, E. Krousky, K. Masek, M. Pfeifer, P. Pisarczyk, T. Pisarczyk, K. Rohlena, V. B. Rozanov, M. Sinor, J. Ullschmied: Laser interactions with low-density plastic foams, Proc. 28th ECLIM, Roma, 2004, p. 261-265.

[5] J. Limpouch, N.N. Demchenko, S.Yu. Gus'kov, V.B. Rozanov, A. Kasperczuk, T. Pisarczyk, M. Kalal, V.N. Kondrashov, E. Krousky, K. Masek, P. Pisarczyk: Iodine Laser Interactions with Porous Matter, Proceedings IFSA2003, American Nuclear Society, pp. 170-173, 2004.

[6] M. Kalal, J. Limpouch, N.N. Demchenko, S.Yu. Gus'kov, A.I. Gromov, A. Kasperczuk, V.N. Kondrashov, E. Krousky, K. Masek, M. Pfeifer, P. Pisarczyk, T. Pisarczyk, K. Rohlena, V.B. Rozanov, M. Sinor, J. Ullschmied: Interactions of subnanosecond laser -pulses with low-density plastic foams, Proc. Physics and technology of inertial fusion energy targets, chambers and drivers, Daejon, Republic of Korea, 2004, IAEA-TECDOC-1466.

V Training, Education, Outreach and Public Information Activities

1. Training and Education

The 2nd Summer Training Course on the CASTOR Tokamak

A direct touch with experimental reality is a fundamental step for the education of a new generation of plasma physicists cooperating with teams of large-scale experiments in a near future. A year after the successful organization of the first experimental summer school, the **2nd Summer Training Course (SUMTRAIC) on the CASTOR Tokamak** was held at IPP Prague under the aegis of the Czech and Hungarian Associations EURATOM (IPP.CR and HAS). The current run was performed on June 2-11, 2004, with participation of eleven students (graduate and post-graduate), from many European countries (Belgium, Bulgaria, Czech Republic, Estonia, Hungary, Slovakia) and also from Egypt and India (see Fig. 1). The main goal was to demonstrate the basic activities related to a real fusion experiment in practice - measurements, data processing leading to physical results, their presentation and discussion.

A standard procedure of preparatory works began several weeks before the training course. The Czech and Hungarian supervisors divided planned experiments into four main fields – basic diagnostics, probe diagnostics, plasma spectroscopy and measurements of plasma fluctuations. Comprehensible manuals describing particular diagnostics and data processing have been prepared beforehand by the supervisors, and their CD and web versions were made accessible to students.

As usual, the first day of the training course was devoted to an introduction of key elements of the CASTOR (vacuum, power supplies, diagnostics etc.) and to a brief theoretical introduction to the tokamak physics. Then, the students were divided into four groups accordingly to their future interests. Contrary to the first run of the training course, when the students were rotating over all available diagnostics, each group was focused on one particular topic during the whole training course. Such an arrangement has allowed to go into more detail with data processing. Consequently, there was more time for discussion of preliminary results, and finally for modification of experimental set-up, and making additional shots when necessary.

The last day of the course was dedicated to the joint workshop in main lecture hall of IPP Prague. The quality of the students' readings was very high, namely Langmuir probe and bolometric group presentations reached a scientific level. Therefore, the supervisors asked organizers of Symposium on Plasma Physics and Technology held in Prague at the same time to enter the conference with a post-deadline poster summarizing all students' contributions. At the end of the course, all students were awarded a certificate by right of merit.

It was concluded that the second SUMTRAIC more than fulfilled its main goals, set up new collaborations and found new talented physicists among its students. Moreover, the collegiate atmosphere of an international friendship positively influenced its perception by students and supervisors, and namely increased the effectiveness of the course. The SUMTRAIC extension to about 10 days proved to be a good idea. The next training course is envisaged to be organized next September in a similar way. Participation from all over

Europe and also other countries is welcome. More information is available at the course homepage: www.rmki.kfki.hu/plasma/castor.

Fig. 1. SUMTRAIC participants in front of the tokamak building

2. Outreach and Public Information

M. Řípa, V. Weinzettl, F. Žáček,
J. Mlynář

In 2004, the Association EURATOM /IPP.CR for the first time participated in the European PIG workshop, this year held in Padova as the 4th Public Information Meeting. Fresh ideas like the Czech fusion postcards and the video contribution to the Fusion Expo were appreciated. An integration of Czech laboratories into the European fusion community was introduced by the director of IPP Prague P.Chráska at a meeting with German and Swiss jounalists and was also demonstrated by a newly created "The history of CASTOR" (a tokamak device in IPP Prague) web page on the EFDA web

server. Under a new PI leader Milan Ripa (from IPP Prague), a lot of the official EURATOM materials for public were translated into the Czech language.

A significant effort was devoted to prepare the first book focused on controlled thermonuclear fusion, written in Czech. The book "**Řízená termojaderná syntéza pro každého**" (Driven thermonuclear fusion for everyone) treats fusion research history and the present taking into account the IPP contribution. The authors with their book met an unbelievably positive public response that the release of 1000 impressions was out of print till the end of the year. In a combination with the traditional Open Door Days of Czech academic institutions and universities, the interest of the public in fusion was strongly increased, namely from the side of secondary and high schools and their students. As a consequence of the broad PI activities including educational materials and lectures, many new students were attracted to the tokamak department of IPP Prague. However, the basic focus of the PI work was still driven to public media, mainly to daily newspapers, where a high number of articles were published. To reach people, who are usually not covered by scientific sections in media, an idea of joined both sports or artistic and fusion PR activities were used. As example, the bicycling race "Tour de Plasma" and a contribution to the Museum of Art and Design in Benešov (presenting deterministic chaos) can be mentioned. Additionally, the PALS laboratory contributed to the EU project ETHNIC by a presentation for a gipsy minority visited IPP.

The following list includes both activity attributed exclusively to the Association and activity where the Association is only a part of the whole.

LIST OF ACTIVITIES

Books

M. Řípa, V. Weinzettl, J. Mlynář, F. Žáček: **Řízená termojaderná syntéza pro každého. (Driven thermonuclear fusion for everyone)** 1st release. ISBN: 80-902724-7-9. IPP AS CR Prague, 2004. 84 pages

Papers

[1] M. Řípa: **Kdo postaví termojaderný reaktor? Francie či Japonsko? (Who constructs thermonuclear reactor: France or Japan?)**, Mladá Fronta Dnes, January 24, 2004, p. C/8

[2] M. Řípa: **D + T -> He + n + 17.6 MeV**, Technický týdeník, TT4/2004, p. 14

[3] M. Řípa: **Fúze pro každého (Fusion for everyone)**, Česká hlava – svět vědy, 3/2004, p. 10-11

[4] M. Řípa: **Výkonný ekologický zdroj energie na obzoru? (Is a powerful ecological energy source getting near?)**, EKO, 2004, No. 2, p. 18–21

[5] M. Řípa: **Evropa, popularizace jaderné fúze a EFDA (Europe, fusion popularization and EFDA)**, Technický týdeník, 11/5/2004, No.5, p.12

[6] M. Řípa: **O fyzice plazmatu v Praze (On plasma physics in Prague)**, Technický týdeník, 11/5/2004, No.10, p.2

[7] M. Řípa: **Plazmové zplynování odpadu (Plasma waste gasification)**, Eko – ekologie a společnost, XV, 4/2004, p.2-5

[8] M. Řípa: **EURATOM v Česku po sedmé (EURATOM in Czech for the seventh time)**, Akademický bulletin, No.6, 2004, p.15

[9] M. Řípa: **21. symposium o fyzice a technice plazmatu (21st symposium on plasma physics and technology)**, Akademický bulletin, No.9, 2004, p. 12

[10] M. Řípa: **Tour de Plasma**, Cykloturistika, 1/2004

[11] M. Řípa: **Výfukové plyny a vodík (Fumes and hydrogen)**, Eko – ekologie a společnost, XV, No.5/2004, p.30

[12] M. Řípa: **Atomová elektrárna bez odpadů (Nuclear power plant without waste)**, Respekt 29.11.- 5.12.2004, p. 18

[13] M. Řípa: **Termojaderná fúze pro každého (Thermonuclear fusion for everyone)**, 3 pól, prosinec 2004, p. 5

Lectures

[1] M. Řípa: **ITER je cesta (ITER is the way)**, Čáslav, 25/3/2004

[2] M. Řípa: **ITER je cesta (ITER is the way),** Akademická Praha, AS CR, Praha 1, Národní 3, 12/5/2004

[3] M. Řípa: contribution of the Association EURATOM/IPP.CR to the lecture of Rosa Antidormi **A Larger EU** on Public Information Meeting 2004

[4] J. Stöckel: **Fyzika plazmatu a termojaderné slučování (Physics of plasma and thermonuclear synthesis)**, Západočeská Univerzita, Plzeň 3/5/2004

[5] J. Stöckel: **Fyzika plazmatu a termojaderné slučování (Physics of plasma and thermonuclear synthesis)**, FEL ČVUT, in the frame of Physical Thursdays, 2/12/2004

[6] J. Stöckel: **Fyzika plazmatu a termojaderné slučování (Physics of plasma and thermonuclear synthesis)**, FJFI ČVUT, 18/3/2004

Other

- M. Řípa, J. Stöckel**: Co to je EFDA, ITER (What is EFDA, ITER)** (translation for http://www.efda.org Multilingual Page)
- F. Žáček, V. Weinzettl, M. Řípa: **The history of CASTOR** , EFDA web site, 30/4/2004
- M. Řípa: contribution to the calendar **Od ohniště k tokamaku 2005 (From fireplace to tokamak 2005),** Parentservis Praha, a.s.
- M. Řípa et al.: **6th Tour de Plasma**, 16–19/9/2004
- M. Řípa et al.: **Open Door Days 2004**, 1 student group and more than 100 individuals,12-13/11/2004
- 20 group excursions at IPP
- P. Chráska, J. Stöckel et al.: meeting with German and Swiss scientific journalists including the presentation on an integration of IPP into the European scientific comunity, March 2004
- V. Weinzettl: exposition **Arnoldova (dvojitá kosá) transformace (Arnold double skew transform)**, Museum of Art and Design in Benešov, 2004
- presentation of the PALS laboratory for a gipsy minority in the frame of the EU project ETHNIC, 7/9/2004
- J. Ullschmied: animated presentation of the PALS laboratory used for high and secondary school students (in the frame of the 6th Physical Week on FJFI ČVUT, 23/6/2004)